HUYGENS

TITLE: HUYGENS MISSION POST FLIGHT ENGINEERING ANALYSIS

Doc n° HUY.ASPI.MIS.RE.xxxx

Ed. : n° 01 **Date: 10/04/06**
Rev. : n°

	FUNCTION	NAME	SIGNATURE	DATE
WRITTEN BY	**ENGINEERING**	**P.COUZIN**		**/06**
APPROVED BY	**PROGRAM MANAGER**	**AM SCHIPPER**		**/06**

Internal Diffusion Sheet

P. MAUTE	**X**
JJ.JUILLET	**X**
A.-M. SCHIPPER	**X**
P. COUZIN	**X**
G. ROUYER	**X**
G.CLUZET	**X**

Change Notice

ED.	REV.	DATES	MODIFIED PAGES	CHANGES	APPROVAL
01	00	10/14/06		1st issue	

TABLE OF CONTENTS

1. SCOPE

This document presents the results of the Huygens Mission. It is essentially based on the analysis of the housekeeping parameters returned from the Probe and from the Probe Support Avionics during the mission. Its purpose is to synthesize the outcomes of the post mission, phase one, industry studies and provides the overall picture of the mission from a pure engineering point of view.

It however excludes :

- the analysis of the entry conditions from an aerothermodynamic perspective, performed in RD01 (EADS report)
- the analysis of the descent condition from an aerodynamic perspective, performed in RD02 (Vorticity report)
- the detailed analysis of the thermal behaviour of the Probe during its mission, performed in RD03
- the analysis of the separation conditions, and of the separation mechanisms performance, addressed in RD04 (Contraves report).
- the analysis of the behavior of the science experiments.

The engineering telemetry parameters which will be analyzed are the ones returned in the 4 Probe HK packets (HK1 to HK4), and the PSE HK packet. The exhaustive content of this telemetry stream is available in RD09 “TM/TC Data Tables”.

2. APPLICABLE DOCUMENTS

The tests have been performed according to the following documents:

- AD01: ESOC checkout sequences
- AD02: Spacecraft Data Operations Handbook (SDOH) DOPS-SMD-HUY-DB-004, Issue 1.0, June 1996

Reference documents for the present report are:

- RD01: Entry and Descent Level 0 post flight analysis
  Doc. n° HUY.EADS.MIS.TN.0006 Issue 01 Rev 0
- RD02: Preliminary analysis of post-flight data
  Doc. n° VOR-RE-0503 Issue 01 Rev B
- RD03: Preliminary Evaluation of Thermal Behaviour during mission
  Doc. n° HUY.ASP.MIS.RE.0004 Iss.02
- RD04: SEPS Flight evaluation
  Doc. n° HUY-CONT-3C00-TN-010-Rev-B
- RD05: FAR Design Report
  Doc. n° HUY.AS/c.100.RE.0403
- RD06: delta FAR Design Report
  Doc. n° HUY.Axxxxx
- RD07: Huygens User's Manual
  Doc. n° HUY.Axxxxxxx
- RD08: HUYGENS PRE-SEPARATION HEALTH ASSESSMENT AND OPERATIONS SYNTHESIS REPORTt
  Doc. n° HUY.ASPI.MIS.RE.0002
- RD09: TM/TC Data Tables
  Doc. n° HUY.Axxxx
- RD10: Pérez-Ayúcar M., Couzin P., Lebreton J.-P., Witasse O, *Huygens Radio Link In-Flight Performance*. Proceedings of the 3rd International Planetary Probe Workshop, Anavyssos, Greece, 2005
- RD11: Pérez-Ayúcar, A. Sarlette, P. Couzin, T. Blancquaert, O. Witasse, J.-P. Lebreton. *Huygens Attitude Reconstruction Based on Flight Engineering Parameters*. Proceedings of the 3rd International Planetary Probe Workshop, Anavyssos, Greece, 2005

- RD12: HUYGENS HRA Altitude Data Calibration V1.0
  R. Trautner, RSSD / SCI-SB, ESTEC, Feb.2005

- RD13: Huygens Recovery Task Force (HRTF) final Report
  Doc. n° HUY-RP-12241, 27/07/2001

- RD14 : Huygens pre separation health assessment and operations synthesis report
  Doc. HUY.ASPI.MIS.RE.0002, Iss.2, 10/05/05

3. LIST OF ABBREVIATIONS

ACP	Aerosol Collector and Pyrolyzer
AGC	Automatic Gain Control
APIS	Acoustic Sounder (SSP experiment)
BCM	Back Cover Mechanism
BDR	Battery Discharge Regulator
CASU	Central Acceleration Sensor Unit
CCD	Charge Coupled Device
CDMS	Command and Data Management Subsystem
CDMU	Command and Data Management Unit
CDS	Command and Data Subsystem (of the orbiter)
CO	Check Out
CRID	
CUT	Computed Unit of Time
DC	Down Converter
DDB	Descent Data Broadcast
DISR	Descent Imager and Spectral Radiometer
DMA	Direct Memory Access
DSN	Deep Space Network
DT	Dead Time
DWE	Doppler Wind Experiment
EDAC	Error Detection And Correction
EEPROM	Electrically Erasable Programmed Read Only Memory
EMC	Electro-Magnetic Compatibility
ESOC	European Space Operations Center
ESTEC	European Space Research and Technology Center
FDI	Frame Data Interrupt
FSM	Front Shield Mechanism
GCMS	Gas Chromatograph and Mass Spectrometer
HASI	Huygens Atmosphere Structure Instrument
HGA	High Gain Antenna
HK	House Keeping

IR	Infra-Red
JPL	Jet Propulsion Laboratory
LGA	Low Gain Antenna
LNA	Low Noise Amplifier
LSB	Least Significant Bit
MTT	Mission Timeline Table
MTU	Mission Timer Unit
MVDA	
NCO	Numerically Controlled Oscillator
PCDU	Power Conditioning and Distribution Unit
PDD	Parachute Deployment Device
PI	Principal Investigator
PJM	Parachute Jettison Mechanism
POSW	Probe On-board SoftWare
PRT	Probe Relay Test
PSA	Probe Support Avionics
PSE	Probe Support Equipment
RAM	Random Access Memory
RF	Radio Frequency
RFE	Radio Front End
RSS	Radio Science experiment
RSW	Receiver Software
RT	Real Time
RTI	Real Time Interrupt
RUSO	Receiver Ultra Stable Oscillator
SASW	Support Avionics SoftWare
SEPS	SEParations Subsystem
SSP	Surface Science Package
TAT	Time Altitude Table
TC	TeleCommand
TCXO	Transmitter Compensated Crystal Oscillator
TM	TeleMetry
TUSO	Transmitter Ultra Stable Oscillator
TX	Transmitter
USO	Ultra Stable Oscillator

4- INTRODUCTION

The mission of the Huygens Probe to the Saturnian's moon Titan has been performed on the 14th of January 2005, after having been successfully released from the Cassini Orbiter on 25 December 2004 at 02:00 UTC.

The Probe electronics was "woken up" as programmed, 4h28mn before the expected entry into Titan atmosphere. The Probe descent part of the mission started at UTC09:10:20,828 until the surface landing, 2h27mn11s later. From UTC09:11:07 until 1h12mn7s after this landing, Huygens successfully transmitted data, exceeding by far its specified survivability on the surface of 3mn. However, because of an operational mishap described in very much details in HUY_NCR-1, the chain A data stream (see RD05) could not be acquired, and this document therefore presents the analysis of the engineering data received from the Probe chain B only, via CASSINI Orbiter.

The flight performance of each subsystem and function are addressed, and compared to the expected one. When relevant they are put back into the context of the mission and both the real time behavior, and the behavior as deduced from the post flight analysis are reviewed.

The subsystems and functions analyzed in the following are :

- CDMS
  - Coast phase measurement, Probe wake up
  - Entry acceleration measurement and entry detection (nominal and back up detection process)
  - Spin measurement
  - Altitude measurement (AGC, algo, RAU's)
  - CDMU
  - Probe on board SW
- power distribution and pyros (status and currents)
- power generation (battery perfo)
- RF link (Tx perfo, PSA, SASW, AGC, NCO)

In addition some system level statistics on the mission return are presented.

Nota 1 : for matter of consistency, all over the document the times will be expressed in UTC.

5- OVERALL ARCHITECTURE

The reference design document of the Huygens Probe are the FAR Design report (RD05) and the Delta FAR design report (RD06). All the analyses presented in the following will refer to this design. However, to simplify the interpretation , Fig. 1 recalls the main elements of the electrical architecture of the Probe.

Nota : the reason why the chain A data stream from the Probe could not be acquired is that the "USO" in the receiving part, circled in red in Fig.1, was not switched ON during the Probe mission.

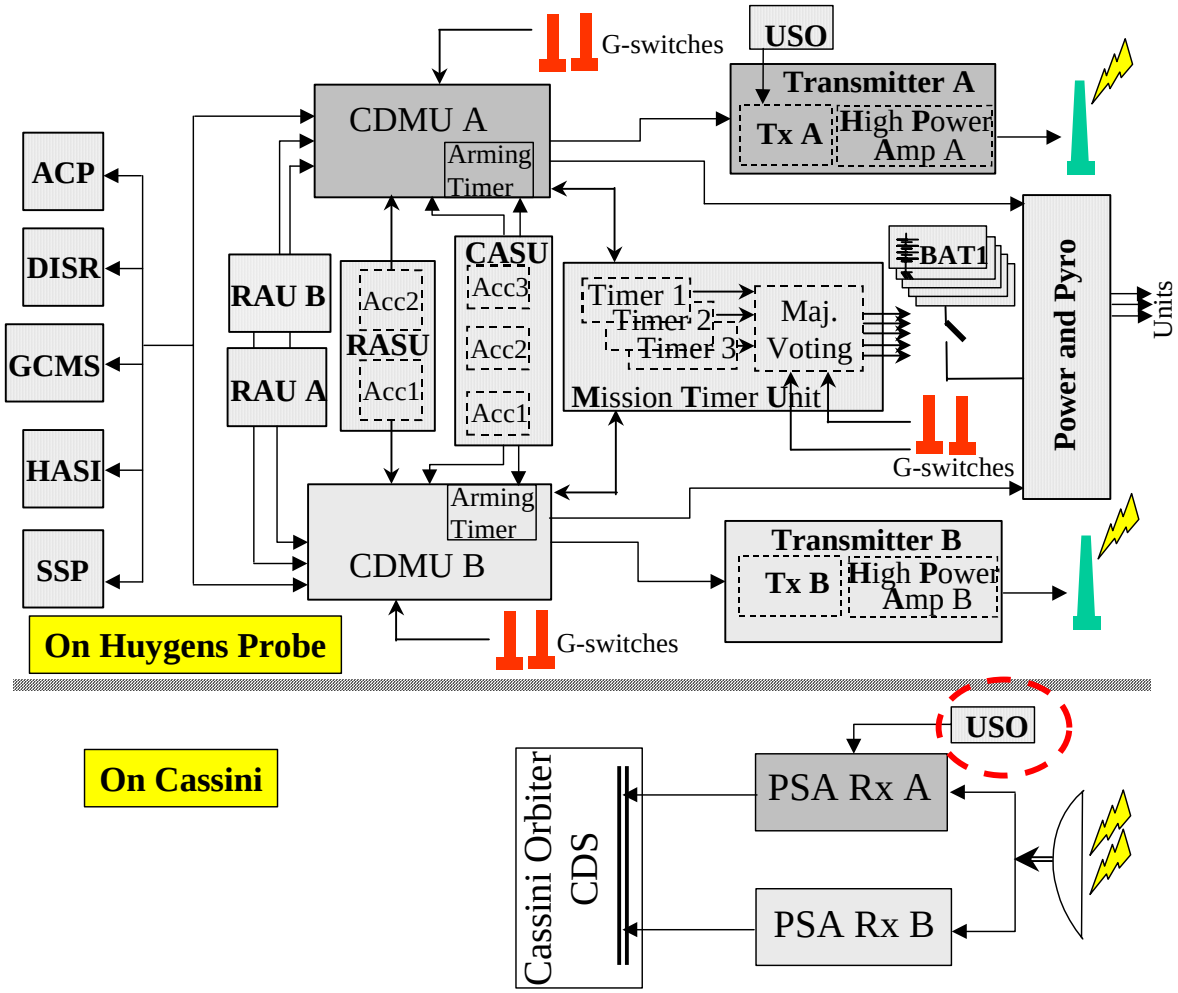

Figure.1 : overall electrical architecture

6- PROGRAMMED MISSION TIMELINE

The table below presents the timeline of events programmed to be executed by the Arming Timer electronics, and the Probe on board Software (POSW). The times are expressed wrt PCDU On event before S0, and wrt S0 detection after. One of the objective of the present analysis is to reconstruct the timeline of events as they have actually been performed during the mission; this will be presented in section xxx. The present table 1 aims to ease the understanding of the analysis.

Tp (sec)	OPERATION
0	PCDU on
0	CDMU A & B, CASU, RASU on
16	TUSO on
16,125	TX-A & TX-B on
30,125	GCMS 1 on
1080,13	HASI 1 on
2320,38	Send ACP Engineering Mode TC
0	S0 detection
1,5	Ta detection/ Arm pyro group 1 (PDD & BCM)
2,125	Reset PDD pyro selection relay
2,25	Reset BCM 3 pyro selection relays
2,375	Set PDD pyro selection relay
6,375	PDD current limiter fire
6,625	Reset PDD pyro selection relay
8,625	Set BCM 3 pyro Norm. Selection relays
8,75	Set BCM 3 pyro Red. Selection relays
8,875	BCM 3 current limiter fire
12,875	Reset BCM 3 pyro selection relays
16,375	TUSO on (2nd switch on)
16,625	TXs on (2nd switch on)
26,67	Arm pyro group 2 (FSM)
34,875	Set FSM 3 pyro selection relays
37,125	ACP 1 on
39,25	ACP 2 energize caps and valves, purge
38,875	FSM 3 current limiter fire
39,375	Reset GCMS inlet pyro selection relay
39,5	Reset GCMS outlet pyro selection relay
39,625	Reset DISR cover pyro selection relay
42,875	Reset FSM 3 pyro selection relays
47,64	Arm pyro group 3 (GCMS & DISR cover)
46,375	ACP 3 on
49,375	HASI 1 on (2nd switch on)
51,83	HPA on
52,375	Set GCMS inlet pyro selection relay
56,03	HASI 2 on : booms start to deploy
55,625	SSP on

56,375	GCMS inlet current limiter fire
60,375	Reset GCMS inlet pyro selection relay
60,5	Set GCMS outlet pyro selection relay
64,5	GCMS outlet current limiter fire
68,5	Reset CGMS outlet pyro selection relay
68,625	Set DISR cover pyro selection relay
72,625	DISR cover current limiter fire
85,625	Reset DISR cover pyro selection relay
86,375	DISR 1 on
160	ACP collection starts
186,375	GCMS 1 on (2nd switch on)
207,02	HASI 2 off
216,375	ACP 1 on (2nd switch on)
226,375	ACP 3 on (2nd switch on)
303,49	Arm pyro group 4 (PJM)
362,21	ACP 2 off
902,375	Set PJM 3 pyro selection relays
906,375	PJM 3 current limiter fire
910,375	Reset PJM 3 pyro selection relays
1737,94	GCMS 2 on
1922,49	Proximity sensor on
4926,38	DISR 1 on (2nd switch on)
6486,38	SSP on (2nd switch on)
6599,13	DISR 2 on
6606,38	ACP 3 off
6606,63	ACP 1 off
8007	DISR turn on surface lamp

Table 1 : Timeline of the Mission events as designed

7- COAST PHASE MEASUREMENT AND PROBE WAKE UP

7.1 COAST PHASE

On the 21/12/04 at UTC07:00, the 3 Mission Timer Units timers have been loaded to wake-up to the Probe 23 days 21h 42mn 22s later, i.e. the 14th of January 2005 at UTC04:42:22.

The Real Time counter parameter reports with each telemetry packet the time elapsed since Probe turn ON. This parameter then allows to precisely date the time of Probe wake up :

Probe wake up time = UTC04:41:18

The difference with the programmed time is 61s. This is very consistent with the measurement performed during the flight checkouts F13 and F14 (see RD08) which predicted a drift of 57s.

It is nevertheless not possible to determine which of the 3 timers have commanded the probe turn ON.

7.2 PROBE WAKE-UP G-SWITCHES

As shown in Fig.1 and described in RD05, 2 g-switches are implemented to serve as back up to the coast Timers operation. As the MTU has performed nominally, it is not possible through the available TM to get information on the performance of the Probe wake up back up solution. One shall note however that these 2 g-switches are similar to 2 g-switches used as Entry detection back-up. As explained in the next chapter, we have on the contrary the demonstration that the entry back up has operated fully nominally.

8. CENTRAL ACCELEROMETERS AND G-SWITCHES

8.1 ENTRY ACCELERATION

These are the accelerations acquired from the 3 CASU accelerometers. These accelerometers primarily aim to support the nominal Probe atmospheric entry detection process and initiate the descent sequence (T0 detection). Detailed analyses of the measured entry profile and the entry detection are performed from aerodynamic and aerothermodynamic points of view in RD01 and RD02 where perfect adequacy with the simulations is demonstrated. These accelerometers are then sampled and reported in telemetry until the end of the mission although they are then not linked to any decision anymore.

The characteristic of this telemetry is :

- sampling rate 8Hz
- telemetry rate 1Hz (1 sample/s from each accelerometer
- HK TM in HK4 TM packet, delayed by 24 x 16s = 6mn24s
- 1 LSB = 39mg (Earth g)
- worst case measurement accuracy at entry detection Arming point (Ta) = 4.68%
- worst case measurement accuracy at entry detection point (S0) = 5.55%
- measurement range = 0 to 10g

Figure 2 reports the measurement acquired from the 3 accelerometers during Entry. The events corresponding to the different steps of the nominal and back up entry detection process (T0 and Ta detection) are identified.

This figure shows that

- all 3 accelerometers have nominally operated, providing very consistent entry deceleration measures
- the "1 LSB noise" anomaly flagged during some of the flight checkouts, summarized in RD08 §5.5, is not present, somehow a posteriori justifying the "use as is statement".

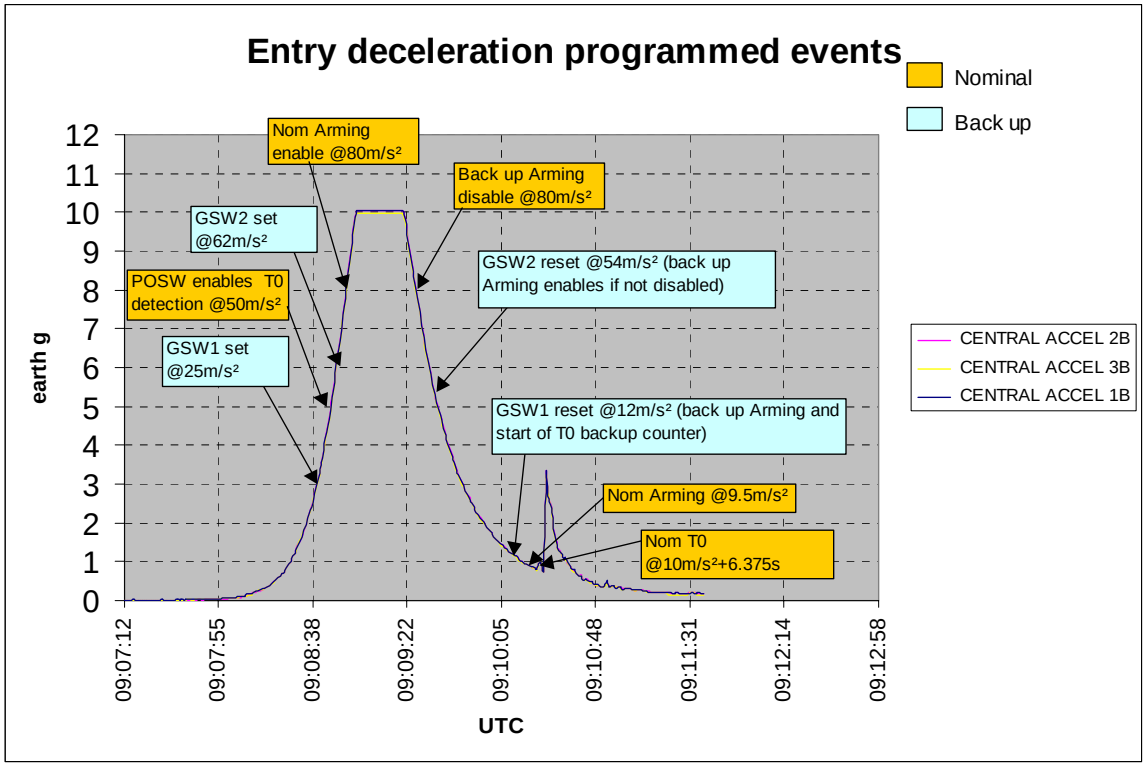

Figure.2 : Entry profile from CASU

Figures 3 and 4 hereafter are zooms of the measured entry profile in the area of S0/T0 detection and entry devices activations and the main entry detection/descent initiation events are marked.

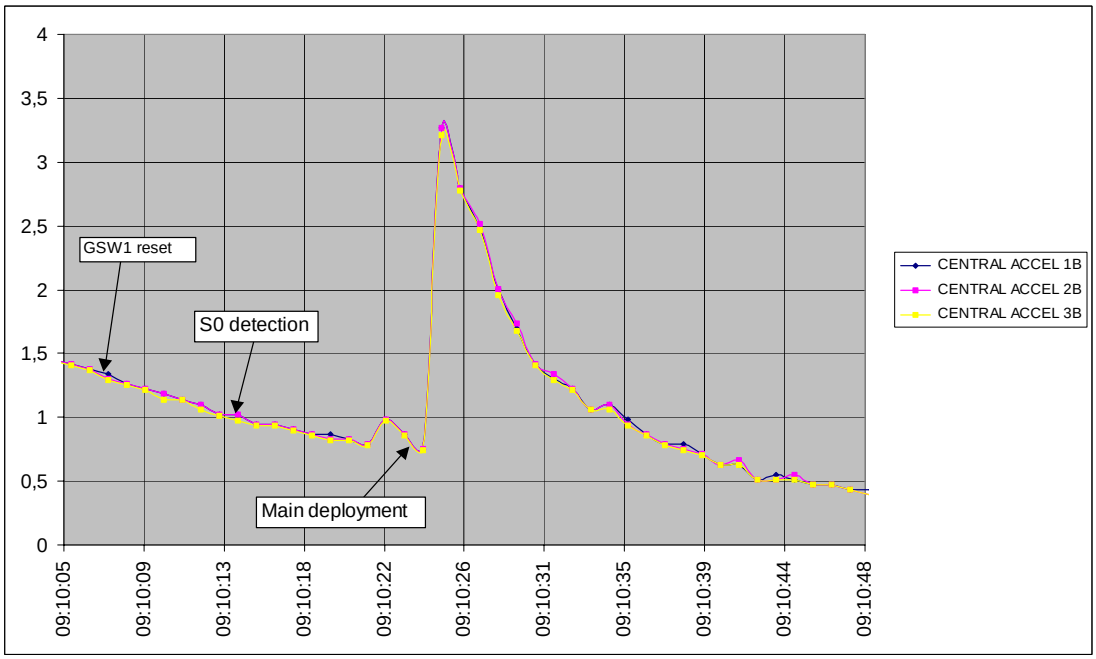

Figure 3 : Entry Profile – zoom

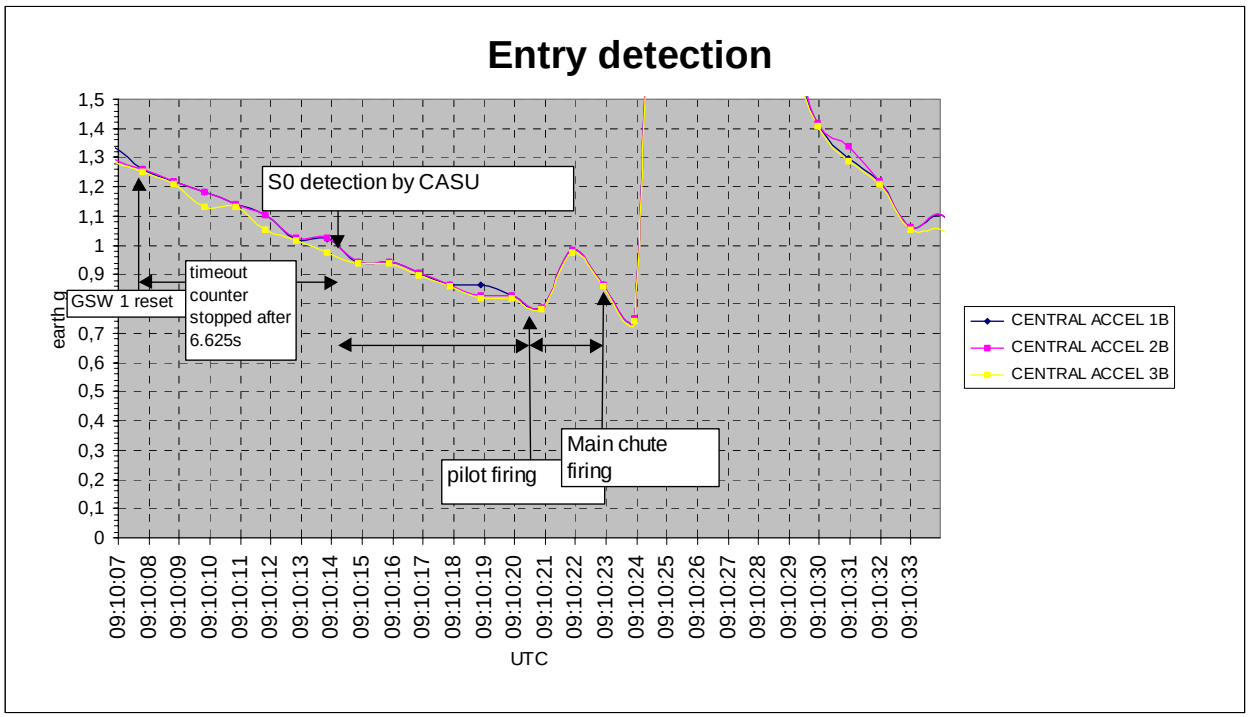

Figure 4 : Entry Profile - zoom

Aerodynamic conditions at which the PDD was fired are addressed in RD01 and RD02.

8.2 TIMES AND DATATION ISSUES

An important point related to the start of the descent phase is the precise measurement of the T0 occurrence. Because all the post T0 events on board the Probe, the engineering telemetry and the science data are dated with respect to this time, the accurate determination of the "T0 time" allows the correlation of the post T0, then pre T0 Probe data to UTC.

In fact 3 times have to be considered :

- the PDD firing time
- the T0 time
- the DDB time origin

The PDD time is the time at which the pilot chute mortar pyros are fired. The T0 time is the time at which the descent timeline starts; it is used as a reference for the datation of the Probe engineering data. There is obviously a relationship between these 2 times : only one of the 2 chains actually fires the pilot mortars, the one which detects T0 the first; for that chain T0 time= PDD firing time. For the other chain, T0 time = PDD firing time+inter chain delay.

The DDB Time is the time distributed to the science experiments and used to date the science data. The DDB time is reset to "0" after detection of T0, ie. at T0 time, however as detailed in Appendix 2, the DDB time may not reset exactly at T0.

Three distinct tasks are then to be done :

1- determine precisely T0 time from the telemetry analysis,

2- determine the time difference between T0 Time and DDB Time=0.

3- identify which of the 2 chains has actually fired the PDD mortar, and subsequent pyros,

8.2.1- T0 time

It is first reminded that only the chain B telemetry is available, then only T0 time from chain B can be established. Referring to appendix 2, which uses the precise S0 time (125ms resolution) recorded by the POSW, one obtains :

T0_time_chain_B = UTC09:10:20,828

The datation of all engineering parameters on board the Probe is based on this time.

8.2.2- DDB Time=0

As explained in appendix 2, DDB Time sent on chain B is reset 250ms after T0 time on chain B leading to :

DDB_time_chain_B_=_0 at UTC09:10:21,078

Which is thus the time origin for science data datation.

8.2.3- Chain A – Chain B synchronization : ICD calculation

The CASU acceleration data telemetry rate is not high enough to allow to discriminate between A and B chains. By using also acceleration measured by HASI servo accelerometer, sampled at 3Hz, one can get the precise time at which the PDD firing event has physically occurred. The negative peak visible in Figure 5 can indeed be attributed to the Probe reaction to the mortar firing. Because this peak initiates BEFORE T0 is detected by the chain B, it becomes clear that the PDD mortar firing has been performed by the chain A, 125 to 500ms before T0_time_chain_B.

This means that all the mission timeline events have very presumably be commanded by the chain A, ie. the chain from which no data was received.

In the same way, the instruments have received DDB_time from both A and B chains all along the mission. Since chain A has consistently been reported as valid by the instruments telemetry, DDB_time_chain_A was nominally used to time stamp the science data. As addressed in appendix 2 a realistic time difference between DDB_time_chain_A and DDB_time_chain_B is +/-100ms, consequently,

DDB_time_chain_A =_0 at UTC09:10:21,078+/-100ms

is thus the time origin for science data datation.

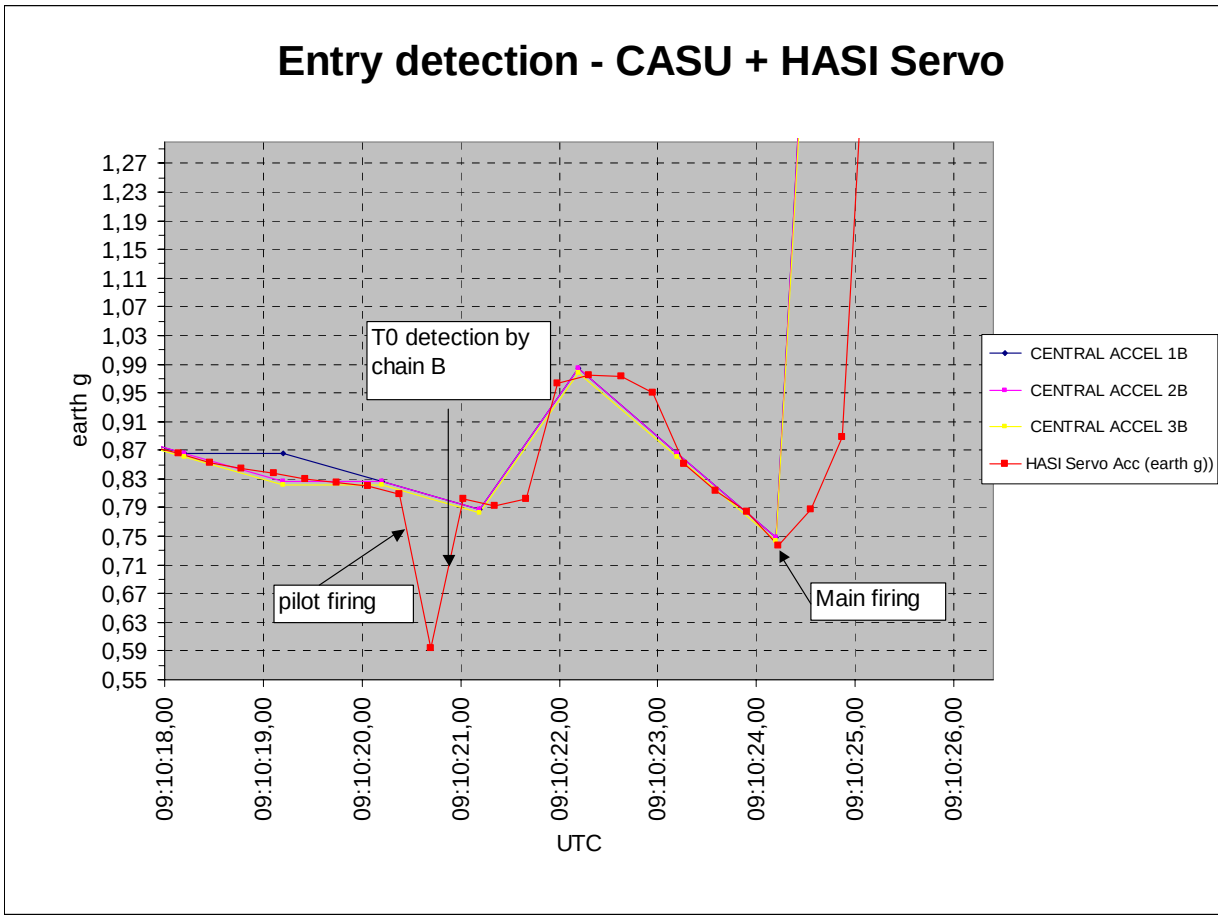

Figure 5 : chain A – chain B time shift

8.3 DESCENT DECELERATION

The Probe deceleration measured by the 3 CASU accelerometers is displayed in Figure 6 hereafter. The stabilizer chute deployment event appears clearly, in consistence the predicted timeline in Table 1. Other noticeable features are :

- the 3 accelerometers exhibit a remarkably similar behavior all over the descent.
- the surface touch down event, at UTC11:38:11(see Fig.10 for details). The descent has therefore lasted **2h27mn50s**, only 2mn10s less than the maximum predicted descent time. This issue is addressed in details in RD02.
- After touchdown, the CASU accelerometers measure the Titan gravity, as detailed in Figure 7 (accelerometers data are averaged; Titan gravity is about 1.4m/s^2).
- 3 distinct regions can be identified :
  - o after entry until the stabilizer is deployed, the deceleration profile is smooth indicating a relatively stable attitude,
  - o After the stabilizer deployment, an apparent instability area occurs until about UTC10:45, called “rough ride”,
  - o Then until surface touchdown the Probe comes back to a seemingly more stable attitude.

Considering the poor resolution of the measurements in these regions, a more quantitative evaluation cannot be made.

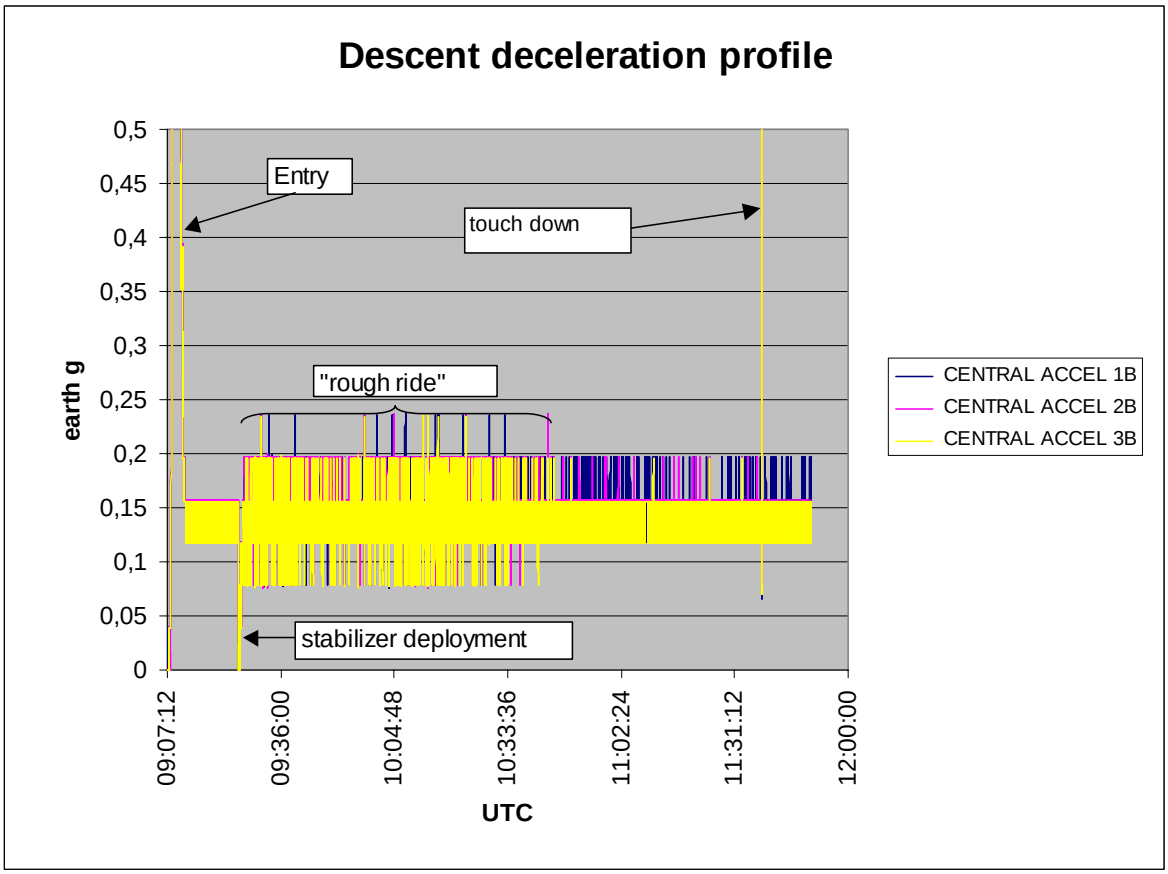

Figure 6 : Descent deceleration profile

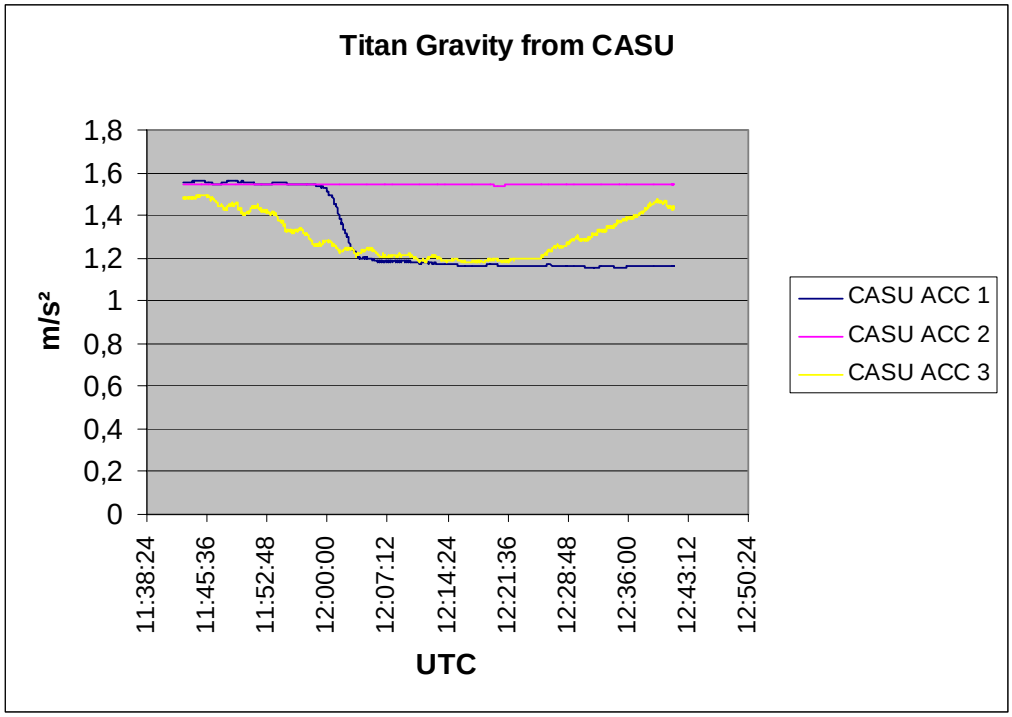

Figure 7 : Titan gravity from CASU data

A zoom in the early descent part allows to identify the front shield release event, as highlighted in Figure 8 below. The occurrence of this event is perfectly aligned with the programmed timeline in Table 1 (remember as stated in §5.2.3 that the actual pyros firing was performed by the chain A).

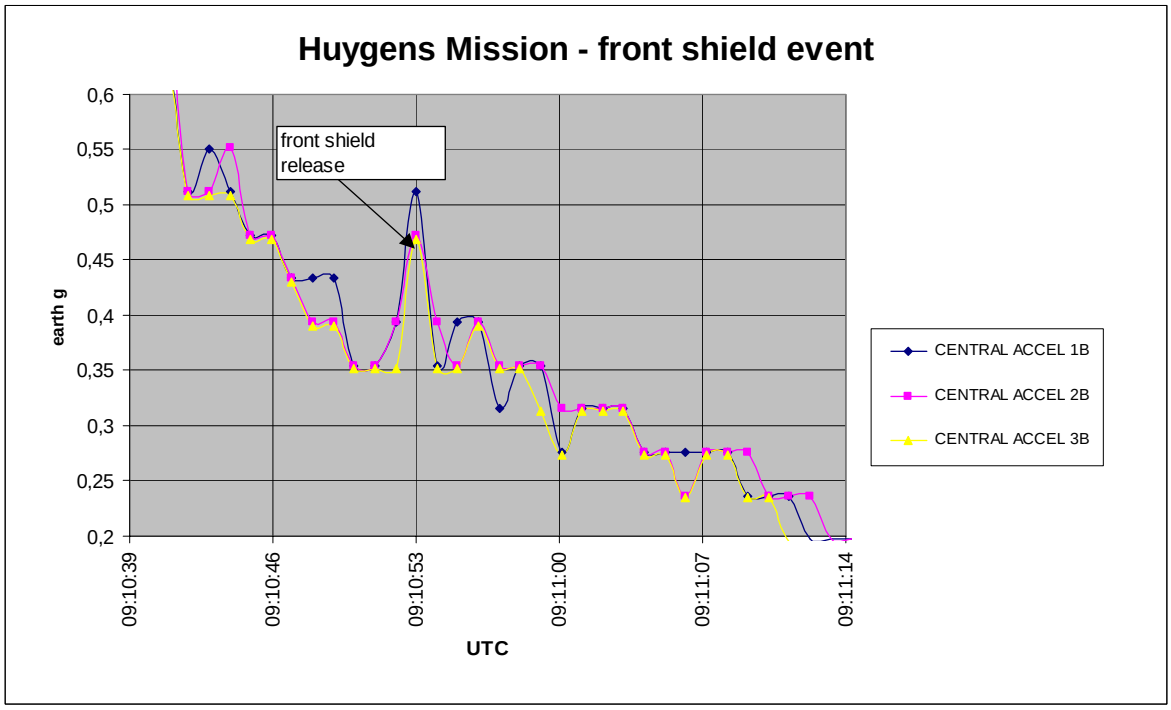

Figure 8 : Front shield release event

A zoom in a later part of the descent part clearly shows the stabilizer deployment event, as highlighted in Figure 9 below. The time of this event is perfectly aligned with the programmed timeline in Table 1 (as mentioned, the actual firing has been performed by the chain A).

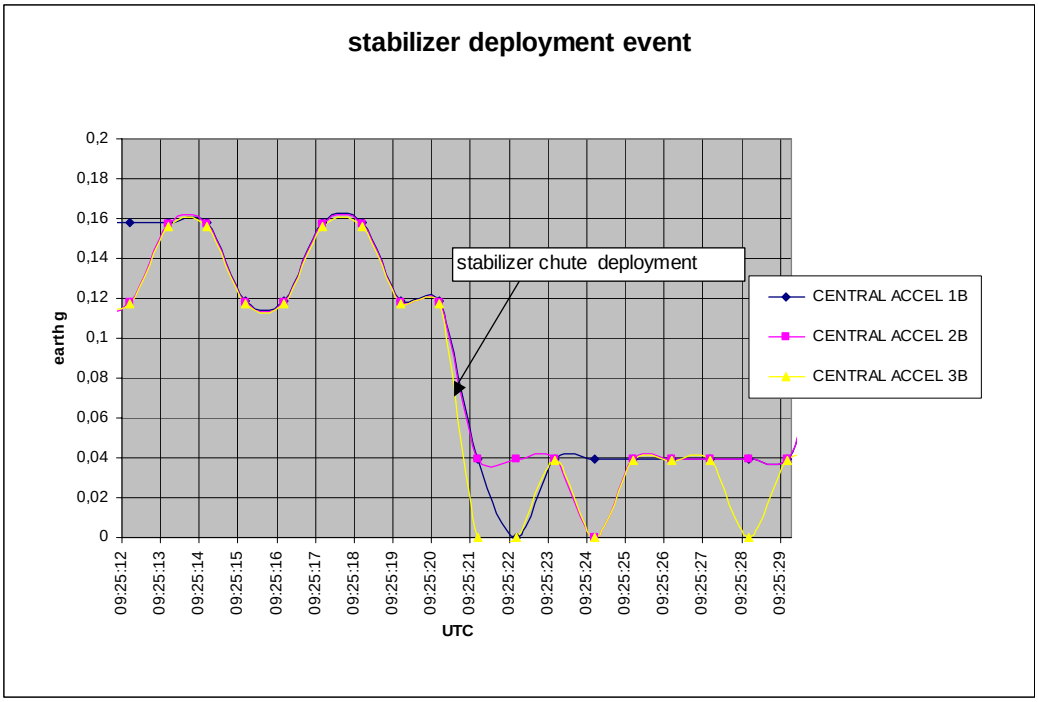

Figure 9 : stabilizer chute deployment event

Finally a zoom around the surface impact time in Fig.10 shows the conditions at touchdown. This impact is very consistently measured in the same way by the 3 CASU accelerometers, however the telemetry rate does not permit to interpret neither the absolute g value (1.2 earth g are measured), nor the impact time with an accuracy better than 1s.

The impact time is measured by CASU at UTC11:38:11

In the 2-3 seconds after the impact, the telemetry seems to indicate some bouncing of the Probe on the surface; it is indeed difficult to explain this either by a motion of the experiment platform, far too rigid, or by a "bouncing" at the level of the accelerometers sensors, their response time being too fast to be visible in TM.

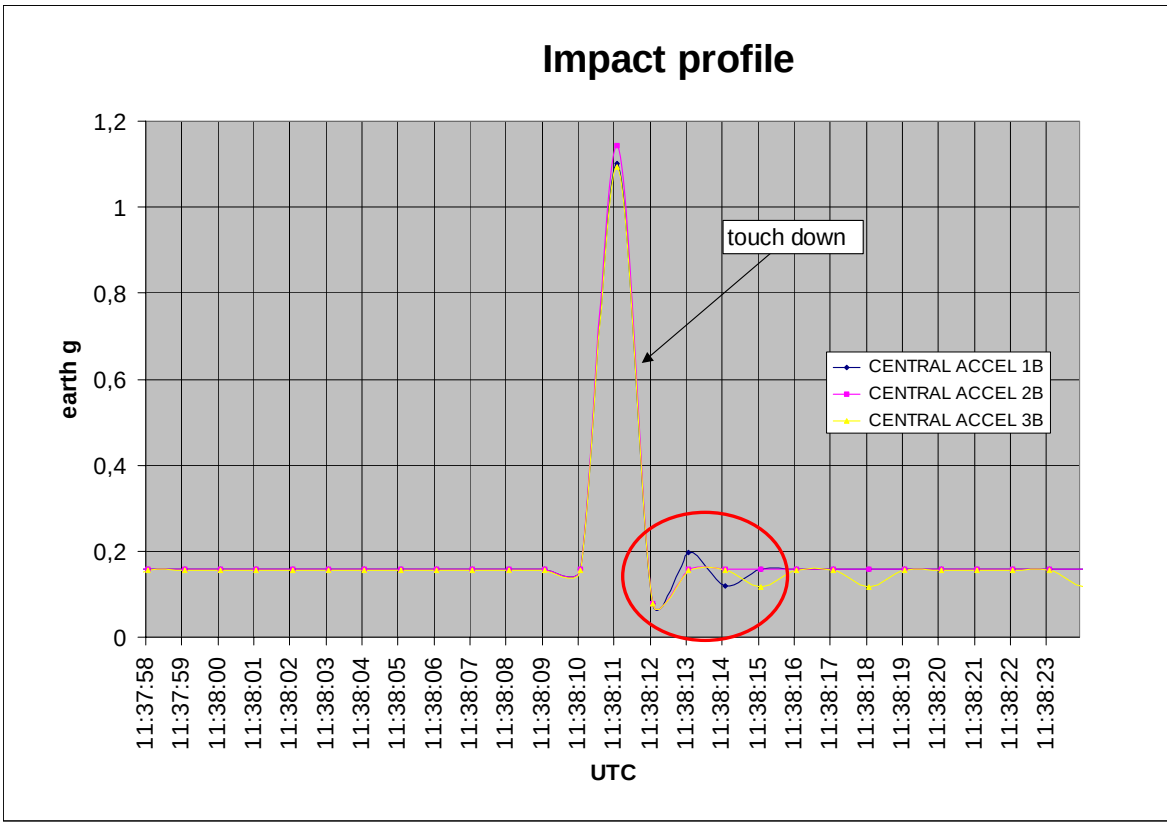

Figure 10 : touchdown event

8.4 ENTRY DETECTION G-SWITCHES

As described in RD05, 2 g-switches per chain are implemented as back up to the operation of the CASU accelerometers. It is possible through the received telemetry to have trace of all the g-switches set and reset. The TM results are summarized in the table hereunder;

UTC	TM code	TM name	TM value	Comment
09:04:58	S2024W	T0/Ta G-S 1/2 B	0000h	
09:05:02	S2025W	T0 G-S T-OUT B	0	To not detected
09:08:39,825	S2024W	T0/Ta G-S 1/2 B	FF00h	G-switch1 set 29,5 m/s²
09:08:49,825			FFFFh	G-switch2 set 59,8 m/s²
09:09:33,825			FF00h	G-switch2 reset 54,5 m/s²
09:10:07,824			0000h	G-switch1 reset 12,8 m/s²
09:10:14,453	S2025W	T0 G-S T-OUT B	6.625 s	Back-up count stop

As reported in blue in Fig.2, the g-switches have operated at the expected thresholds.

At UTC09:10:07,824, the back up entry detection count down has started, triggered by the G-switch 1 reset. As reported from S2025W parameter, this 20s long timeout has stopped 6.625s later because S0 has been detected by the accelerometers based detection process. This is illustrated in Fig. 4.

As a remark, if the nominal process had not worked for any reason, the back up would have then attempted to initiate the descent activities at about 200Pa and Mach 1.1. This is obviously, as expected, beyond the “guaranteed” conditions of operation but is likely to have led to a quasi nominal mission.

9. SPIN AND RADIAL ACCELERATION

9.1 SPIN AND RADIAL DECELERATION IN FLIGHT MEASUREMENT

The Probe spin is calculated from the radial acceleration measured by the 2 RASU accelerometers. The algorithm used to extract the spin data is presented in RD05, Chap 2.5. Two points have to be highlighted :

- because the measures acquired from the RASU are unipolar, the spin amplitude is calculated, but the spin direction cannot be derived.
- any "negative" radial acceleration being cut to "0", the spin calculation algorithm introduces a positive bias if, because of the Probe attitude, some radial deceleration values become opposite to the spin direction.

This spin information is not used by the Probe system and simply distributed to the experiments via the 2s period Descent Data Broadcast. Detailed analysis of the measured spin profile is performed in RD01.

In addition to the spin itself, the raw data under the form of the radial acceleration is also reported in telemetry.

The characteristic of this telemetry is :

Spin

- telemetry rate 0.5Hz
- HK TM in HK3 TM packet,
- 1 LSB = 4.705e-3m/s² (1,12rpm is hence the minimum measurable spin rate with RASU).
- worst case measurement accuracy : see Fig.11.
- measurement range = 0 to 17.6rpm

Radial acceleration

- sampling rate 8Hz
- telemetry rate 4Hz
- 7th order low pass anti aliasing filtering at 2Hz
- HK TM in HK2 TM packet
- 1 LSB = 4.705e-3m/s²
- worst case measurement accuracy : see Fig.12
- measurement range = 0 to 120mg

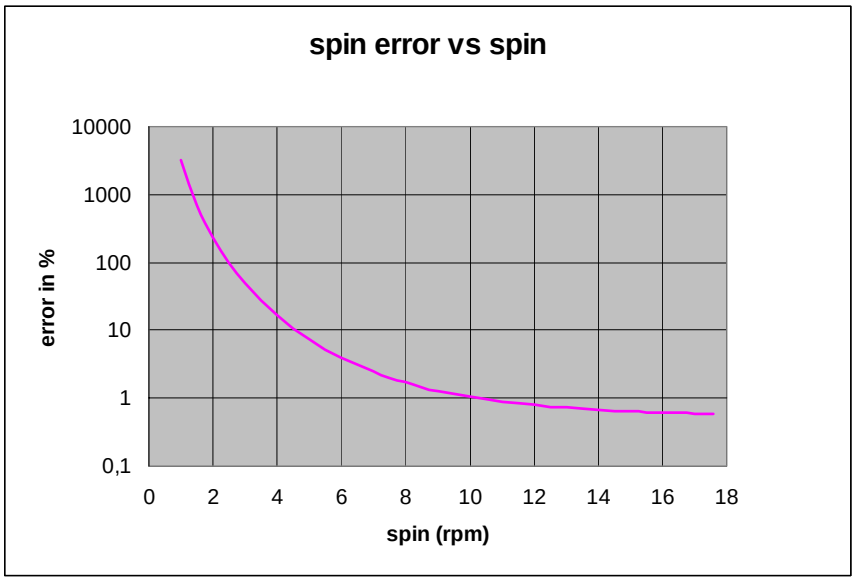

Figure 11 : spin measurement error

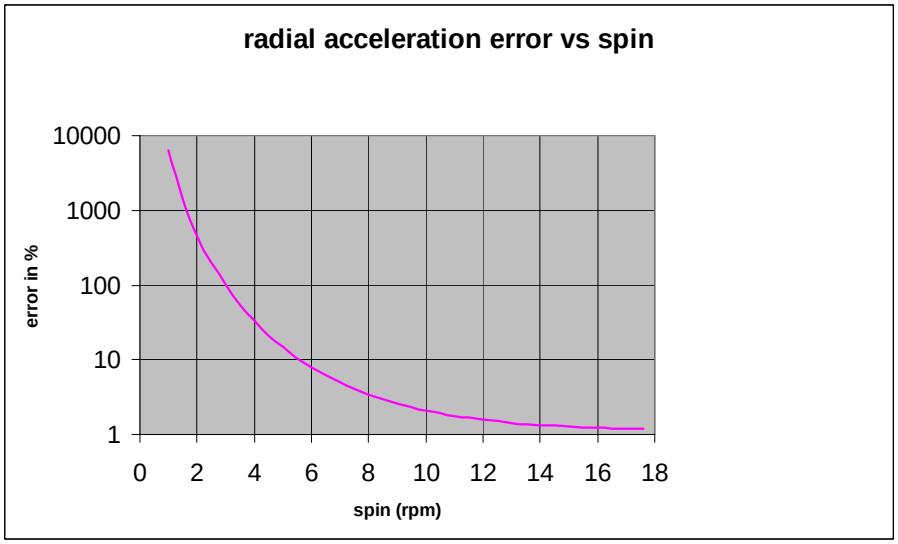

Figure 12 : radial acceleration measurement error

Figure 13a reports

- the measurement acquired in flight from the radial accelerometer connected to the chain B. In order to simplify the interpretation, the radial accelerations are transformed in rpm.
- the spins calculated from the 2 radial accelerometers and distributed in the DDB A and DDB B.

This figure shows that

- the radial acceleration is extremely noisy, as somehow anticipated, due to the variations in the Probe attitude during the various parts of the descent,
- the spin algorithm has well succeeded in extracting a seemingly consistent spin value from the

noisy acceleration, to be distributed to the experiments,

- even if only one radial acceleration sensor data could be retrieved (the one sent by the chain B), it was possible to retrieve the spin as measured by the chain A from SSP experiment HK data set (curve in pink below). Both A and B spins are extremely consistent, indicating that the raw data (radial acceleration from RASU Acc 1) was also very similar to the available RASU Acc 3 data set.

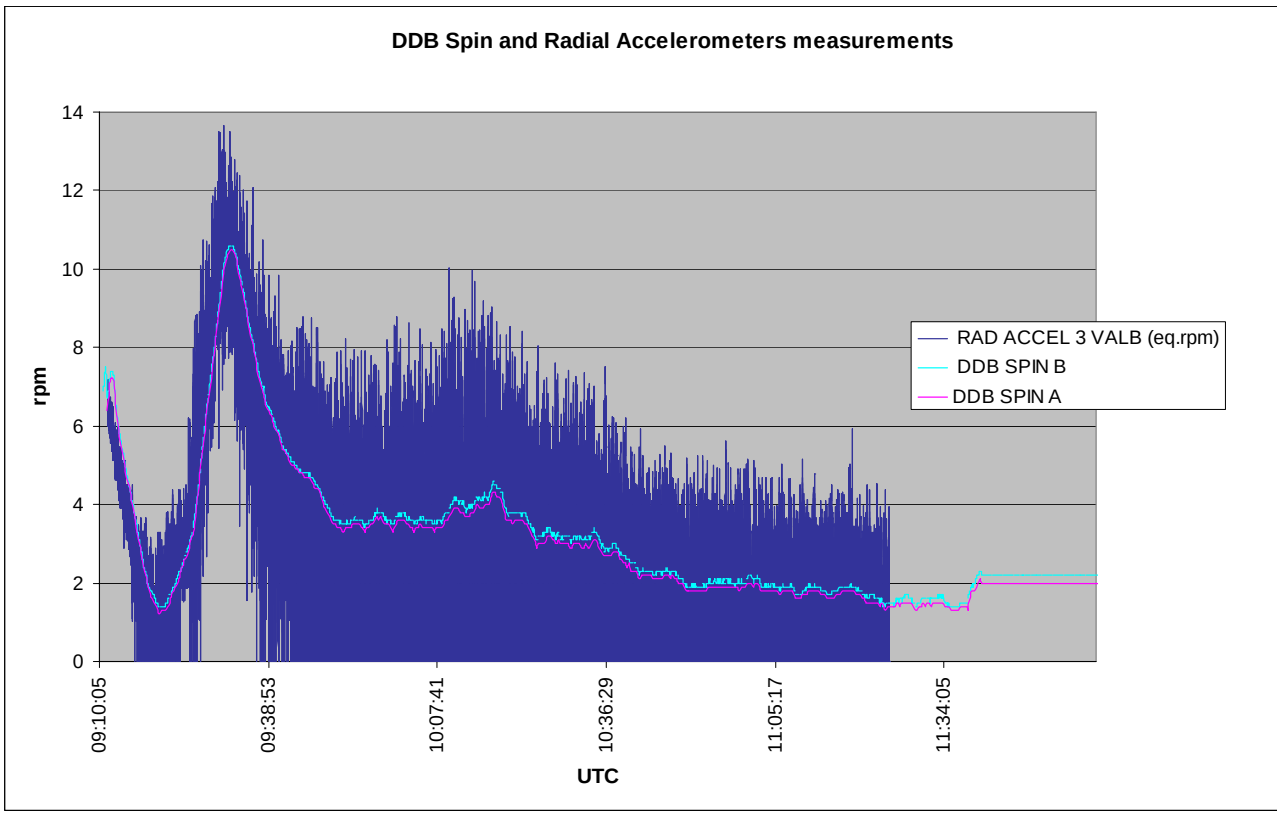

Figure 13a : radial acceleration and spin as measured in flight

Fig.13b gives another representation of the same parameter. The predicted altitude (TAT) is here plotted vs. the DDB Spin; the predicted alt=f(spin) profile is superimposed.

Fig.13 a and 13b show a discrepancy between the predicted and measured profiles; especially the fast decrease of the spin in the first 15mn was not expected. Expected spin profiles are also detailed in RD05, while this "spin anomaly" is detailed in RD01 and better evidenced in the next chapter,

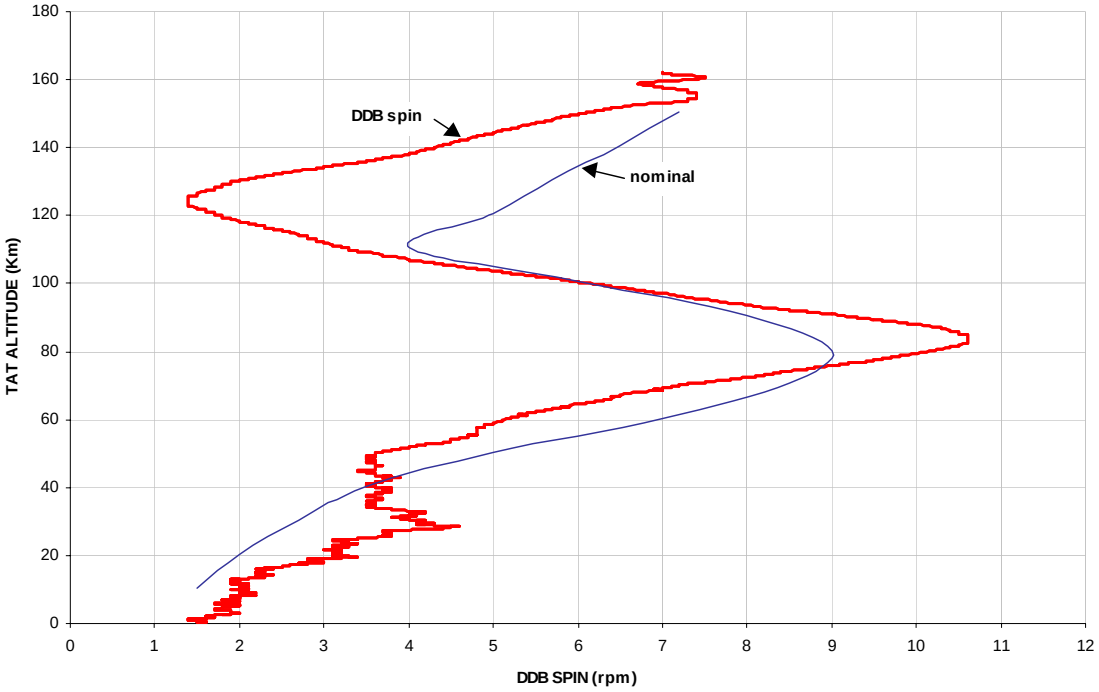

Figure 13b : TAT altitude =f(DDB spin) as measured in flight

9.2 SPIN POST FLIGHT RECONSTRUCTION

The analysis of the spin and radial deceleration measurement has led to 2 different issues :

1- A discrepancy has been found in the RASU accelerometers distance to CoG between the flight software data (coherent with the User Manual) and an evaluation performed in the frame of the document "Probe reference data for post flight analysis". This discrepancy and the related analysis are presented in Appendix 2. It appears that a distance error has marginally affected the spin calculation algorithm in flight. The spin measurement after correction of this error is shown in Fig. 14.

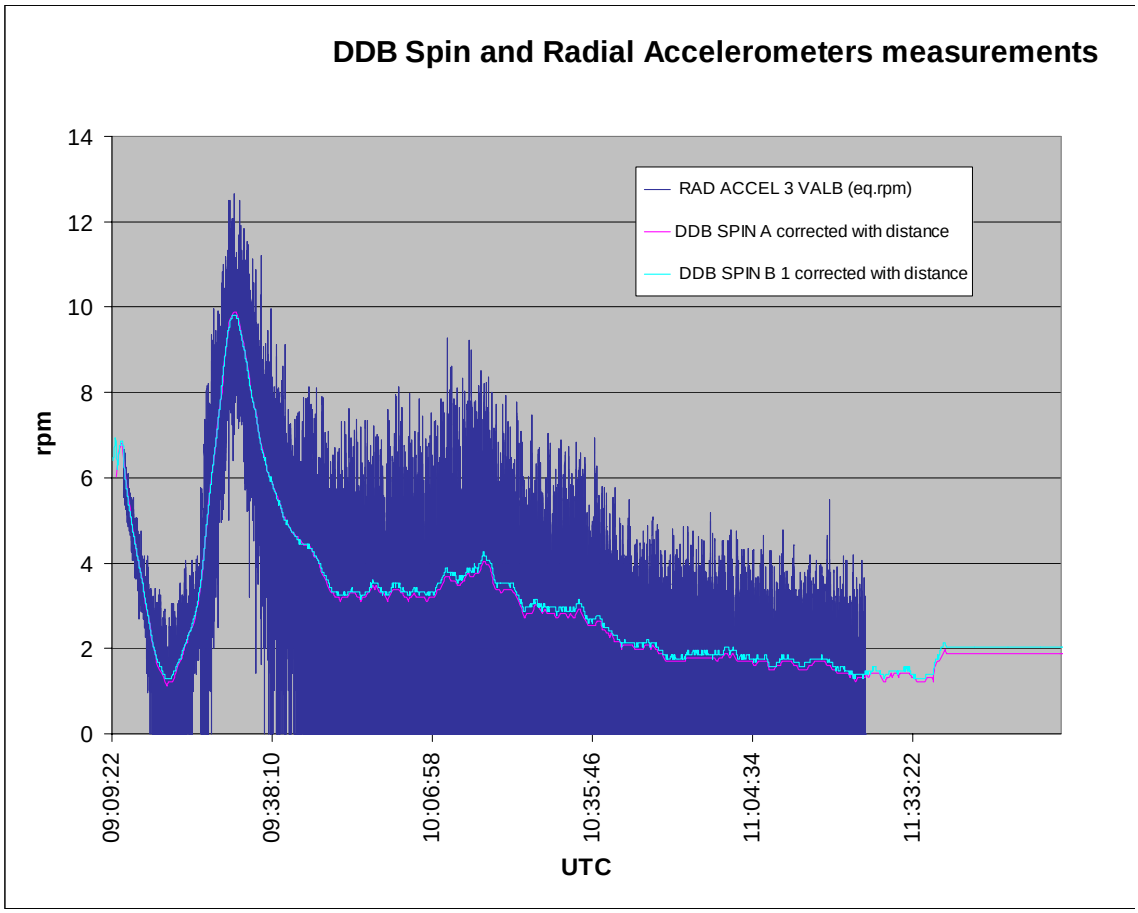

Figure 14 : radial acceleration and spin after correction

2- A more detailed analysis of the spin anomaly mentioned in previous chapter is first shown in Fig.15. The spin apparently starts to rise around UTC09:19, while this should have occurred at the stabilizer deployment time, at UTC09:25. The initial decrease of the spin is also much too fast and much too strong. At this last time, it can be verified that the spin rate increases faster, due to the increase of the descent velocity of the Probe, and that the Profile becomes more disturbed, in consistency with the start of the "rough ride" noticed on the CASU accelerometers profile, in yellow in Fig.15. The attitude of Huygens under the stabilizer is much less stable than under the main chute.

The figure 16 permits to better interpret the spin anomaly : negative radial acceleration values have been reconstructed based on the realistic assumption that the radial acceleration is comprised of an average component due to the spin modulated by higher frequency changes in the Probe attitude due to pendulum or wobble motions. Introducing these missing negative values, it becomes clear that the spin actually reaches zero around UTC09:19. No further conclusion related to the spin direction can be drawn from the radial acceleration parameter, and we will make use of a totally different parameter, the AGC value measured by the PSA receiver, to definitely state on the spin issue. This will be addressed in chapter xxx.

See also RD12 for a synthetic discussion on the Probe Spin.

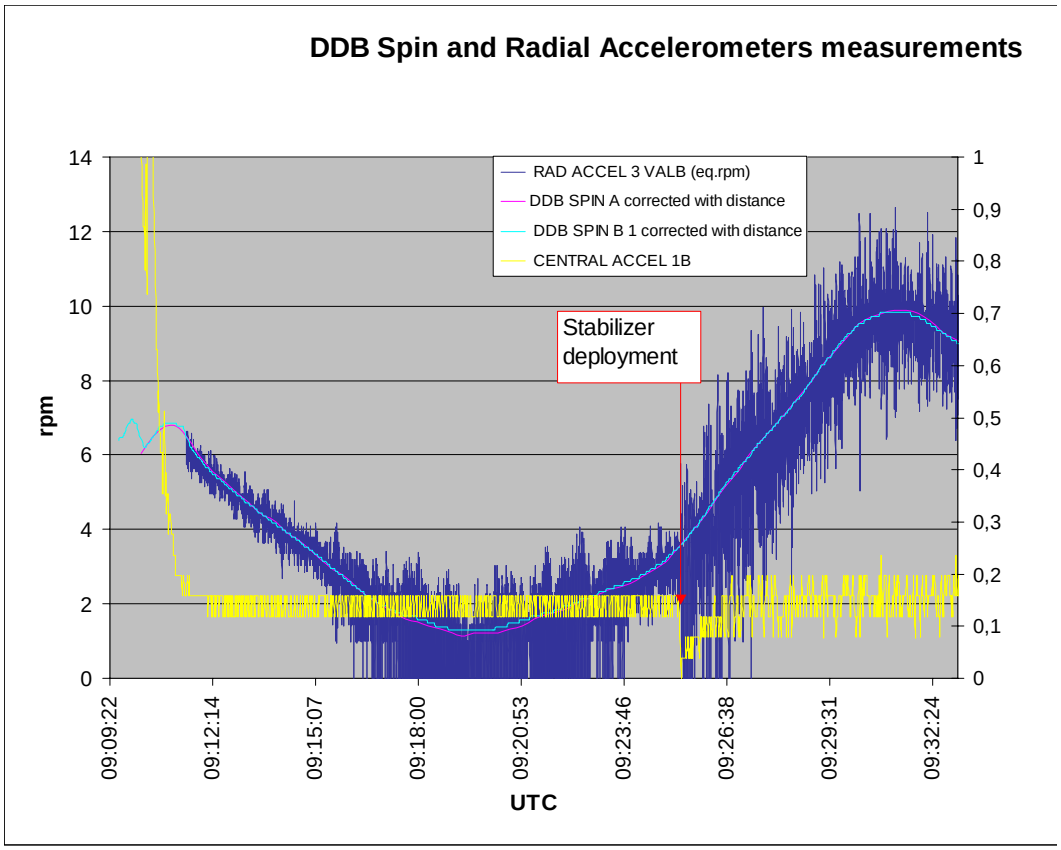

Figure 15 : Spin anomaly as seen by RASU

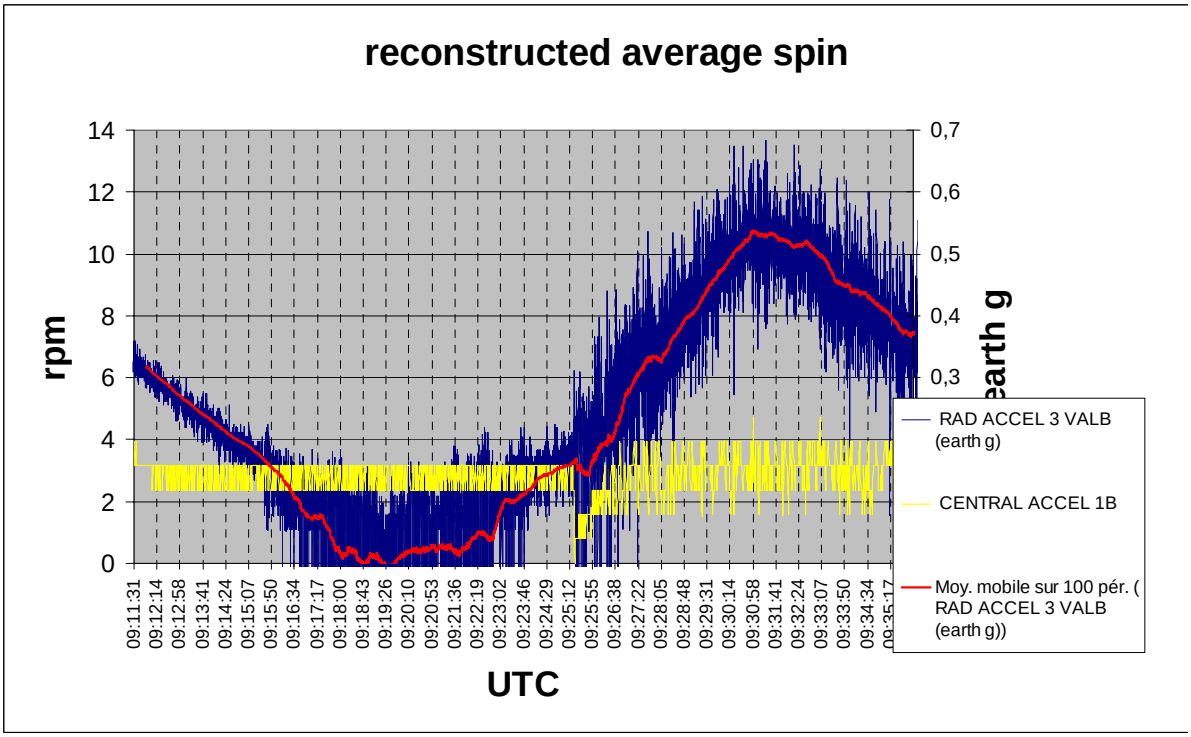

Figure 16 : Spin anomaly as reconstructed from RASU

9.3 PROBE ATTITUDE POST FLIGHT RECONSTRUCTION

To better quantify the motion of the Probe during the descent, the figures 17a to 17j present the frequency analysis in 2D of the radial acceleration (TM rate=4Hz), over 9 time slots. Considering the measured frequencies, they definitely cannot be linked to periodic changes in the spin, but rather to modulation imposed by periodic changes in the Probe attitude. In more details, it brings out from the plots that :

- the motion under the main chute is mainly composed of an oscillation frequency of about 0.8Hz, plus a 1st harmonic of that frequency at 1.6Hz. This 0.8Hz frequency can be associated to the natural pendulum frequency under the Main (see RD02),
- the motion under the stabilizer, during the "rough ride" part of the descent is primarily composed of an oscillation frequency of about 1Hz. This could be associated to the natural pendulum frequency under the stabilizer (see RD02),
- the motion under the stabilizer in the last part of the descent seems more complex and composed of 2 main components : one of ~1Hz, the other one changing from 0.7 to 0.5Hz

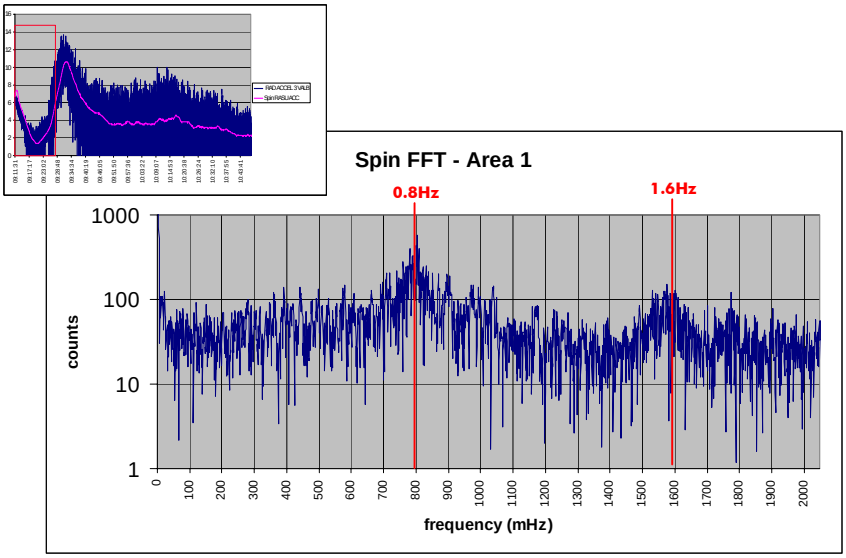

Figure 17a : frequency profile

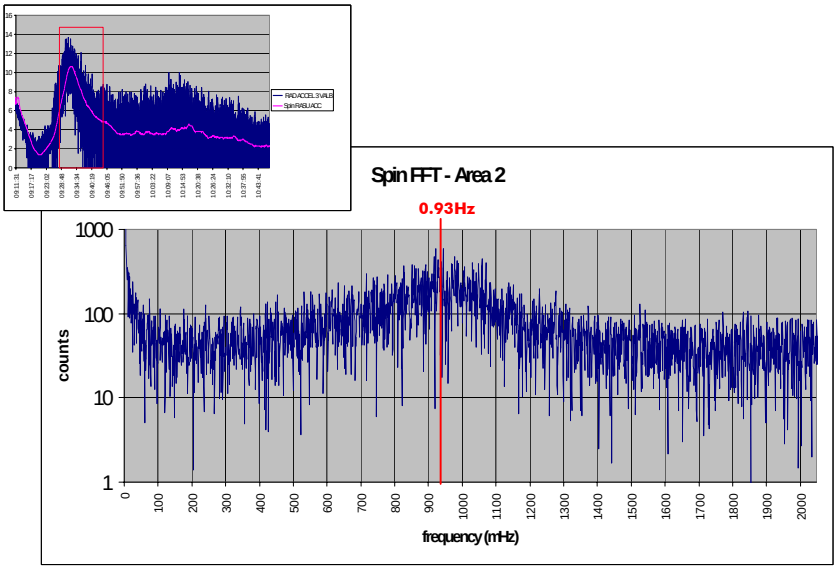

Figure 17b : frequency profile

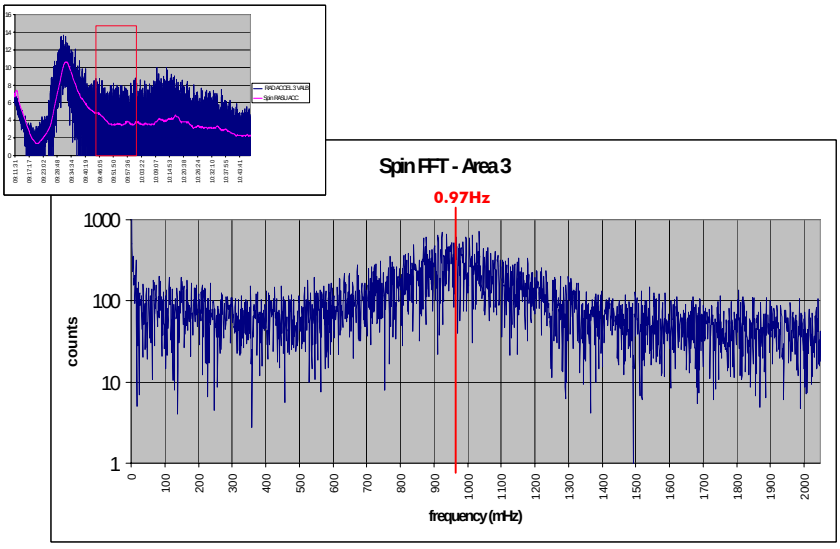

Figure 17c : frequency profile

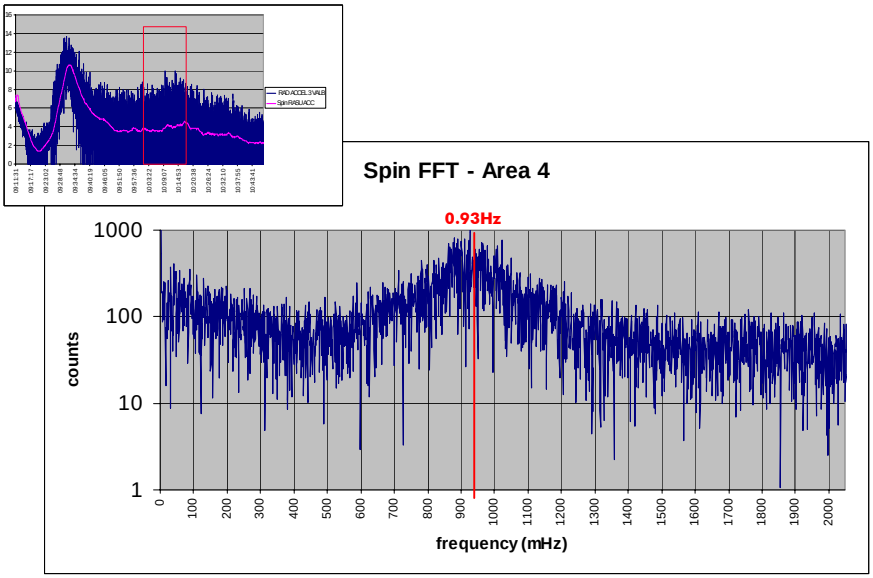

Figure 17d : frequency profile

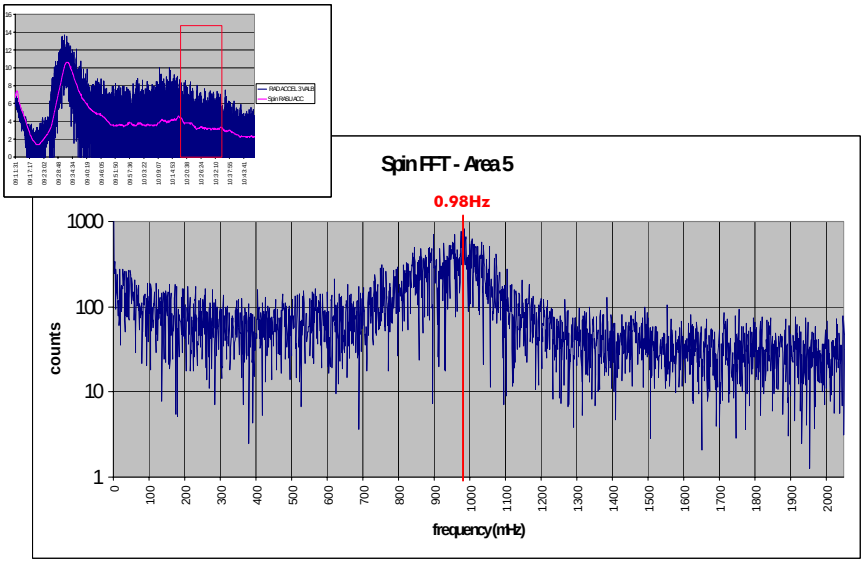

Figure 17e : frequency profile

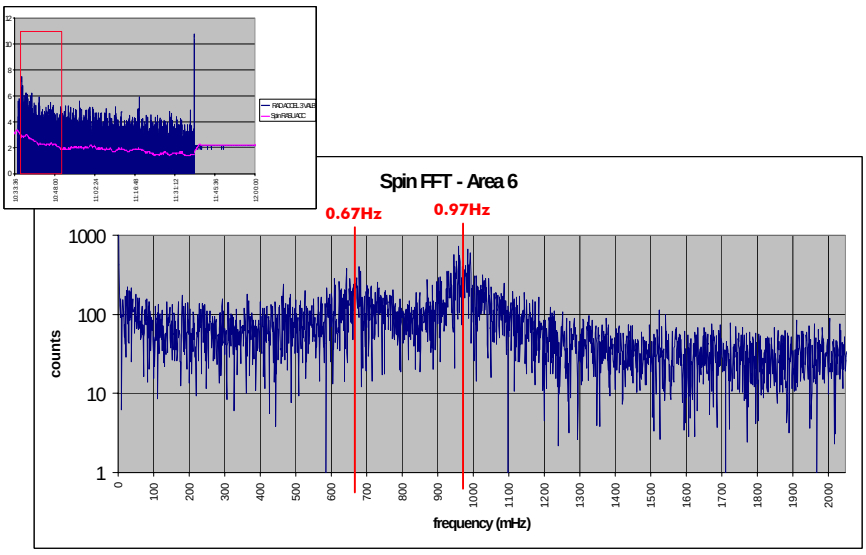

Figure 17f : frequency profile

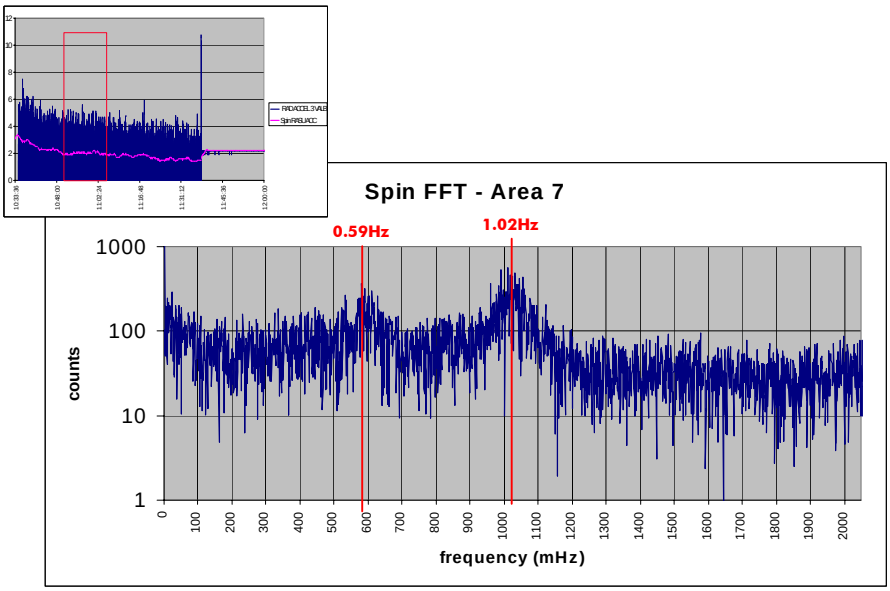

Figure 17g : frequency profile

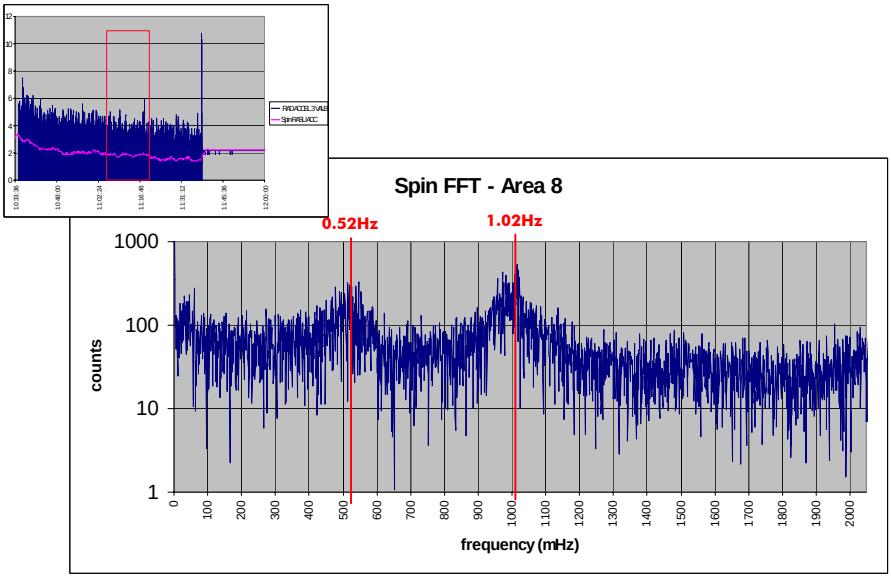

Figure 17h : frequency profile

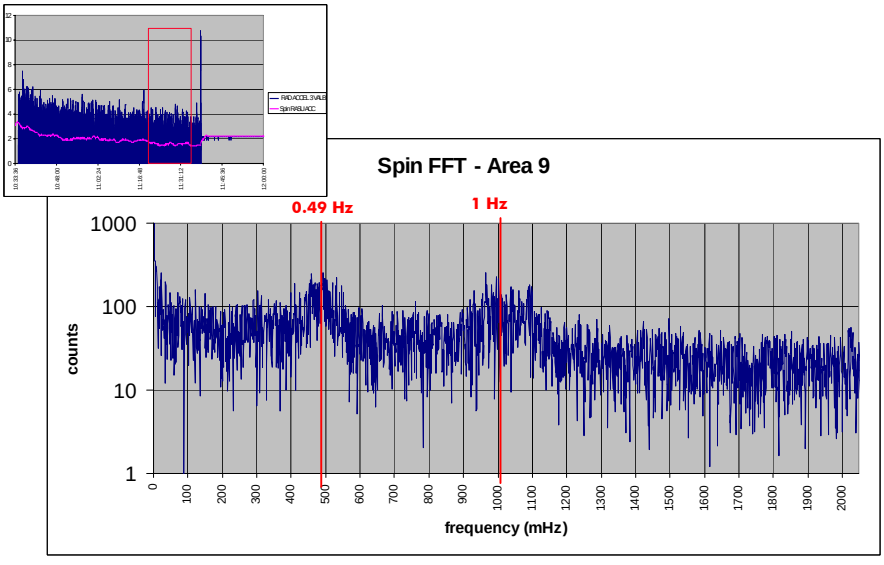

Figure 17i : frequency profile

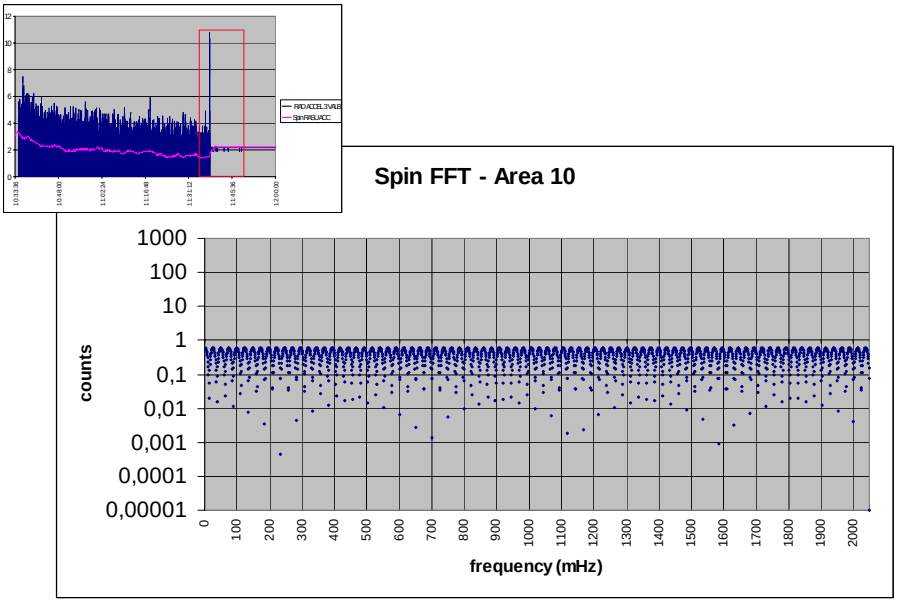

Figure 17j : frequency profile

9.4 INITIAL SPIN

The Figure 18 below is a zoom on the spin profile in the early part of the descent. As a matter of fact, the spin calculation algorithm, based on a heavy low pass filtering of the radial acceleration data applies a delay of some 68s wrt real time; it shall also be highlighted that the spin data is calculated and distributed in the DDB from the Probe turn ON time. Consequently, the first spin TM data is fully valid (no algo initialization effect), and refers to the spin as it was at the end of the Entry. Fig.18 shows, together with the spin, the entry profile measured by CASU. It appears that :

- the DDB spin at the end of the entry phase is below 7rpm, slightly less than the spin calculated after the Probe separation from CASSINI (see RD04). It is worth mentioning that, according to Fig.11, the accuracy of the spin measurement, including the calculation algorithm, is in the order of 2%. The value reported in TM and displayed here shall therefore be taken as a consolidated value,
- the DDB spin increases by 0.5rpm (7%) in 15s, then decreases by 0.8rpm (11.5%) in the next 18s until the PDD is fired and the pilot, then the Main is deployed. From that event, the spin increases again up to 6.8rpm in about 30s, then starts to decrease as better shown in Fig.14. about 1mn after T0.

Because of the amplitude of the DDB Spin change, together with the relatively high average spin value (and therefore good measurement accuracy), it is strongly believed that the feature evidenced in Fig.18 corresponds to real Probe spin changes. At that time no explanation to this behaviour is given.

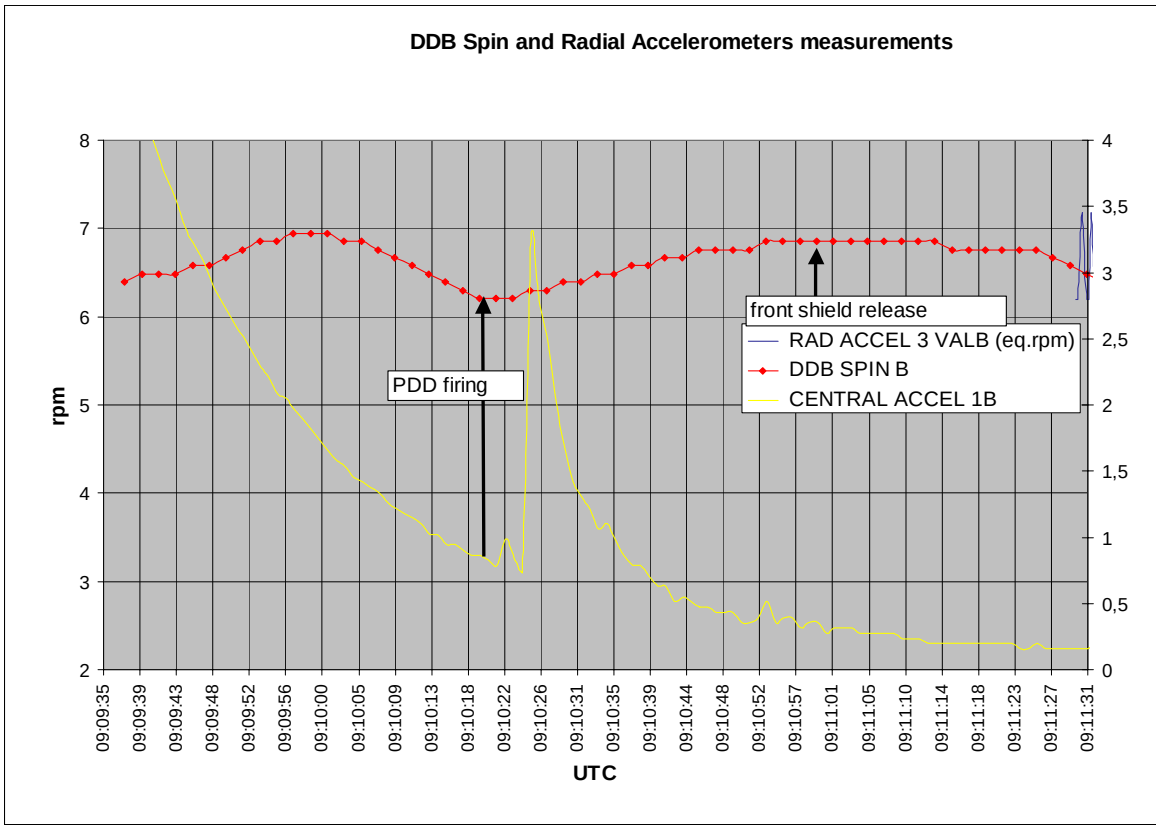

Figure 18 : spin and Entry deceleration profiles around T0

9.5 RADIAL ACCELERATION AT LANDING

Fig.19 shows the changes in the radial acceleration, sampled at 4Hz, at the instant of touch down together with the Central accelerometers impact profile, sampled at 1Hz. This demonstrates :

- a very good consistency between the 2 data sets : the impact is detected between UTC11:38:11,00 and UTC11:38:11,1
- a bouncing-like effect of the radial acceleration during about 7-8s after impact time. Considering the shape of the bouncing, the most probable explanation is that the Probe has oscillated for a few seconds before stabilizing. The minimum angle of inclination, ie. the angle reached in the RASU axis is constrained by Fig.20 values (only the positive angles can be derived) and attains 18°. After stabilization the Probe is inclined by 0.75° in RASU direction. See RD11 for further discussions on the Probe attitude on the surface.

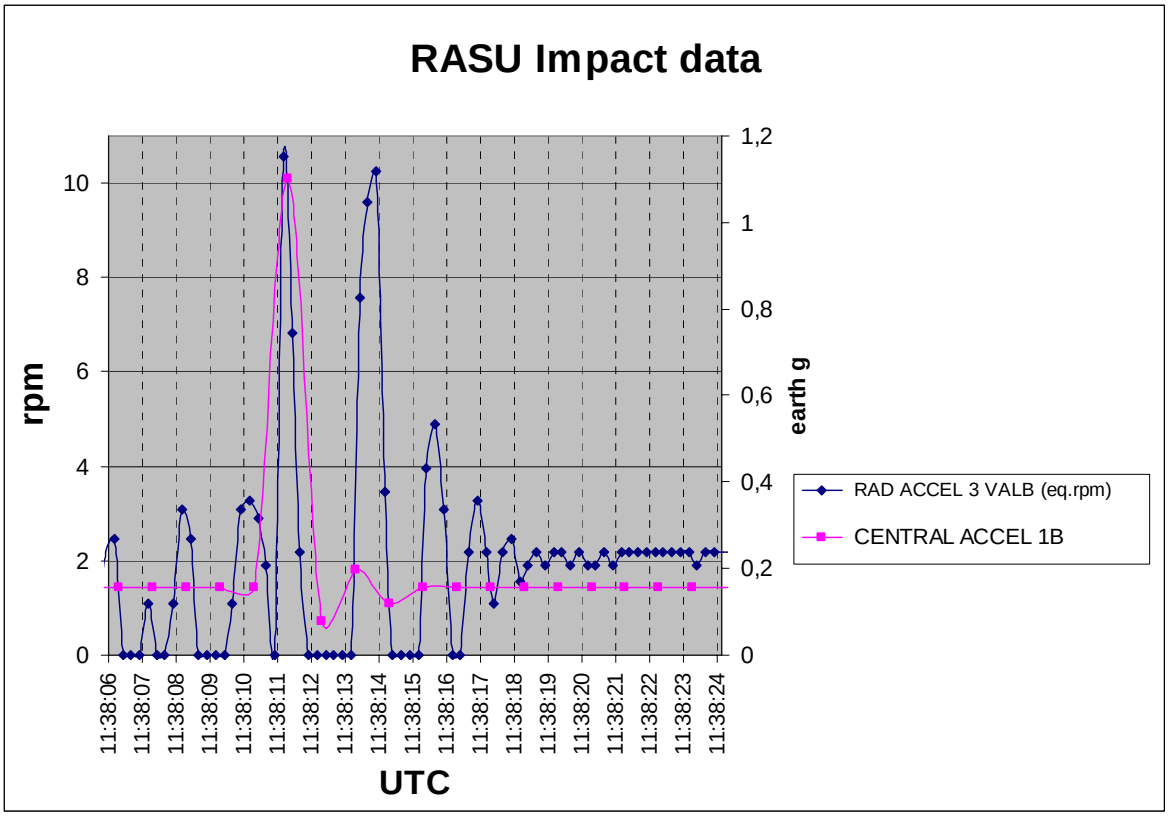

Figure 19 : spin and Entry deceleration profiles around T0

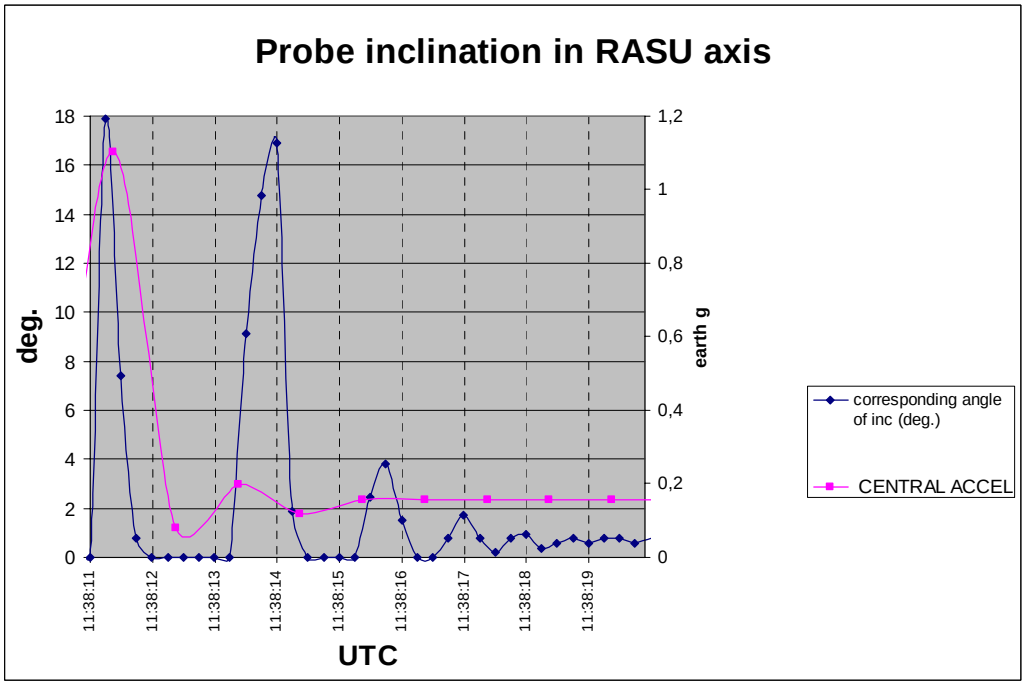

Figure 20 : Probe inclination on the surface in RASU axis

10. ALTITUDE MEASUREMENT

10.1 ALTITUDE IN FLIGHT MEASUREMENT

The Probe altitude is processed from the stored Time Altitude Table, then from the altitude provided by the 2 hot redundant Radar Altimeter Units (RAU's) after they have proved to be properly locked and in any case below the predicted altitude of 25km. The processed altitude is distributed to the experiments via the DDB Altitude every 2s. A description of the altitude determination algorithm can be found in RD05 and RD07. An overall description of the altimeters operation can be found in RD07

In addition to the altitude data, the RAU's also provide an AGC signal indicating the strength of the returned signal.

The 2 RAU altitudes are acquired by the 2 CDMU's which means that the available TM HK stream on the chain B includes the altitude information reported by the 2 RAU's.

The characteristic of the telemetry is :

RAU altitude

- telemetry rate 0.5Hz
- HK TM in HK3 TM packet,
- 1 LSB = 10m.
- worst case measurement accuracy : 5%.
- measurement range = 150m to 10km guaranteed, 150m to 60km as a goal.

RAU AGC

- telemetry rate 1Hz
- HK TM in HK1 TM packet,
- 1LSB = xxx
- worst case measurement accuracy : xxxxxx
- measurement range = 0 to 4V

In addition lock status of both RAU's are available.

The figure 21 presents the altitude data distributed to the instruments via the DDB B, in red, with the predicted altitude envelope in blue and green. It shows that :

- when the altimeters have locked consistently, the descent profile has joined the theoretical max profile,
- an anomaly has occurred around UTC10:25 and has disappeared around UTC10:45. During that period, the DDB altitude was about half of the estimated real altitude.

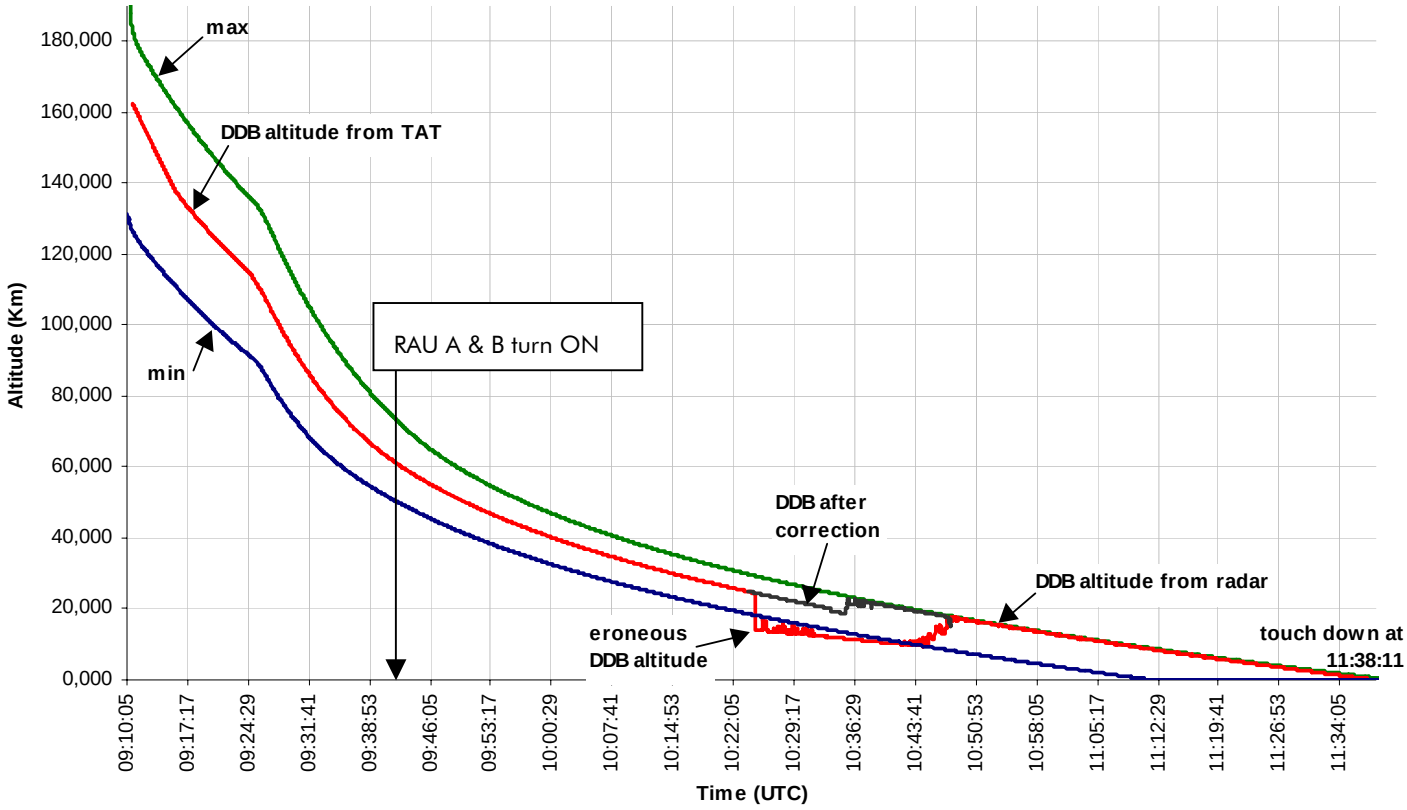

Figure 21 : DDB Altitude in Flight

Figure 22 provides details on the noticed anomaly, and insight to the altitude calculation algorithm performance. It appears that :

- RAU A first lock has occurred at the altitude of ~36km; RAU B first lock has occurred at the altitude of ~45km, thus much higher than the minimum guaranteed altitude of operation.
- the altitudes reported by the 2 altimeters (RAU raw) are inconsistent compared to the prediction until an altitude of 17km on RAU A and 22km on RAU B. From 35km, RAU B displays an altitude which is about half of the real altitude. From about 24km, RAU A locks to an altitude which is about half of the real altitude.
- Shortly after 25km, when the RAU's data are considered by the altitude determination algorithm, both RAU's are consistently locked, but to an altitude which is about half the real one. As a consequence, this false altitude is validated by the algorithm and reflected in the DDB altitude (in yellow).
- At the predicted altitude of 20km, RAU B locks to a valid altitude. Then, at the predicted altitude of 15km, RAU A locks to a valid altitude implying that the DDB altitude locks to a valid altitude also, consistent with the "max" descent profile.
- From the time the RAU's lock to a correct altitude, the lock is not lost and the altitude measurement remains very consistent. As shown in Fig. 23, both altimeters lose the lock at 140m, fully in line with the min range of operation.

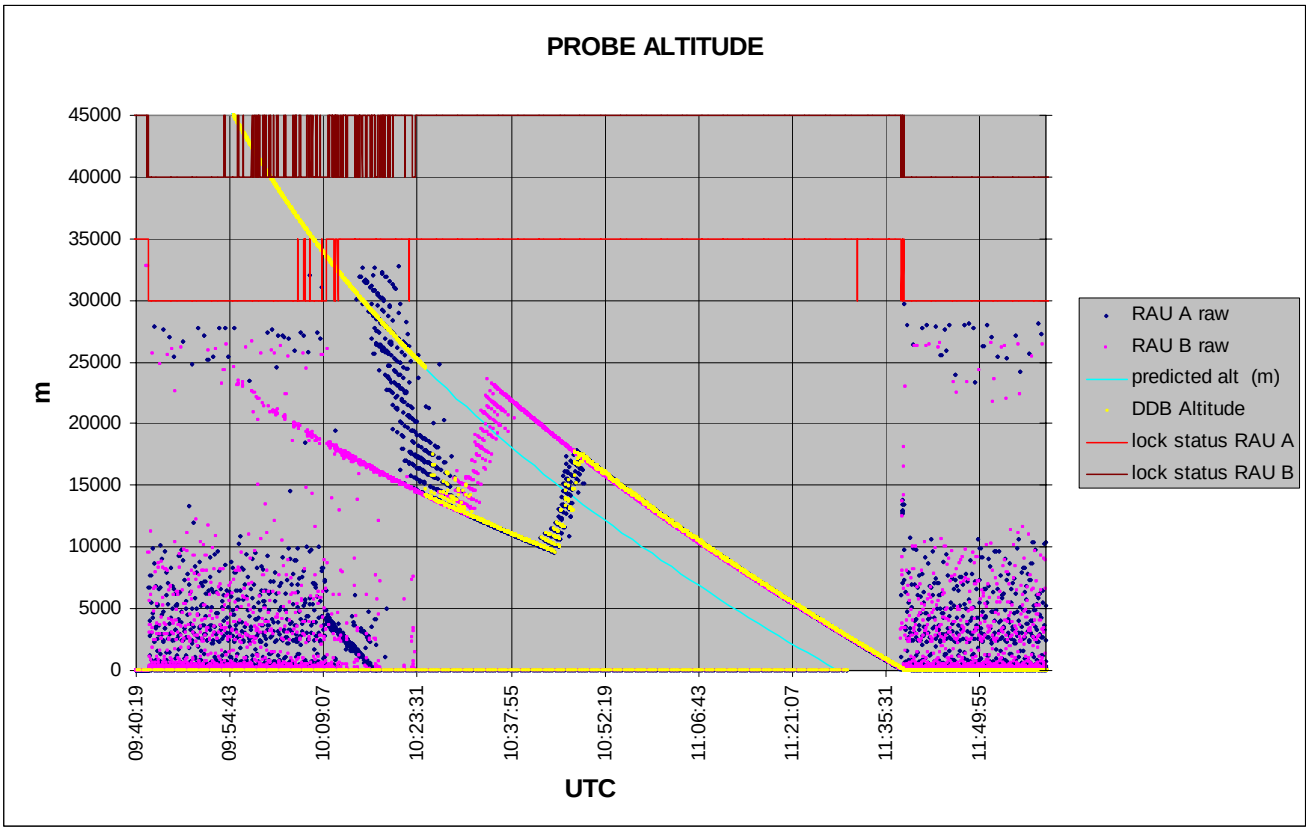

Figure 22 : RAU's anomaly

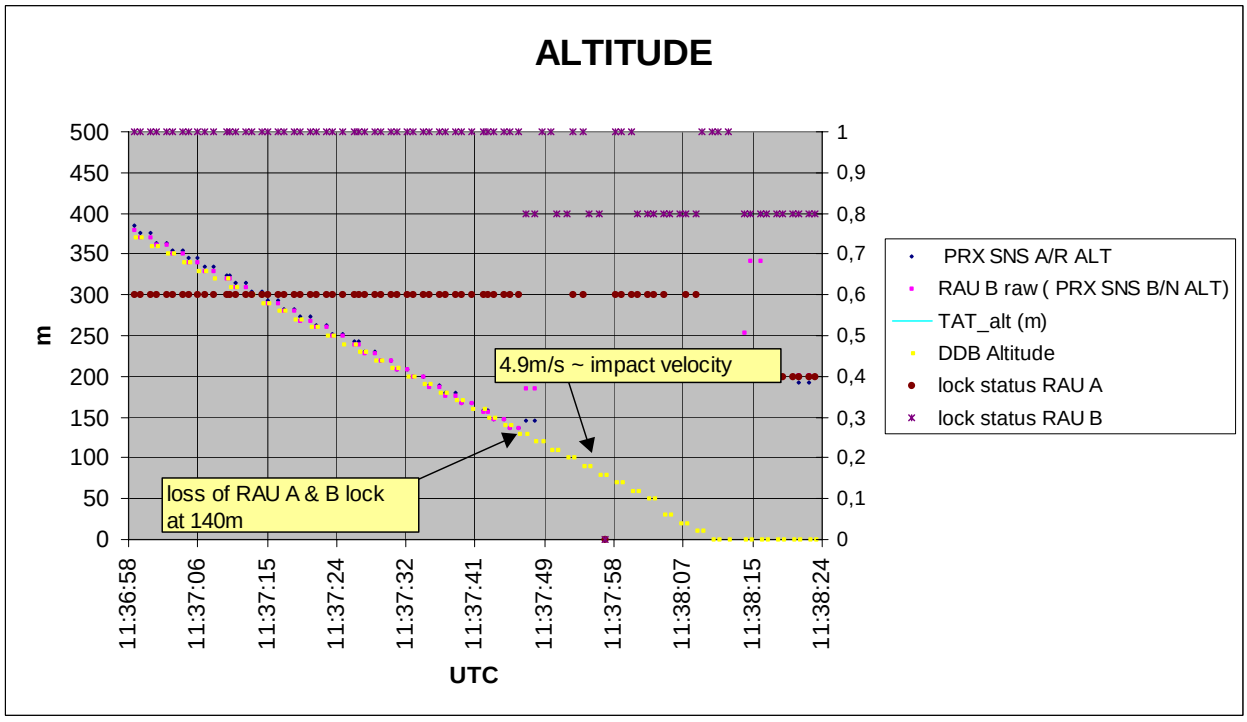

Figure 23 : Altitude in the last part of the descent

As a synthesis, both altimeters, although in lock from a RF point of view, have had a similar and faulty behavior until the real altitude of about 17km (22km for RAU B). This flaw, located in the digital part of the altimeters, has led to the report of totally invalid altitudes of half of the real altitudes. Because the algorithm was not designed to cope with consistent simultaneous failures of the 2 altimeters, the erroneous altitudes have been reflected in the DDB. Fortunately, from about 17km, the 2 altimeters have returned to an healthy operation and the DDB has reported the real altitude. As a consequence, the DDB altitude data has switched from ~10km back to ~17km.

This faulty behavior of the 2 altimeters could not be seen during the nominal development and test plan of the Proximity Sensor because no test in realistic conditions at altitude higher than some 3000m was ever planned nor performed. It was however already noticed in the frame of a balloon test flight performed in December 2004 (few weeks before the real mission), and essentially attributed to a non representative configuration of the test (see test results analysis in RD12). From that information it becomes obvious that the faulty operation is due to a design flaw, common to all altimeter units, not a failure of the flight units.

10.2 VELOCITY AT IMPACT

From Fig.23, one can draw an estimate of the Probe velocity at impact. This gives 4.9m/s.

It is pointed out that the lock of the altimeters being lost at 140m, this figure assumes that the descent velocity has remained constant in the last 140m, ie. the last 30s of the descent.

10.3 GROUND PROFILE

As explained in the previous chapters, the 2 altimeters have properly measured almost simultaneously, every 2s, the altitude of the Probe above the surface. Considering that because of some wind the Probe had a lateral velocity, it could in theory be possible to extract the profile of the terrain flown over by Huygens. The accuracy of the reconstruction is strongly dependent upon the absolute accuracy of the altitude measurement; the reconstruction is therefore likely to be more accurate at low altitude. Practically, the reconstruction is achieved by subtracting the instantaneous altitude to a fitted altitude representing the "level 0" of the flown-over ground.

The Figure 24 presents the profiles obtained from the 2 RAU's expressed as a function of the mission time in UTC, for the last 45mn of the descent, ie from the time the 2 RAU's lock to the correct altitude at ~17km (the peak at the end of the descent is not representative; it corresponds to the loss of lock of the RAU's at 140m). Assuming a lateral descent velocity of 2m/s, one obtains Figure 25. Figure 26 is a zoom in the last 11mn of the descent.

One can draw two conclusions :

- the profiles derived from the 2 RAU's show some consistency : the ground 5km from landing is relatively smooth with max "relief" amplitude of 22m. The steepest slopes are in the order of 7%,
- the profiles calculated in the last 11mn of the descent (or ~600m from landing point) are remarkably consistent between the 2 altimeters. At this time, in the direction of the descent, Huygens has flown over a slightly descending, constant slope of ~ –2.2%

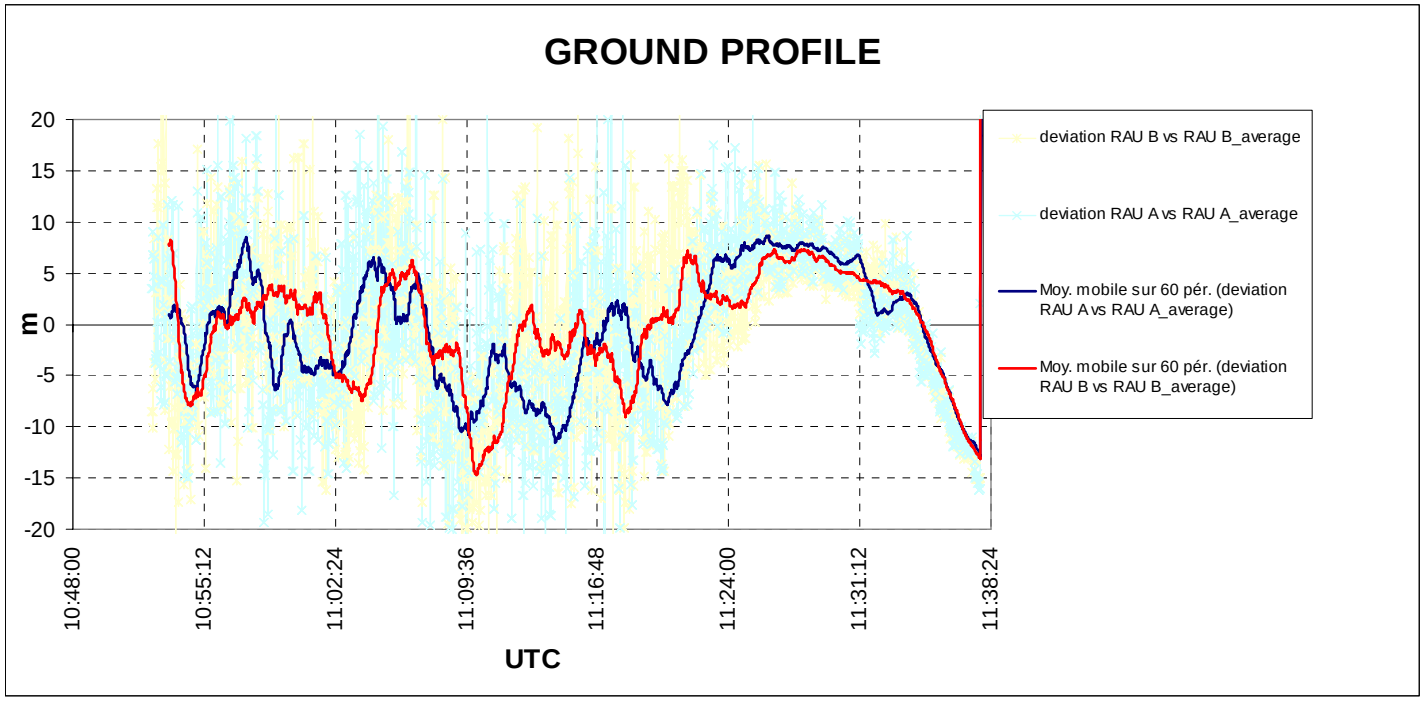

Figure 24 : Ground profile in the last 45mn of descent as derived from RAU's

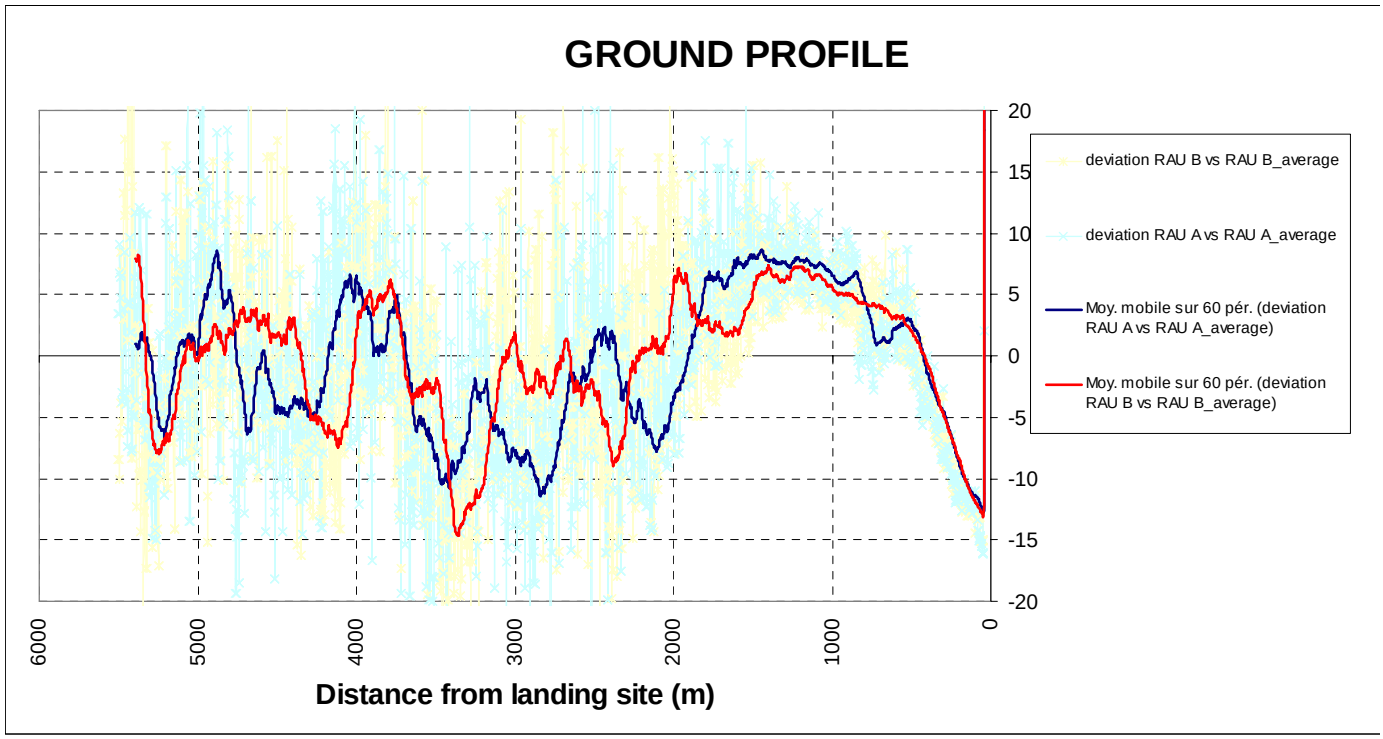

Figure 25 : Ground profile as derived from RAU's assuming a 2m/s lateral velocity

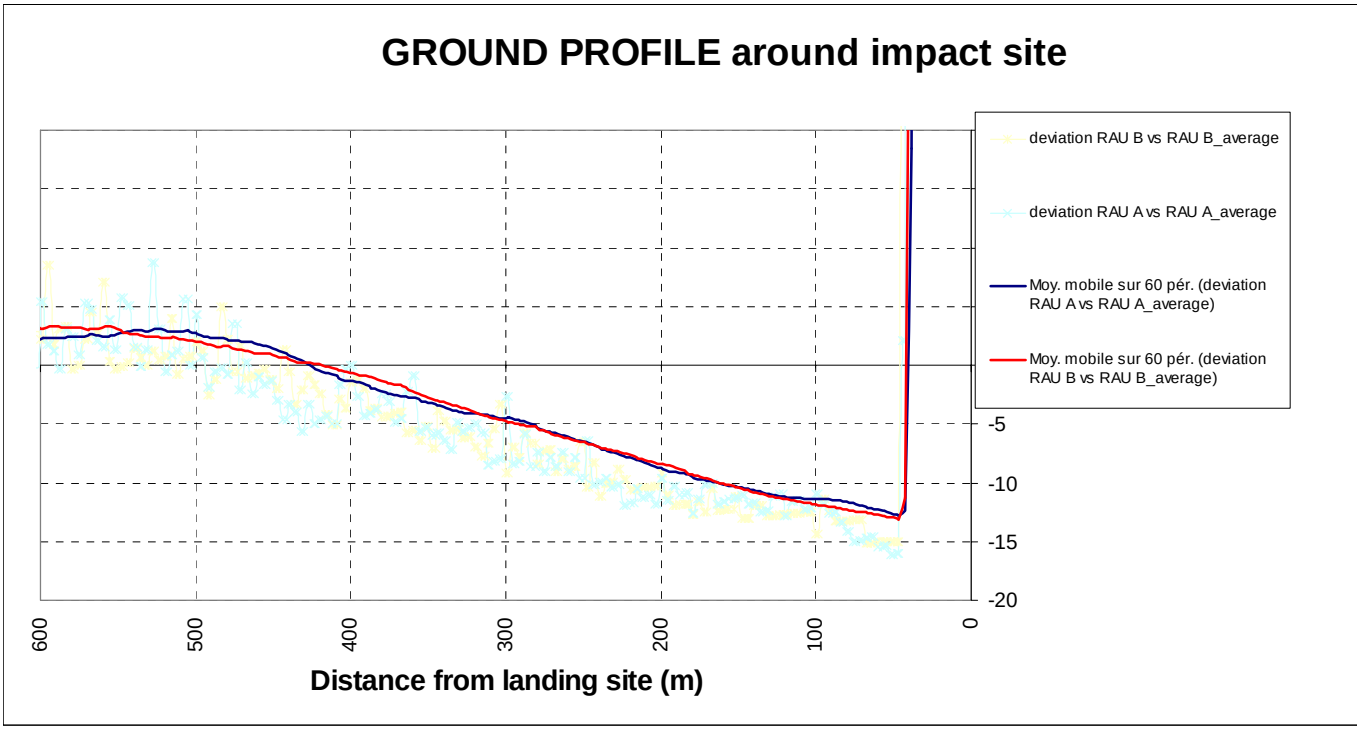

Figure 26 : Ground profile as derived from RAU's assuming a 2m/s lateral velocity - zoom

10.4 AUTOMATIC GAIN CONTROL

This parameters reports the RAU control loop gain. The raw values are shown in Fig.27 with the altitude measurement. After application of the relevant transfer function, this AGC value is turned in Fig.28 into gain of the intermediate frequency amplifier. This plots evidences two phenomena :

- 2 regions are identified, the region 1 where the IF amplifier gain is higher and decreases rapidly, corresponding to a surface with low reflectivity, and the region 2 where the IF gain is pretty constant (after compensation of the altitude effect) and low, corresponding to a surface with higher reflectivity,
- the separation between these 2 regions is relatively sharp indicating a transition between 2 surfaces of different nature. It is seen at ~UTC10:42 when the Probe is at an altitude of about 23km. It is remarkable to notice that the lock of RAU B to the right altitude occurs at the same instant, possibly giving some clue to the faulty behavior of the altimeters discussed in the previous sections.

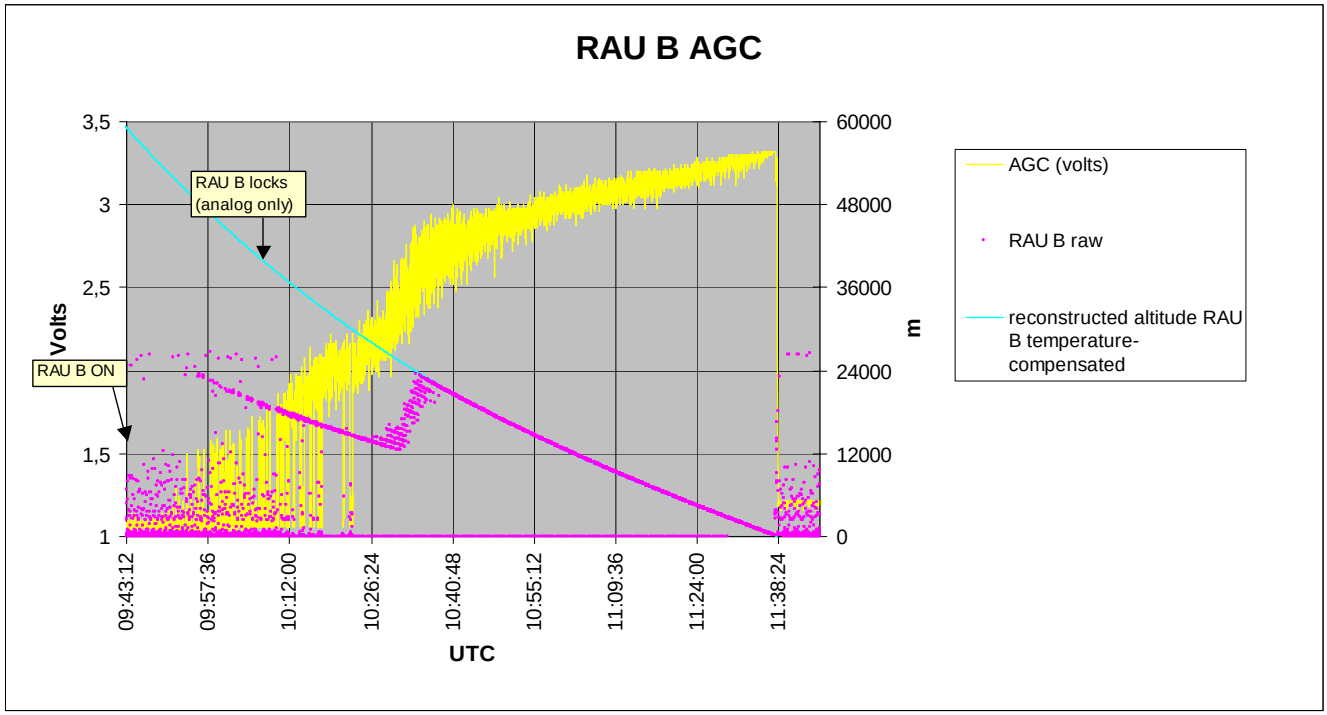

Figure 27 : RAU B AGC variations during descent

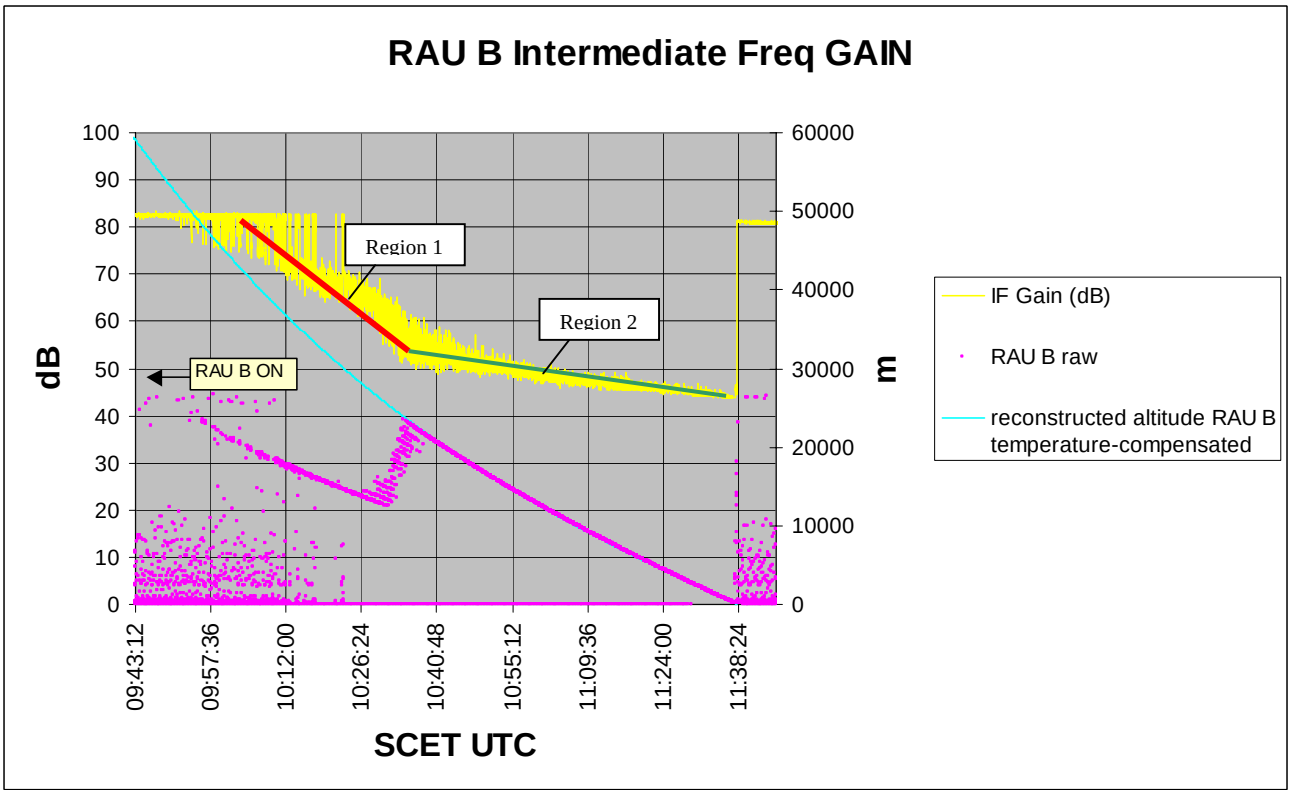

Figure 28 : RAU B IF gain variations during descent

11. COMMAND AND DATA MANAGEMENT UNIT

We will review here the values of the few parameters dealing with the behavior of the CDMU in flight. For already explained reasons only the TM related to CDMU B is available.

11.1 HARDWARE STATUS

At start-up the POSW has performed hardware checks and has reported its initialization status. As shown in the table below, no anomaly is seen on chain B : both the CDMU B hardware and POSW software are healthy at Probe turn ON. In addition, there has been no single bit error over the whole mission.

There is no data from chain A. However all the experiments have reported chain A as valid which means that all checks performed at start-up on CDMU A were OK and that no failure has been detected later on by the software running of CDMU A.

UTC	TM code	TM name	TM value	Comment
09:11:22	S2010H	CDMU INIT STAT B	HEALTHY	
09:11:23	S2007H	OVERRUN CNT B	0000	
09:11:23	S2006H	EXCEPTION CNT B	0000	
09:11:23	S2001H	RAM SNG ERR B	0000	
09:11:23	S2008H	RAM DBL ERR B	0000	
09:11:23	S2002H	INVALID TC CNT B	0001	Default value. No Inhibition TC
09:11:23	S2003H	VALID TC CNT B	0002	Predefined ACP TCs in MTT have been sent
09:11:24	S2016W	CPU B FAULT REG	HEALTHY	
09:11:24	S2004H	FXD POINT OVFL B	0000	
09:11:24	S2005H	FLT POINT OVFL B	0000	
09:11:24	S2017W	RAM FIRST FAIL B	#FFFF#16	No failure
09:11:24	S2018W	POSW B PROM CHK	0000	
09:11:24	S2020W	POSW B INIT TIME	1.89 s	Criterion : < 6.5 s
09:11:25	S2023W	POSW B HLT MSW	HEALTHY	
09:11:25	S2022W	POSW B HLT LSW	HEALTHY	
09:11:25	S20134	CDMU CHAIN B	CHAIN_B	
09:11:25	S20135	PROC VAL PORT B	VALID	
09:11:25	S2019W	POSW B HIGH WTR	7425 (10%)	Criterion : < 80%

11.2 REFERENCE VOLTAGES

The Figure 29 presents the measurement of the CDMU B reference voltages used as calibration for the analogue acquisition chain. These voltages have stayed in accordance with the expectation within 0 LSB. The CDMU B analog measurement chain has therefore perfectly functioned during the whole mission, which validates the quality of all the analogue acquisitions performed (acceleration data, current telemetry, …).

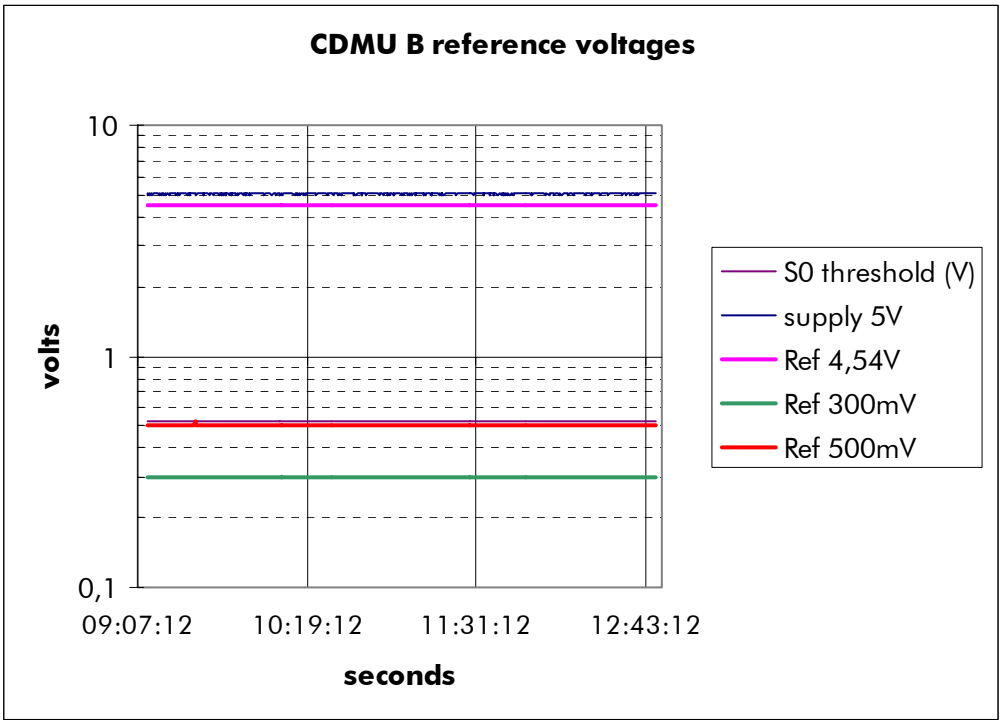

Figure 29 : CDMU reference voltages

11.3 ON BOARD CLOCK STABILITY

This point has been an important issue in the last years prior the mission since the drift of the CDMU TM oscillator is a contributor to the total frequency drift of the received data stream, and therefore impacts the receiver bit synchronizer performance found faulty during a flight test in 2000. This is widely documented in RD13, and an outcome of the recovery task force has been to force an increase of the CDMU internal, therefore the quartz oscillator temperature and thus reduce as much as possible its additional drift, by performing an early turn ON of the Probe . This feature, known as “pre-heating” has been the driver to wake up the Probe 4h38mn before planned Entry.

The present chapter is a post flight assessment of the efficiency of the pre heating. As documented in RD13, two TM parameters are used to reconstruct the CDMU clock drift, the CDMU DC/DC converter temperature and the PSA receiver Frame Data Interrupt (FDI) Start signal. Fig.30 below displays these parameters over the mission time.

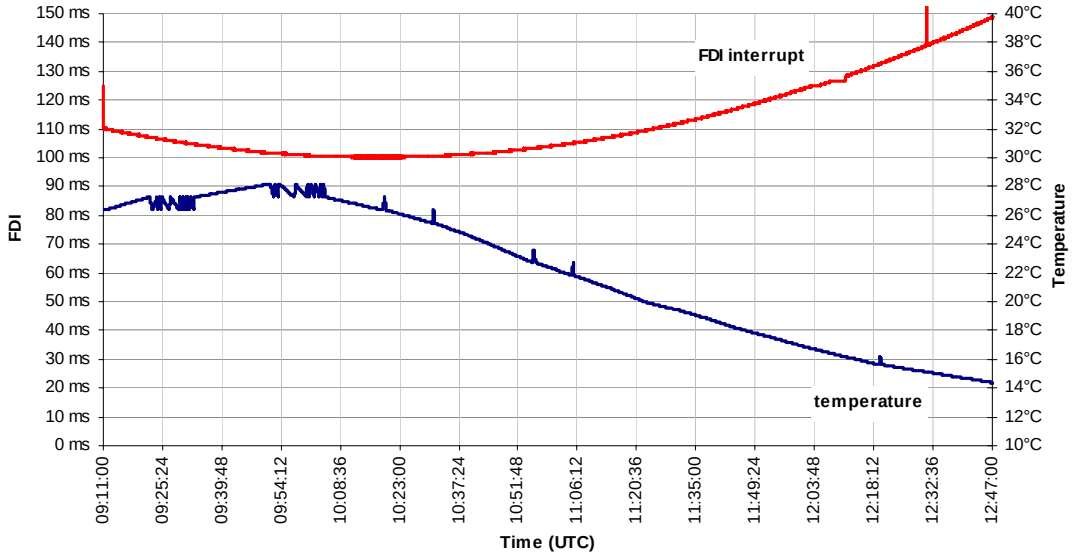

Figure 30 : CDMU B DC/DC Conv temperature and Chain B FDI Start

The data stream frequency drift is actually the sum of all the frequency drift contributors, Huygens-Cassini Doppler effect, CDMU Oscillator drift and Cassini RTI drift (offset for the Huygens mission duration), which can be expressed by :

$\Delta f_{data} \approx \Delta f_{doppler} + \Delta f_{T°drift} + Offset_{Huygens/Cassini}$

From the FDI TM one can obtain directly $\Delta f_{doppler} + \Delta f_{T°drift}$ represented in Fig.31.

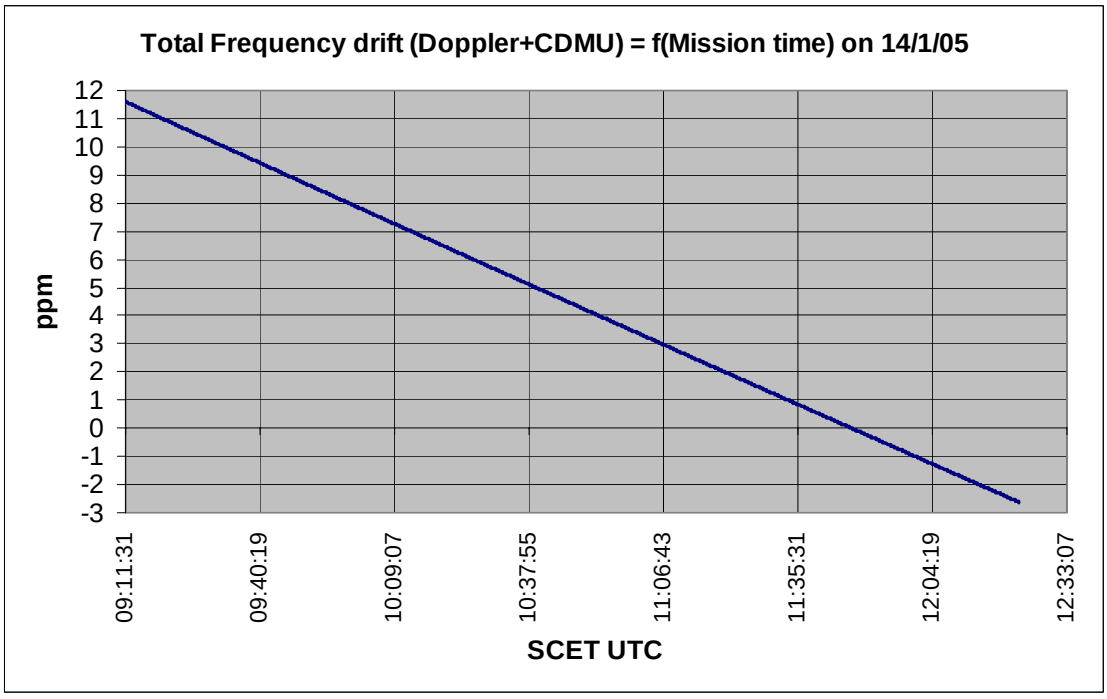

Figure 31 : CDMU B DC/DC Conv temperature and Chain B FDI Start

After removing the Doppler effect (output of mission analysis), one deduces in Fig.32 the contribution of the CDMU clock drift as a function of the descent time counted from the establishment of the RF link.

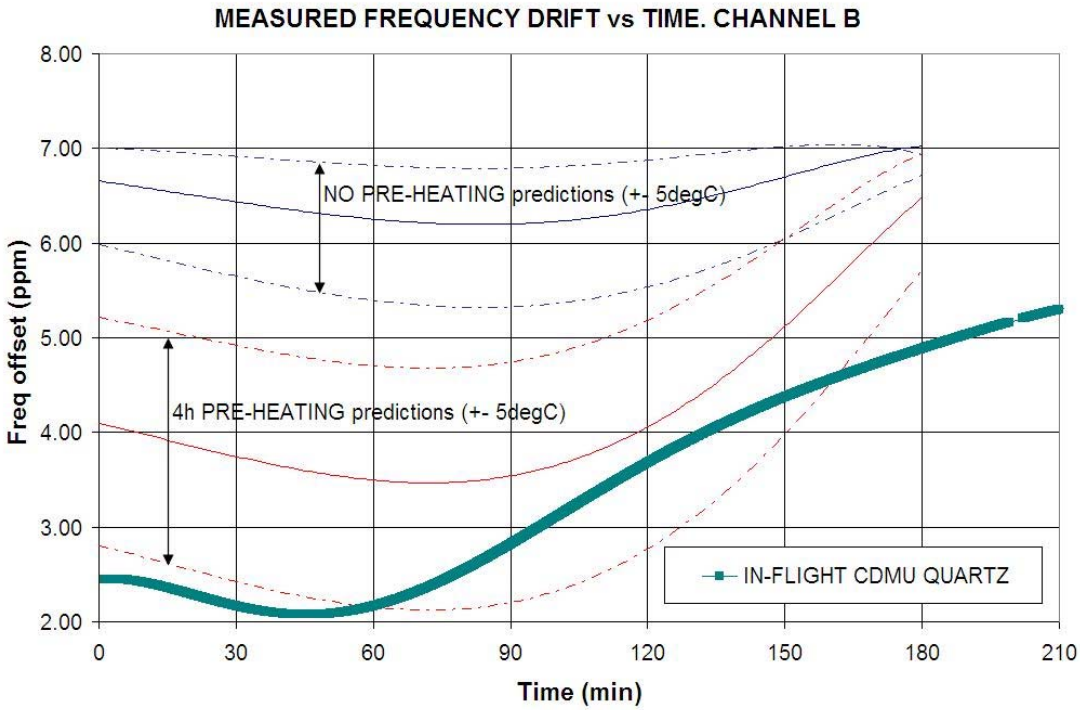

Figure 32 : CDMU B Clock drift compared to prediction

Fig.32 shows that the effect of the pre heating has been overall more efficient than predicted : the frequency offset due to the CDMU TM oscillator drift is strongly reduced especially in the first hour of the mission when the loss of bit sync is critical (see RD13). This is due to a very favourable CDMU temperature during the descent (see discussion on the thermal behaviour of the Probe in RD03), and has provided ample margins to the PSA receiver bit synchronization mechanism.

12. PROBE ON BOARD SOFTWARE

Some telemetry parameters, directly linked to the POSW operation, have already been reviewed in §xxxx (CDMU H/W Status.). Some other parameters provide some clue in the performance of the Mission Timeline function as well as the POSW workload.

12.1 MISSION TIMELINE

The Figure 33 reports the total number of telecommands issued by the Probe On Board Software running in the CDMU B during the whole mission, pre and post T0. The total number (47) is in full accordance with the Mission Timeline Table, with the "pre heating" changes demonstrating that the CDMU B has executed nominally this timeline.

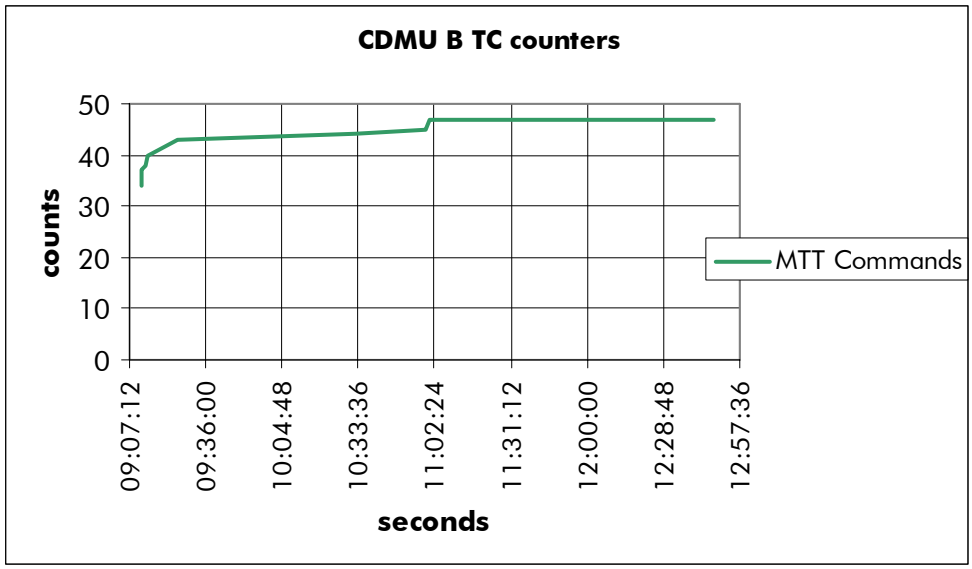

Figure 33 : Commands issued by CDMU B

A TM/TC cross check is performed in Table below : the main status are dated in UTC. It shows a correct execution of all the timeline commands. The delay between the command and the observation of its effect is also in line with the telemetry sampling rate, once the link is established.

CMD Time	CMD Name	TM Time	Delta	TM Name	Value
04:41:35	TUSO R power ON	09:11:22		TUSO R LIMIT ST	ON
04:41:35	TX B power ON	09:11:24		TX B LIMIT ST	ON
04:41:49	GCMS 1 R power ON	09:11:22		GCMS 1 R LIMIT	ON
		09:11:00		GCMS B MODE	RUN_POST_T0
		09:11:00		GCMS B PROC VAL	CDMU_A_ACT
04:59:19	HASI 1 R power ON	09:11:23		HASI 1 R LIMIT	ON
		09:10:48		HASI B MODES	TITAN
		09:10:48		HASI B CDMU ACT	CDMU_A_ACT

09:10:15	**To detection**				
09:10:52	ACP1 R power ON	09:11:22		ACP 1 R LIMIT	ON
		09:11:18		ACP B OP MODE	DESCENT
		09:11:02		ACP B CDMU ACT	CDMU_A_ACT
09:10:54	ACP 2 R power ON	09:11:23		ACP 2 R LIMIT	ON
09:11:01	ACP 3 R power ON	09:11:22		ACP 3 R LIMIT	ON
09:11:07	Pyro 2 GCMS IN set	09:11:22		GCMS IN SRS B	SQUIB SEL
09:11:07	**HPA power ON**				
09:11:11	HASI 2 R power ON	09:11:24	00:00:13	HASI 2 R LIMIT	ON
09:11:11	SSP R power ON	09:11:23	00:00:12	SSP R LIMIT ST	ON
		09:11:20		SSP B PROC VAL	CDMU_A_ACT
09:11:15	Pyro 2 GCMS IN reset	09:11:38	00:00:23	GCMS IN SRS B	SQUIB NO SEL
09:11:15	Pyro 2 GCMS OUT set	09:11:22	00:00:07	GCMS OUT SRS B	SQUIB SEL
		09:11:22		DISR 1 R LIMIT	OFF
		09:11:22		GCMS 2 R LIMIT	OFF
09:11:23	Pyro 2 GCMS OUT reset	09:11:54	00:00:31	GCMS OUT SRS B	SQUIB NO SEL
09:11:24	Pyro 2 DISR cover set	09:11:24	00:00:00	DISR CO SEL B ST	SQUIB SEL
		09:11:24		CMD COUNTER B	34
09:11:28	Pyro 1 and 2 fire A	09:11:40	00:00:12	CMD COUNTER B	35
09:11:41	Pyro 2 DISR cover reset	09:11:41	00:00:00	DISR CO SEL B ST	SQUIB NO SEL
09:11:41	DISR 1 R power ON	09:11:54	00:00:13	DISR 1 R LIMIT	ON
		09:11:50		DISR B MODE	INIT
		09:12:54		DISR B MODE	DESCENT
		09:11:56		CMD COUNTER B	37
09:13:21	GCMS 1 R redundant ON	09:13:32	00:00:11	CMD COUNTER B	38
09:13:42	HASI 2 R power OFF	09:13:48	00:00:06	HASI 2 R LIMIT	OFF
09:13:51	ACP 1 R power red. ON				
09:14:01	ACP 3 R power red. ON	09:14:04	00:00:03	CMD COUNTER B	40
09:16:17	ACP 2 R power OFF	09:16:27	00:00:10	ACP 2 R LIMIT	OFF
09:25:17	Pyro 2 PJM set	09:25:30	00:00:13	PAR J3 SRS B	SQUIB SEL
		09:25:30		PAR J2 SRS B	SQUIB SEL
		09:25:30		PAR J1 SRS B	SQUIB SEL
09:25:25	Pyro 2 PJM reset	09:25:46	00:00:21	PAR J3 SRS B	SQUIB NO SEL
		09:25:46		PAR J2 SRS B	SQUIB NO SEL
		09:25:46		PAR J1 SRS B	SQUIB NO SEL
		09:25:32		CMD COUNTER B	43
09:39:13	GCMS 2 R power ON	09:39:22	00:00:09	GCMS 2 R LIMIT	ON
09:42:17	Proximity sensor A ON	09:42:20	00:00:03	PRX SENS B LIMIT	ON
10:32:21	DISR 1 R power red. ON	10:32:28	00:00:07	CMD COUNTER B	44
10:58:21	SSP R power red. ON	10:58:36	00:00:15	CMD COUNTER B	45
11:00:14	DISR 2 R power ON	11:00:27	00:00:13	DISR 2 R LIMIT	ON
11:00:21	ACP 3 R power OFF	11:00:26	00:00:05	ACP 3 R LIMIT	OFF
11:00:22	ACP 1 R power OFF	11:00:26	00:00:04	ACP 1 R LIMIT	OFF
		11:00:28		CMD COUNTER B	47

12.2 CPU LOAD

The CDMU B CPU workload is plotted in Fig.34. It is expressed in terms of ms, a 100% load

corresponding to 125ms. The shape of the curve showing a dependency of the workload to the mission time due to the location in the MTT and in the Time Altitude Table is as expected and was noticed during all flight checkouts. The absolute values (~47% load in average, 50% worst case) are also fully consistent.

It shall be underlined that the RAU's anomaly having led to a jump in altitude, its, very remarkable, effect of the of the CPU load is "nominal".

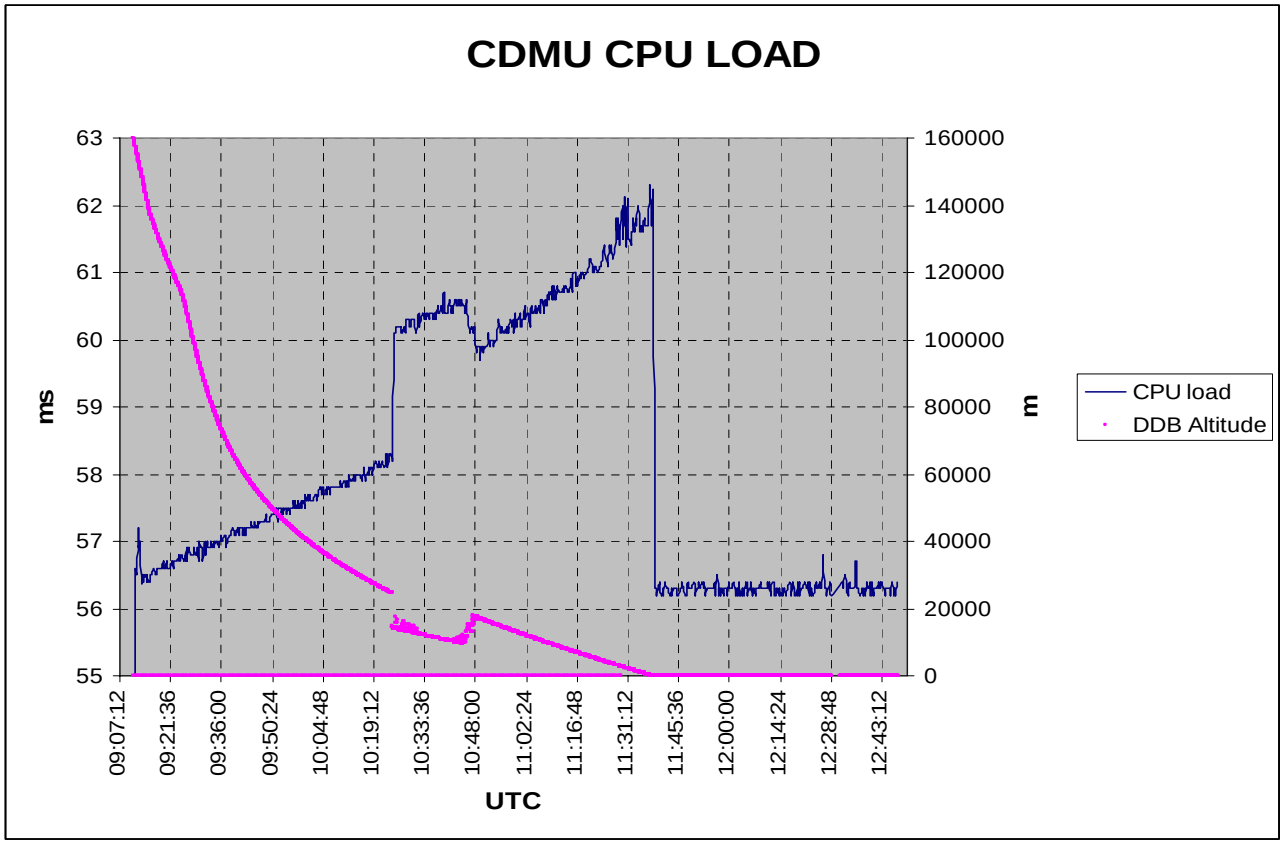

Figure 34 : CPU load vs mission time.

13. POWER SUBSYSTEM

The Electrical Power Subsystem is composed of the Power Conditioning and Distribution unit, the Pyro box and the batteries. In addition to the relays and LCL's status, the set of telemetry parameters used for the evaluation are :

Battery Voltages

- telemetry rate 16Hz
- HK TM in HKxxx TM packet,
- 1LSB = xxx
- worst case measurement accuracy : xxxxxx
- measurement range = 0 to 78V

Main Bus Voltage

- telemetry rate 16Hz
- HK TM in HKxxx TM packet,
- 1LSB = xxx
- worst case measurement accuracy : xxxxxx
- measurement range = 0 to 28V

BDR's currents

- telemetry rate 16Hz
- HK TM in HKxxx TM packet,
- 1LSB = xxx
- worst case measurement accuracy : xxxxxx
- measurement range = 0 to xxxA

LCL currents

- telemetry rate 16Hz
- HK TM in HKxxx TM packet,
- 1LSB = xxx
- worst case measurement accuracy : xxxxxx
- measurement range = 0 to xxxA

13.1 BATTERY VOLTAGES

Due to the loss of chain A TM, only the Batteries 3,4 and 5 voltages are available. These voltages shown in Fig.35 are :

- fully consistent with the voltages measured during the batteries depassivation activity performed

before separation (see report in RD14)

- fully consistent with the characterization performed with flight spare batteries on ground in mid 2004.
- Identical for all 3 batteries and indicating no cell level anomaly.

The batteries voltage remain almost constant for the whole mission duration, until landing. After landing, until loss of the RF link the voltage decrease is still minimum. This indicates that, when data reception stopped, the Probe was still capable to nominally operate from a power point of view, and most probably did. This will be addressed later in that chapter.

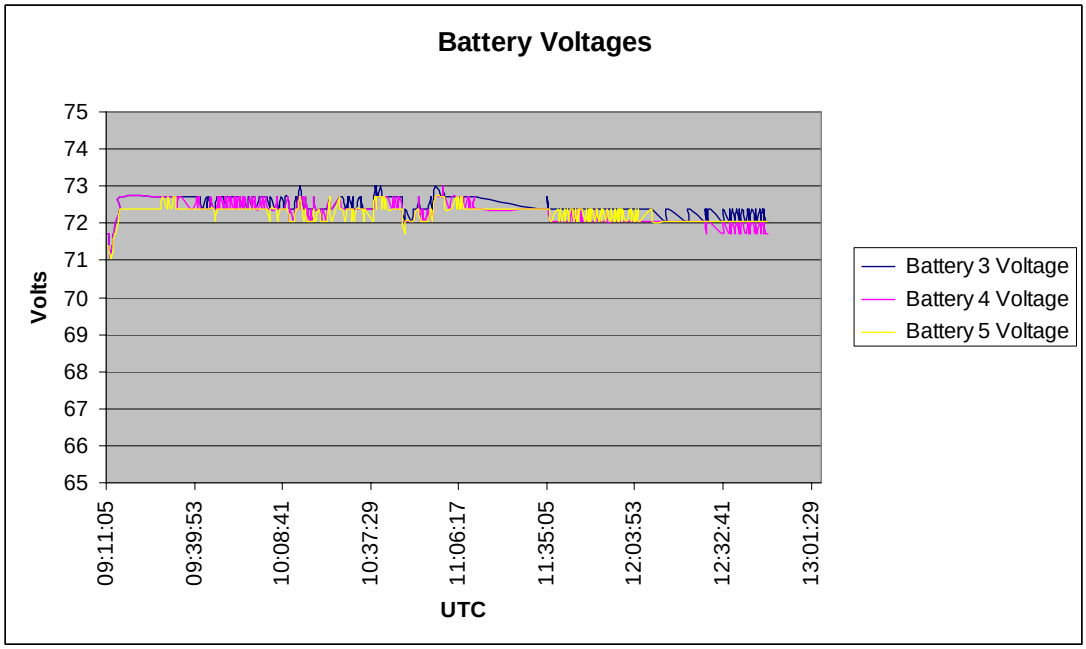

Figure 35 : Batteries voltage

13.2 BUS VOLTAGE

Fig.36 shows that the regulated 28V bus distributed to all the units has nominally remained perfectly stable all along the mission.

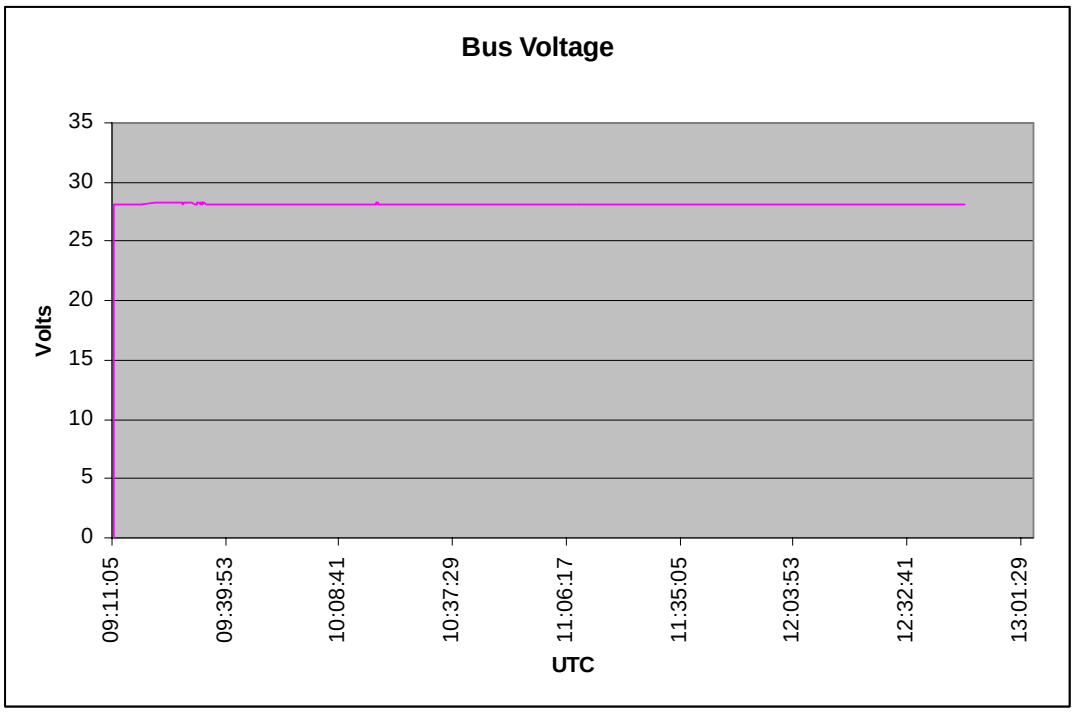

Figure 36 : Bus voltage

13.3 BDR CURRENTS

Fig.37 shows the evolution of the 3 Battery discharge regulators respectively connected to the batteries 3, 4 & 5. This shows that as designed, an identical current has been drawn from the batteries 3 and 4, while a higher current has been drawn from battery 5, which was not used during coast phase to supply the MTU.

The ratio between batt 5 and batt 3 & 4 BDR currents, known as BDR balancing is displayed in Fig.37. The average value of 1.127 is well in line with the designed 1.14+/-5%

Some more insight to the batteries voltage are given by plotting on the same graph, eg. for battery 5, the BDR 5 current and the battery voltage. Fig 38 shows that the small battery voltage variations correspond pretty well to the BDR current variations (higher BDR currents correspond to lower battery voltage).

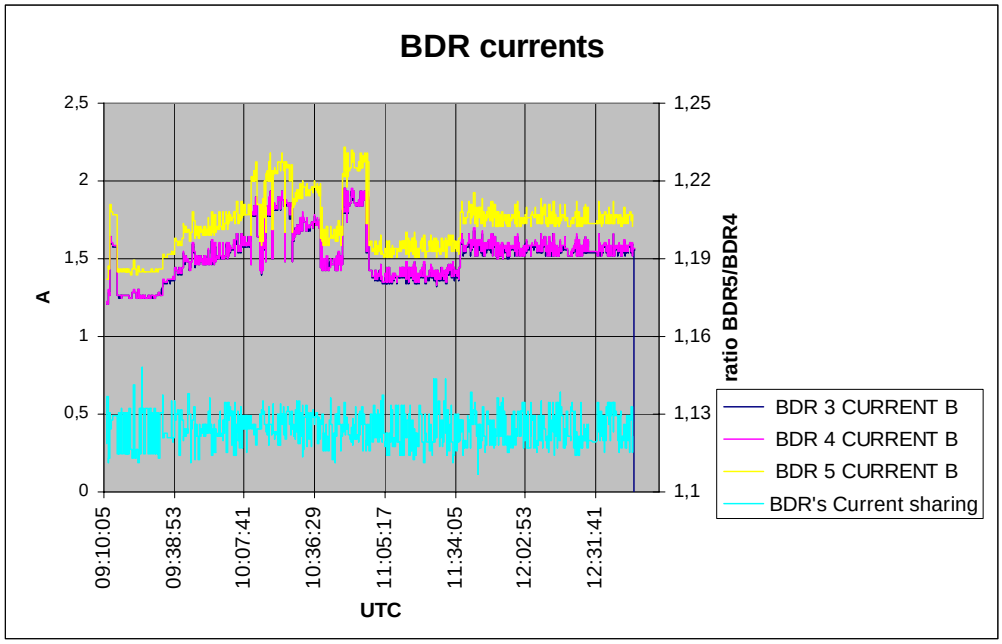

Figure 37 : BDR currents

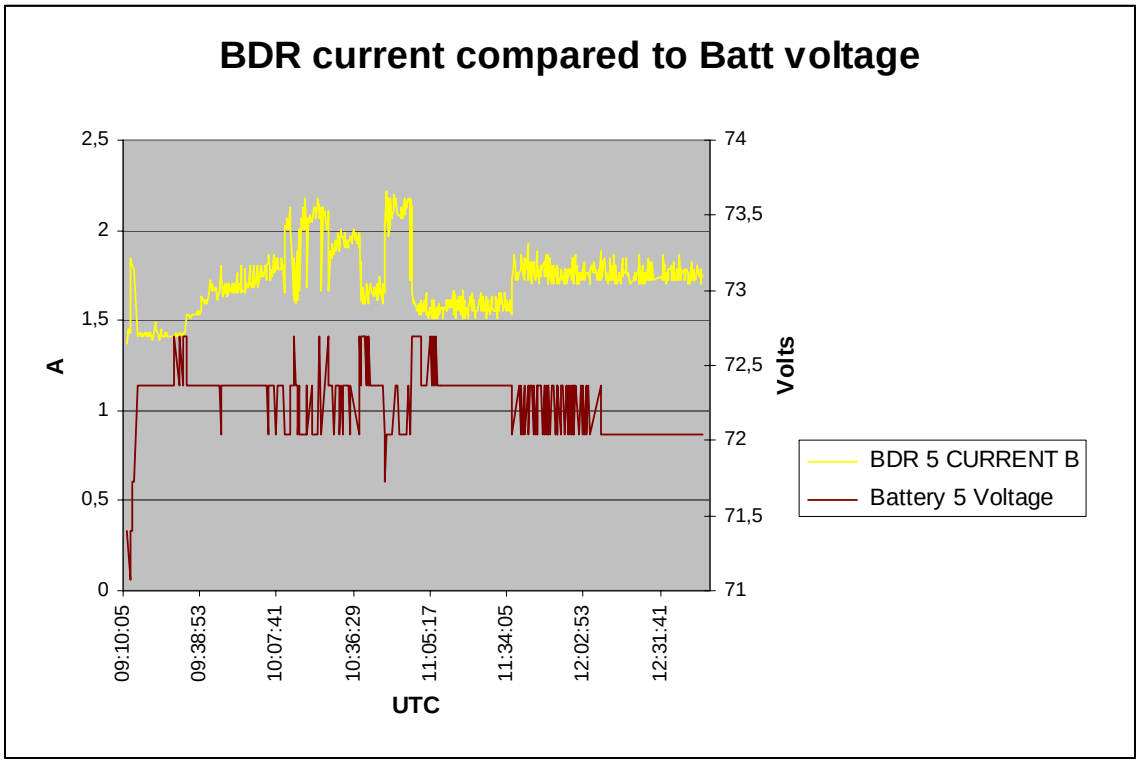

Figure 38 : BDR currents vs Batt voltage

13.4 LCL STATUS AND CURRENTS

Because of the loss of chain A telemetry, only half of the current limiters status and current values (the redundant ones) is available. Fig.40 shows that the LCL activation is consistent with the mission timeline in table 1.

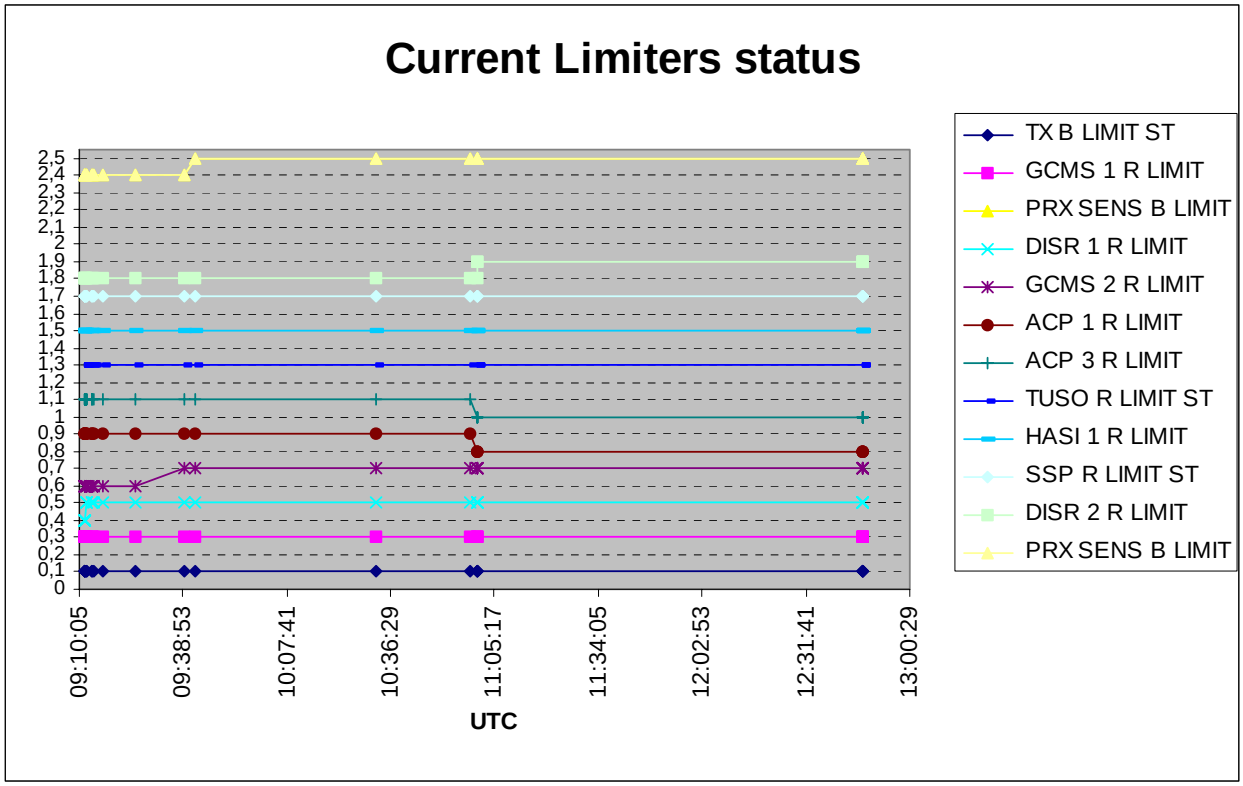

Figure 40 : Current Limiters status

The Figures 41a to 41g show the current consumption profiles from to the available telemetry. These profiles are compared to the predicted ones used to construct the pre mission power budget. The predicted profiles are traced for the planned mission duration, ie. from the Probe turn ON to the surface landing, while the measured profiles are plotted from the TM link availability, shortly after entry, until loss of contact with Huygens. These profiles then only partly overlap in time.

Considering that only the redundant LCL's TM is recorded (acquired by CDMU B), the mission power profiles are very well in line with the prevision; the only significant difference is coming from ACP 3 line for which a higher consumption was generally expected. ACP team have explained the measured behaviour by a discrepancy in the predicted figures.

It is pointed out that Fig.41h actually comprises the power consumption of CDMU B and RAU B. Fig.41i includes the contributions of Pyro box and PCDU.

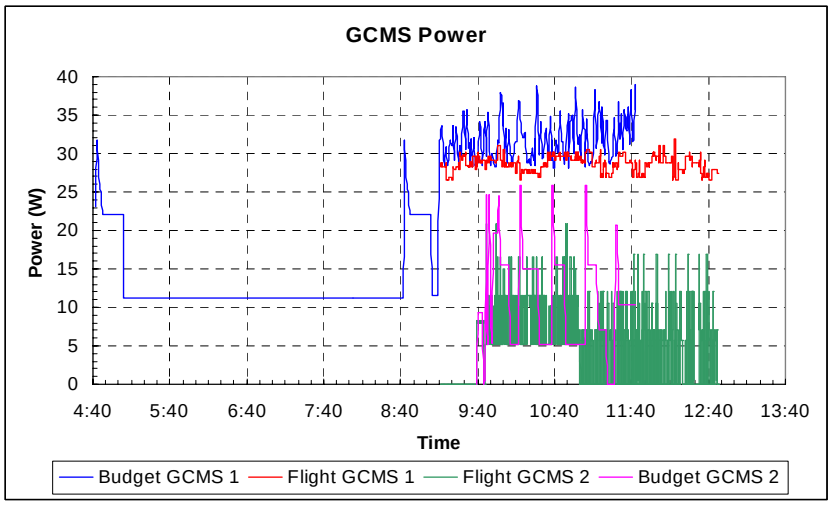

Figure 41a : GCMS R Current consumption

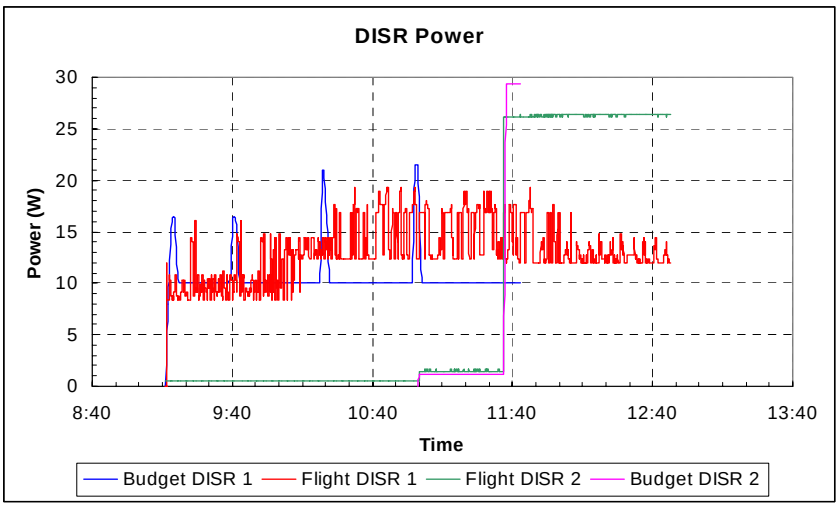

Figure 41b : DISR R Current consumption

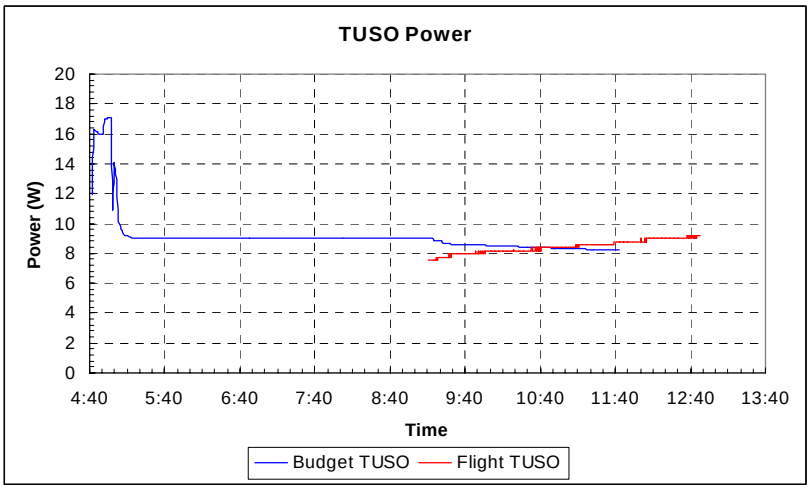

Figure 41c : TUSO R Current consumption

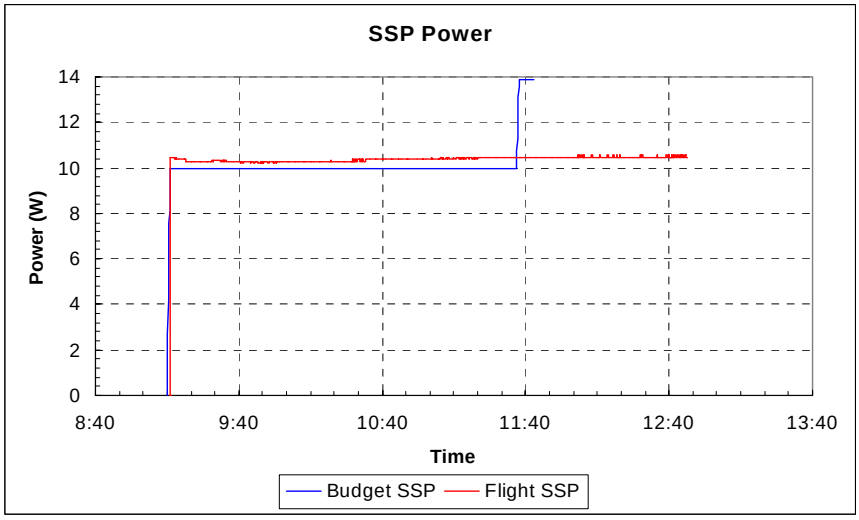

Figure 41d : SSP R Current consumption

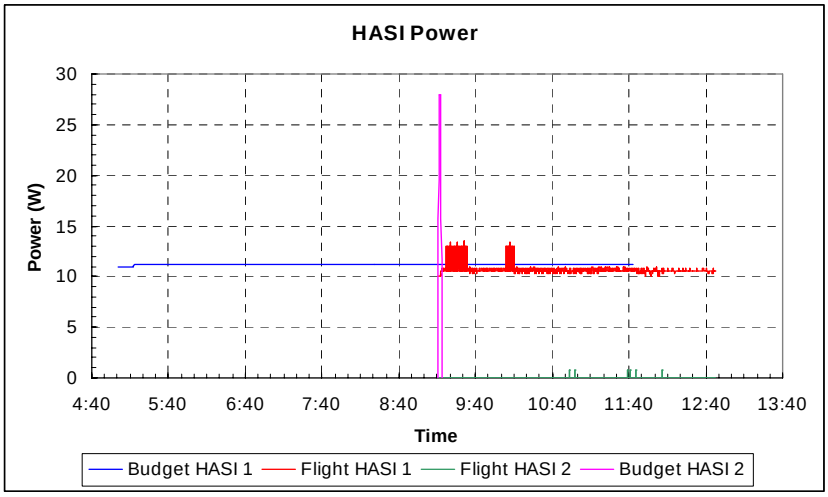

Figure 41e : HASI R Current consumption

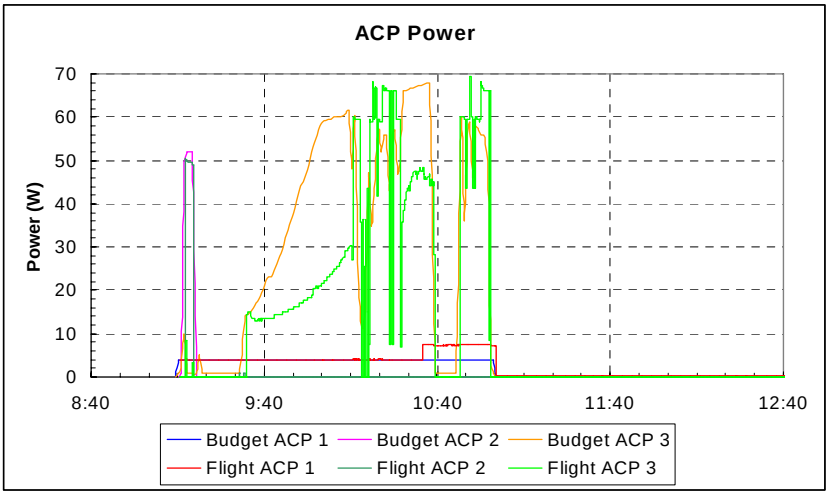

Figure 41f : ACP R Current consumption

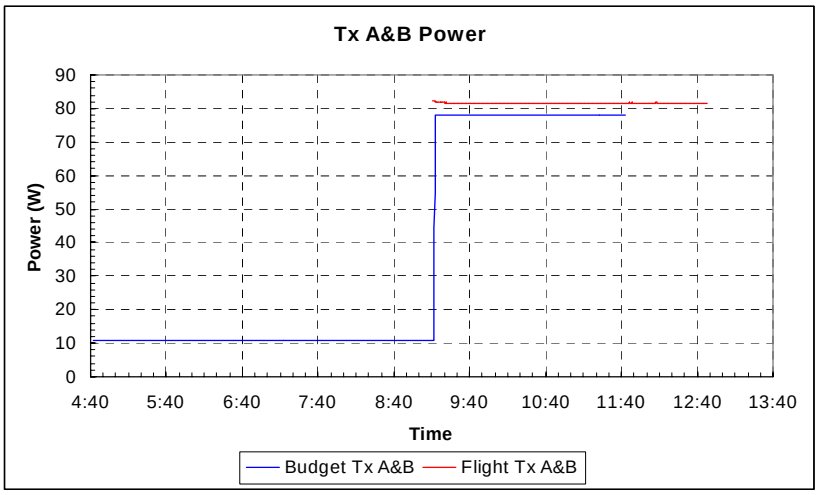

Figure 41g : Tx B Current consumption

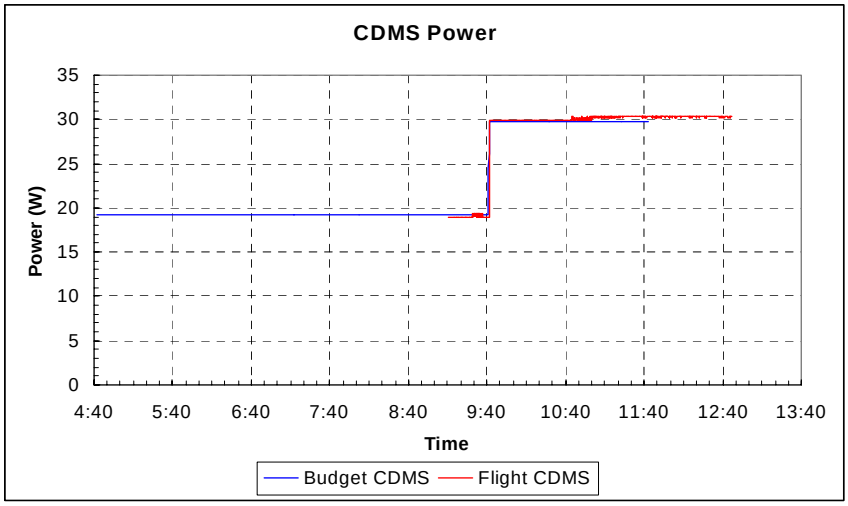

Figure 41h : CDMS Current consumption

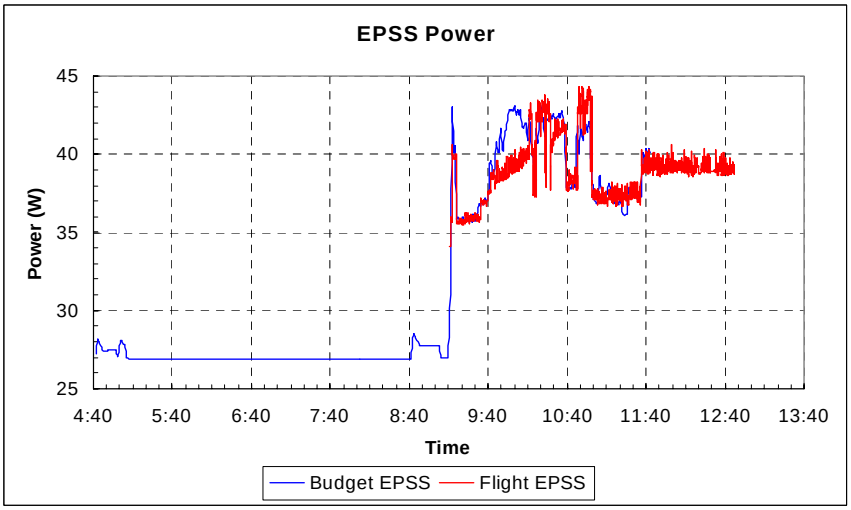

Figure 41i : EPSS Current consumption

13.5 POWER AND BATTERY

Fig.42 displays the total descent and surface power budget. In order to have comparable data, the non existing current TM has been extrapolated from existing data. The main differences between the profiles originate from the ACP discrepancy mentioned before. In the same way Fig.43 shows the power and energy profiles over the whole mission duration; the missing TM, again is extrapolated from the existing one. At touch down of the Probe, about 1200Wh were consumed. When the link with Huygens was interrupted, 2100Wh were taken from the batteries.

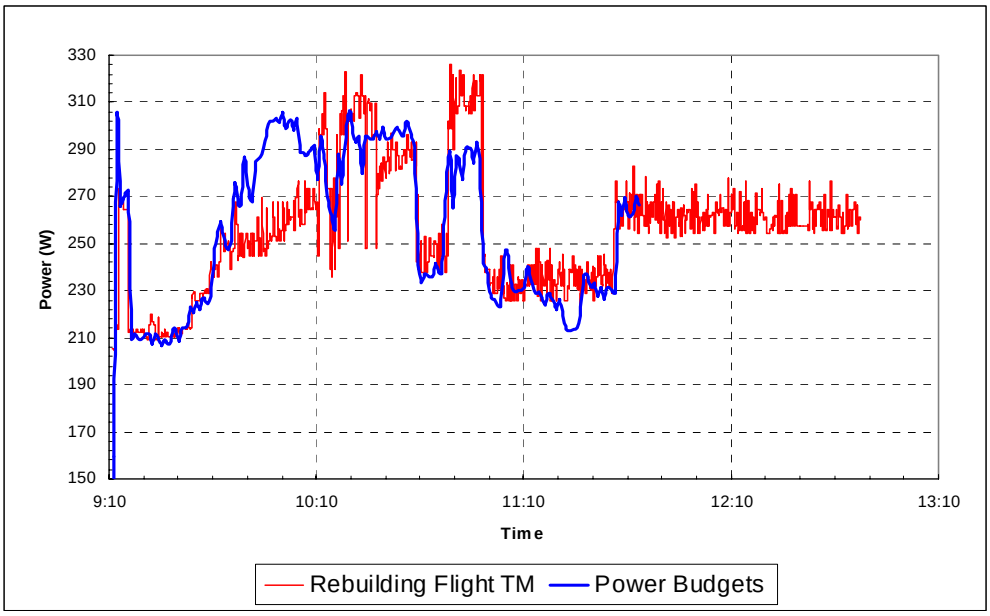

Figure 42 : Total power consumption during descent and surface phases.

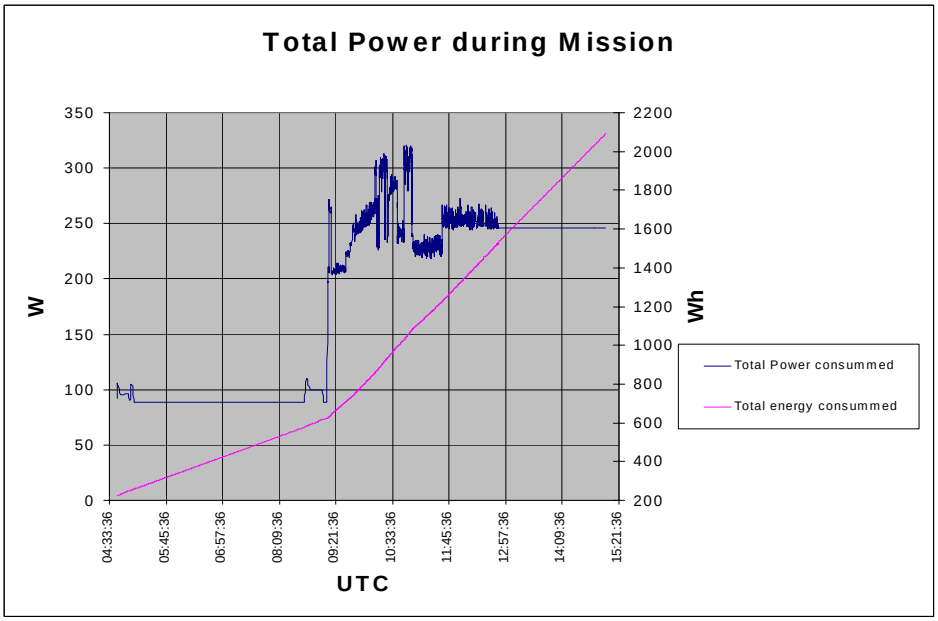

Figure 43 : Total Power and energy profiles during the entire mission

The available telemetry allows also to calculate, based on some assumptions, the time at which the Probe went OFF on the surface. The energy stored in a battery is indeed dependent upon :

- the battery temperature
- the discharged current from the battery.

Battery temperatures extrapolated from RD03 results over the whole mission (from Probe turn ON at the end of Coast phase) are displayed in Fig.44.

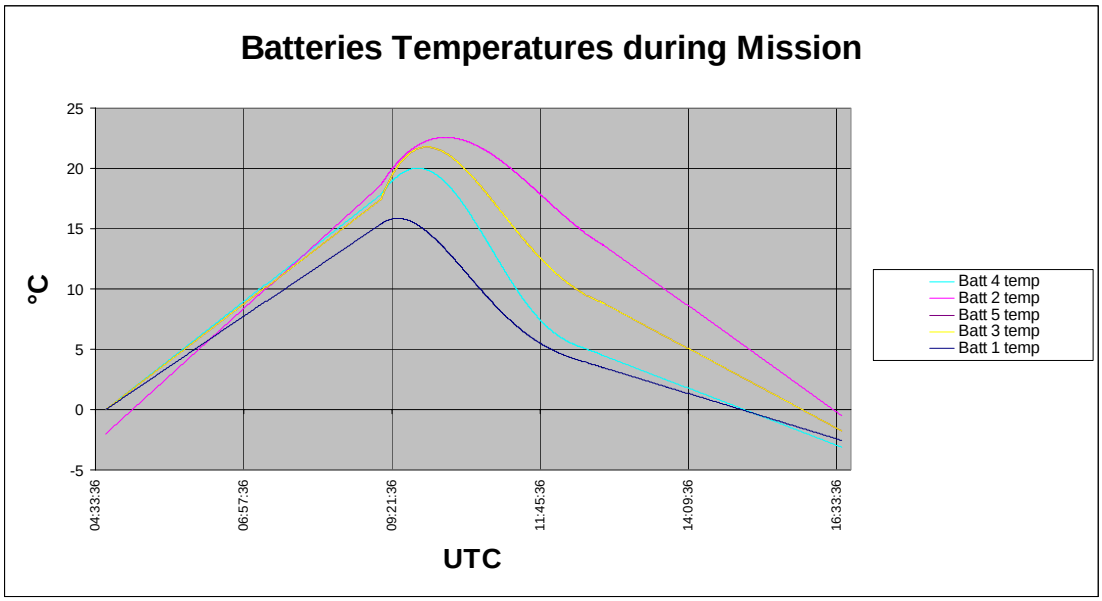

Figure 44 : Total Power and energy profiles during the entire mission

Based on the current consumed during coast phase (on batteries 1 & 5), pre-entry, entry, descent and surface phases, the BDR's efficiency and balancing, and assuming fully charged batteries at separation (consistent with the batteries voltage history), Fig.45 shows the energy left in each battery vs time.

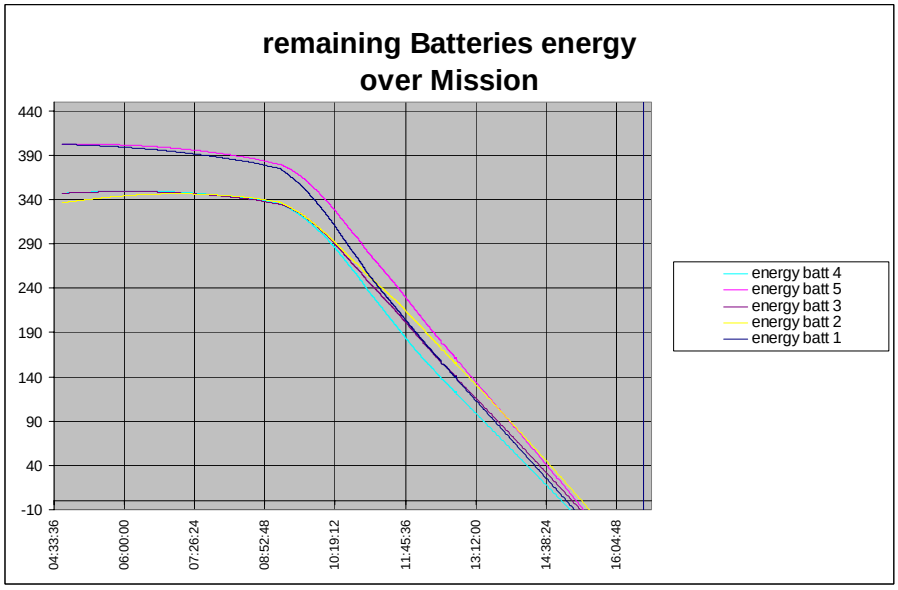

Figure 45 : Energy remaining in each battery

Considering that Probe is expected to have turned OFF after the depletion of 3 batteries, Fig.46 is a zoom of Fig.45, showing for the 3 weakest batteries, the time at which no energy remains in these 3 batteries. Assuming a certain dispersion around the nominal original batteries capacity, one deduces that the Huygens Probe has stopped to operate on the surface between UTC14:52 and UTC15:16. This is 3.5hours after landing, and the Probe remained ON about 2h20mn after the link with CASSINI was interrupted.

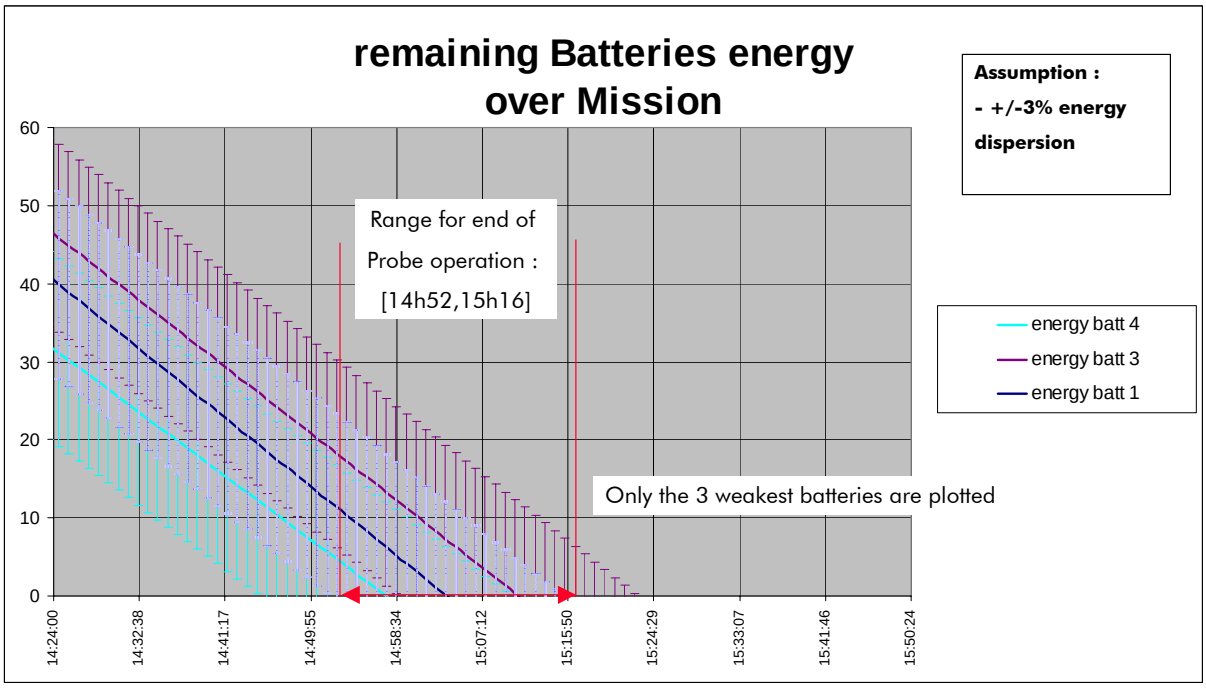

Figure 46 : Energy remaining in 3 weakest batteries

14. DATA RELAY

The data realy subsystem comprises both the transmitting side on the Probe and the receiving side on the Orbiter.

The set of telemetry parameters used for the evaluation are :

Transmitter B power :

- telemetry rate 16Hz
- HK TM in HK2 TM packet,
- 1LSB = xxx
- worst case measurement accuracy : xxxxxx
- measurement range = 0 to 78V

15. HUYGENS MISSION TIMELINE

Tp (sec)	UTC	OPERATION
0	04:41:18,453	PCDU on
0	04:41:18,453	CDMU A & B, CASU, RASU on
16	04:41:34,453	TUSO on
16,125	04:41:34,578	TX-A & TX-B on
30,125	04:41:48,578	GCMS 1 on
1080,13	04:59:18,578	HASI 1 on
2320,38	05:19:58,828	Send ACP Engineering Mode TC
2321,38	05:19:58,828	Send ACP Engineering Mode TC
0	09:10:14,453	S0 detection
1,5	09:10:15,953	Ta detection/ Arm pyro group 1 (PDD & BCM)
2,125	09:10:16,578	Reset PDD pyro selection relay
2,25	09:10:16,703	Reset BCM 3 pyro selection relays
2,375	09:10:16,828	Set PDD pyro selection relay
6,375	09:10:20,828	PDD current limiter fire
6,625	09:10:21,078	Reset PDD pyro selection relay
8,625	09:10:23,078	Set BCM 3 pyro Norm. Selection relays
8,75	09:10:23,203	Set BCM 3 pyro Red. Selection relays
8,875	09:10:23,328	BCM 3 current limiter fire
12,875	09:10:27,328	Reset BCM 3 pyro selection relays
16,375	09:10:30,828	TUSO on (2nd switch on)
16,625	09:10:31,078	TXs on (2nd switch on)
26,67	09:10:41,123	Arm pyro group 2 (FSM)
34,875	09:10:49,328	Set FSM 3 pyro selection relays
37,125	09:10:51,578	ACP 1 on
39,25	09:10:53,703	ACP 2 energize caps and valves, purge
38,875	09:10:53,328	FSM 3 current limiter fire
39,375	09:10:53,828	Reset GCMS inlet pyro selection relay
39,5	09:10:53,953	Reset GCMS outlet pyro selection relay
39,625	09:10:54,078	Reset DISR cover pyro selection relay
42,875	09:10:57,328	Reset FSM 3 pyro selection relays
47,64	09:11:02,093	Arm pyro group 3 (GCMS & DISR cover)
46,375	09:11:00,828	ACP 3 on
49,375	09:11:03,828	HASI 1 on (2nd switch on)
51,83	09:11:06,283	HPA on
52,375	09:11:06,828	Set GCMS inlet pyro selection relay
56,03	09:11:10,483	HASI 2 on : booms start to deploy
55,625	09:11:10,078	SSP on
56,375	09:11:10,828	GCMS inlet current limiter fire
60,375	09:11:14,828	Reset GCMS inlet pyro selection relay

60,5	09:11:14,953	Set GCMS outlet pyro selection relay
64,5	09:11:18,953	GCMS outlet current limiter fire
68,5	09:11:22,953	Reset CGMS outlet pyro selection relay
68,625	09:11:23,078	Set DISR cover pyro selection relay
72,625	09:11:27,078	DISR cover current limiter fire
85,625	09:11:40,078	Reset DISR cover pyro selection relay
86,375	09:11:40,828	DISR 1 on
160	09:12:54,453	ACP collection starts
186,375	09:13:20,828	GCMS 1 on (2nd switch on)
207,02	09:13:41,473	HASI 2 off
216,375	09:13:50,828	ACP 1 on (2nd switch on)
226,375	09:14:00,828	ACP 3 on (2nd switch on)
303,49	09:15:17,943	Arm pyro group 4 (PJM)
362,21	09:16:16,663	ACP 2 off
902,375	09:25:16,828	Set PJM 3 pyro selection relays
906,375	09:25:20,828	PJM 3 current limiter fire
910,375	09:25:24,828	Reset PJM 3 pyro selection relays
1737,94	09:39:12,393	GCMS 2 on
1922,49	09:42:16,943	Proximity sensor on
4926,38	10:32:20,828	DISR 1 on (2nd switch on)
6486,38	10:58:20,828	SSP on (2nd switch on)
6599,13	11:00:13,583	DISR 2 on
6606,38	11:00:20,828	ACP 3 off
6606,63	11:00:21,078	ACP 1 off
8007	11:23:41,453	DISR turn on surface lamp
8258,38	11:38:11,000	Titan Surface touch down - End of descent phase

Reconstructed Timeline of the Mission events

16. CONCLUSION

APPENDIX 1 : PARAMETERS DATATION

The present note aims to present and justify the precise calculation from telemetry of T0 time, in comparison with the DDB Time and the time of pilot chute firing.

A1.1 BACKGROUND

Each telemetry packet on board the Probe is stamped with 2 counters, both with 125ms resolution :

- the Real Time (RT), which counts the time from the Probe turn ON (or more precisely from ~10s after the Probe is physically powered, after the POSW has completed its initialisation). The RT is monotonously increased, and never reset.
- the Mission Time (MT), which is equal to RT until S0 is detected by the POSW, and resets to 0 at S0. The Mission Timeline Table which drives all the pre and post T0 events is quoted in MT (ie. it loses synchronisation with the RT at T0).

At any time after T0, then, by calculating (RT-MT) one obtains the S0 (and therefore T0) detection time with a 125ms accuracy.
The acquisition of the different housekeeping parameters (voltage, currents, statuses, accelerations, altitude, …) occurs at precise and known times from the RT and MT values in the header of the packet, different for each parameter. These times being set in the Huygens database, it is thus possible to date each parameter with an accuracy better than 125ms wrt the time of the packet in which the parameter appears. The datation process which is then applied to permit to express the times in UTC relates the packet times (RT and MT) to the BIU time (~CASSINI time) after the transfer frames are in turn stamped at reception by the PSA using the BIU time.

The above datation process is automatically implemented on all the retrieved parameters using the so called "datation tool" developed by ESOC.
All the Probe housekeeping parameters currently retrieved from the mission are time stamped using this mechanism.

Another time is maintained on board the Probe to provide the experiments with a time consistent with the mission events, the DDB Time. It is reset to 0 after T0 has been declared, its resolution is 2s and it is maintained in synchronization with the Real Time (see above).

From the above description, one can immediately draw the conclusion that from T0, DDB Time and Mission Time may not be synchronized; a time shift between 0 and 2s being authorized. It shall be noticed that this is a design feature, widely documented.

Another important point is that each chain A and B keeps its own RT, MT and DDB Times (RT A, RT B, MT A, MT B, DDB Time A, DDB Time B) which are in theory not necessarily synchronized between them. However it can be estimated that the RT A and RT B (and consequently DDB Time A and B, MT A and MT B before T0) maintain a synchronisation better than 100ms over the mission duration.

A1.2 RESULTS FROM THE MISSION ENGINEERING PARAMETERS ANALYSIS.

All the times, RT, MT and DDB time are reported in telemetry. HK3 actually reports all 3 times and thus allows to compare them. The table below is an extract of the time parameters retrieve from HK3. It permits to get (line in yellow) :

S0 detection time by chain B = 129350-379 = 128971 CUTs = 16121,375s from Probe ON = UTC09:10:14,453

Consequently, Pilot mortar firing time by chain B = T0 time = 129022 CUTs = UTC09:10:20,828
On another hand, one gets (from line in green in table 1)
DDB Time B = 0 at UTC09:10:21,078

This means that DDB Time B is reset (UTC09:10:21,078 - UTC09:10:20,828) = 250ms after T0 = 2 CUT's after T0.

NB : the correct synchronization of the DDB Time with the RT is verified (DDB Time B = 129022 + 2 = 129024 CUT's = 8064s, which is a pair, integer number of seconds).

```
# DDB T0; 2005-014T09:11:14; Delta_T; 8430.000; ;
# Parameter Characteristics;
# NAME; DESCR; UNIT; PKTYP; TOFSET; TDNEXT;
HBHK34; HK 3B RTC; ; H3B; 0.000; ;
HBHK35; HK 3B MTC; ; H3B; 0.000; ;
S2014D; DDB TIME B; Sec; H3B; -16.750; 2.000;
# Parameter Statistics;
# Name; First Sample Time; Last Sample Time; Samples; Minimum; Maximum; Average;
Sigma;
HBHK34; 2005-01-14T09:11:01.828; 2005-01-14T12:47:49.783; 804; 129350; 233414;
180839; 29865.1;
HBHK35; 2005-01-14T09:11:01.828; 2005-01-14T12:47:49.783; 804; 379; 104443;
51868.1; 29865.1;
S2014D; 2005-01-14T09:10:45.078; 2005-01-14T12:47:47.033; 6432; 24; 13046;
6467.14; 3733.14;
# Parameter values;
                # Sample Time;  Delta_T; HBHK34; HBHK35; S2014D;
                 2005-01-14T09:10:45.078;8401.078;;;24.0000000;
                 2005-01-14T09:10:47.078;8403.078;;;26.0000000;
                 2005-01-14T09:10:49.078;8405.078;;;28.0000000;
                 2005-01-14T09:10:51.078;8407.078;;;30.0000000;
                 2005-01-14T09:10:53.078;8409.078;;;32.0000000;
                 2005-01-14T09:10:55.078;8411.078;;;34.0000000;
                 2005-01-14T09:10:57.078;8413.078;;;36.0000000;
                 2005-01-14T09:10:59.078;8415.078;;;38.0000000;
                 2005-01-14T09:11:01.078;8417.078;;;40.0000000;
                  2005-01-14T09:11:01.828;8417.828;129350;379;;
                 2005-01-14T09:11:03.078;8419.078;;;42.0000000;
                 2005-01-14T09:11:05.078;8421.078;;;44.0000000;
```

Table 1 : RT, MT and DDB Times from HK3

The synchronization principles and the mission results are illustrated in Fig 1.

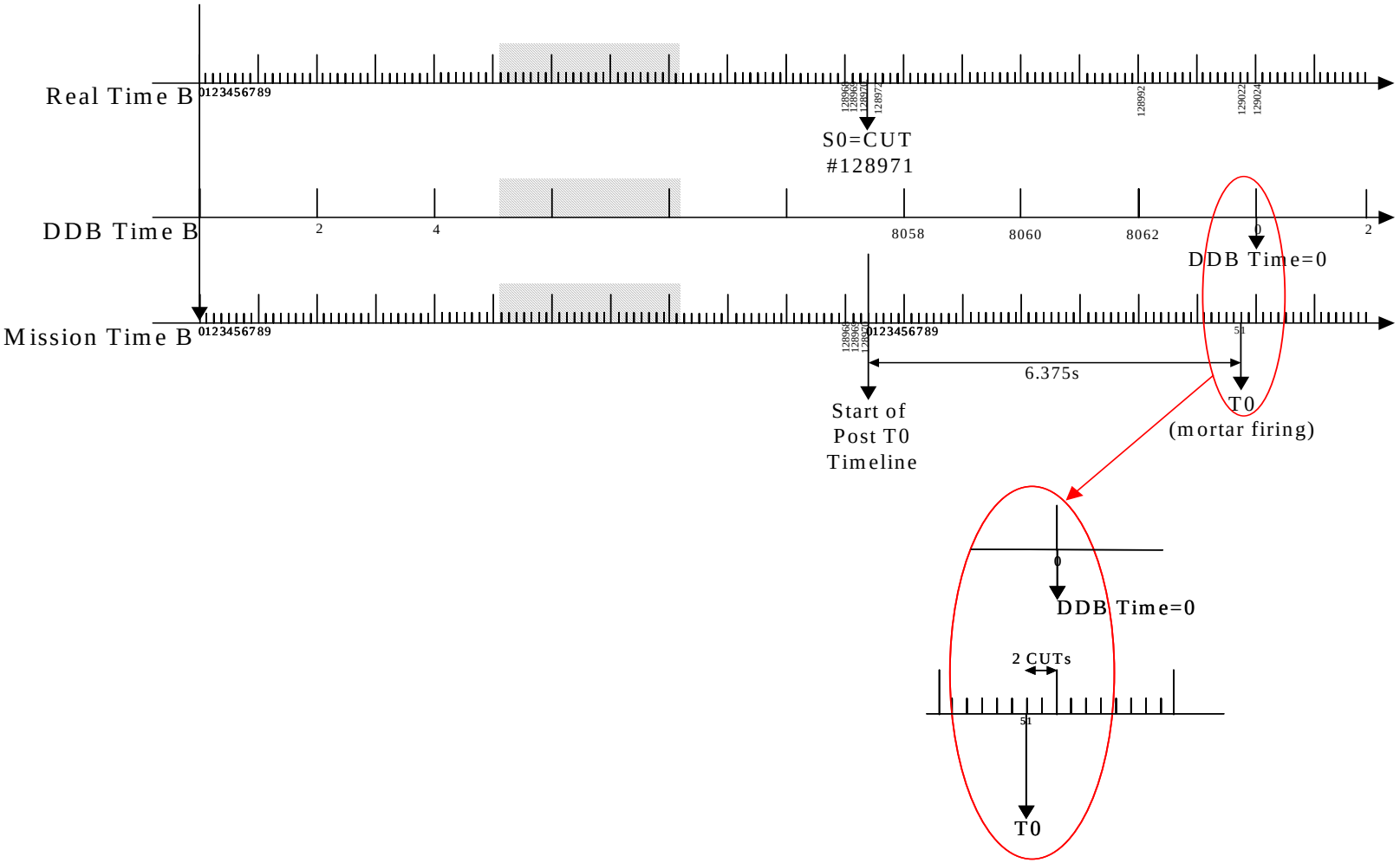

Figure 1 : T0 detection and time synchronization during mission

A1.3 CONSEQUENCES

As far as the engineering parameters are concerned, the datation process is independent upon the exact T0 time. As recalled in the beginning of the note, the reference to UTC is achieved via the time stamping of the frame by the BIU time on board CASSINI.
As far as the science data datation is concerned, IF THE DATATION PROCESS HAS ASSUMED DDB TIME=0 AT T0 then the science parameters stamping should be corrected by adding 250ms to the time ticks : a couple (time, parameter) should be corrected by (time + 250ms, parameter).

Because of the possible time difference of up to 100ms between DDB Time A (received by the experiments during the mission) and DDB Time B (see before), an uncertainty figure of 100ms shall be applied to the 250ms nominal shift.

Nota : a value of 375ms (3 CUT's) has been announced earlier (meeting in Meudon); this value, after multiple cross checks is corrected to 250ms as justified here.

APPENDIX 2 : ANALYSIS OF RASU POSITION DISCREPANCIES

A2.1 SCOPE

We have a discrepancy in the RASU accelero distance from CoG between the flight software data (coherent with the User Manual) and new evaluation performed in the frame of the document "Probe reference data for post flight analysis".

This memo has the objective to establish the correct position of these accelero.

R1 Probe reference data for post flight analysis, HUY.ASP.MIS.TN.0006 (beginning of June 2005)

R2 Huygens MTICD, HUY.AS/C.100.ID.0208 issue 7, 7 june 1996

To be noted: In the following, ACC1 = RASU A and ACC3 = RASU B. the denomination ACC x is used in LABEN ICD.

A2.2 CASU ACCELERO POSITION IN FLIGHT SOFTWARE

The flight software includes the following table:

Data for the Spin Calculation Algorithm

SVT RECORD RAM START=$ **6533** RAM END=$ **654A**

Spin/SVT Table

Constant	Initial value	RAM START	RAM END	RAM DATA	RAM DATA	exp
A1A	0.0000000000	6533	6534	0000	0000	0
B1A	0.0047058826	6535	6536	4D19	E6F9	-7
C1A	0.0000000000	6537	6538	0000	0000	0
D1A	0.0000000000	6539	653A	0000	0000	0
RA	0.4320000408	653B	653C	6E97	8DFF	-1
A1B	0.0000000000	653D	653E	0000	0000	0
B1B	0.0047058826	653F	6540	4D19	E6F9	-7
C1B	0.0000000000	6541	6542	0000	0000	0
D1B	0.0000000000	6543	6544	0000	0000	0
RB	0.3530000446	6545	6546	5A5E	35FF	-1
K1	95.4929661155	6547	6548	5F7E	3307	7
K2	0.0000000000	6549	654A	0000	0000	0

All above are **32-bit floating point data as below**

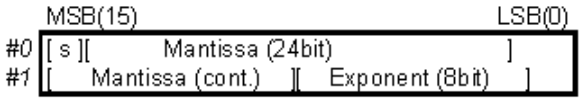

where
s = The sign bit
Mantissa = 2's complement of the 24 bit mantissa
Exponent = 2's complement of the 8 bit exponent

Table 1

RA is the distance of Accelero A, and RB is the distance of accelero B from CoG.

- RA = 432.0000408 mm
- RB = 353.0000446 mm

A2.3 RASU INSERT POSITION

The RASU insert identifiers are the following (from R2):

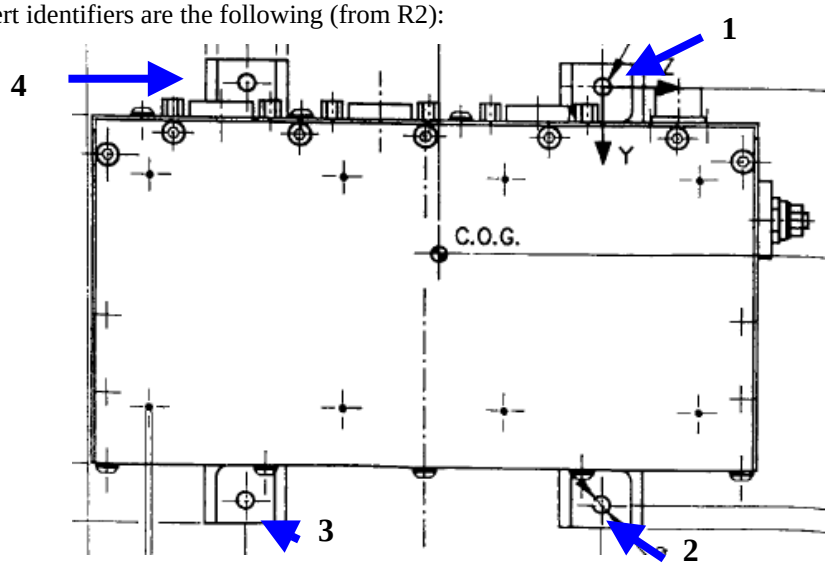

Figure 1

The RASU insert positions are the following (from R2):

Insert	X	Y	Z	Distance from X axis
1 = ref point	73	-370,55	-189,34	416,12
2	73	-308,92	-278,03	415,61
3	73	-384,46	-330,53	507,01
4	73	-446,1	-241,85	507,44

Table 2

The CoG position during the mission is the following (from R1):

Mission phases	X	Y	Z
Begin entry	75,44	1,75	5,38
End entry	82,54	2,48	5,13
Under main with FRSS	65,19	2,64	5,46
Under main without FRSS & DISR cover	81,33	3,67	1,17
Under drogue	71,83	-0,52	3,68
Descent module without any parachute	69,22	-1,46	5,46

Table 3

Hence, the inserts distance from COG during the mission is the following:

Mission phases	Distance from CoG			
	1 = Ref point	2	3	4
Begin entry	420,15	420,53	511,86	511,56
End entry	420,79	421,00	512,33	512,17
Under main with FRSS	421,04	421,30	512,64	512,44
Under main without FRSS & DISR cover	420,00	419,21	510,63	511,29
Under drogue	417,35	417,70	509,03	508,75
Descent module without any parachute	417,36	418,23	509,50	508,80

Table 4

Inserts 1&2, and 3&4 have about the same distance, as it can be verified on Figure 4

These distances questions seriously the RB value of 353mm as presented in §0 above.

A2.4 POSITION PROPOSED IN "PROBE REFERENCE DATA"

The acceleration measurement position is issued from SYSTROM DONNER 4310F engineering sketch:

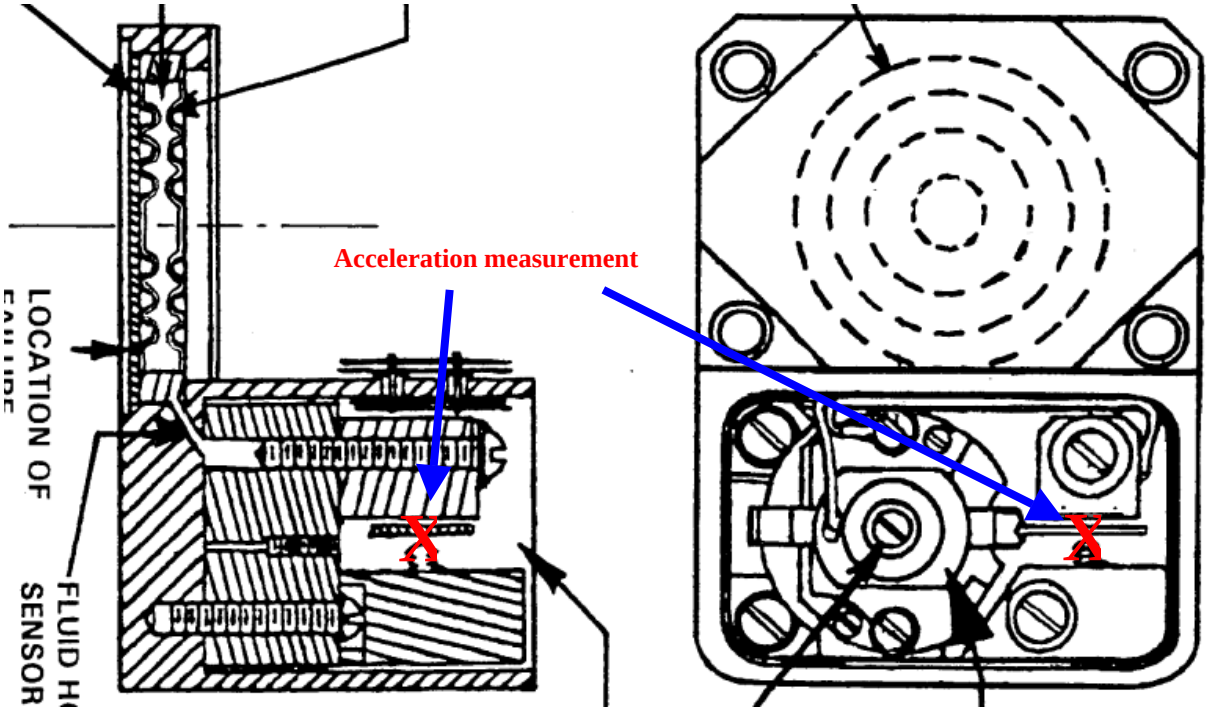

Figure 2

Then this position is placed in the RASU for both accelerometers:

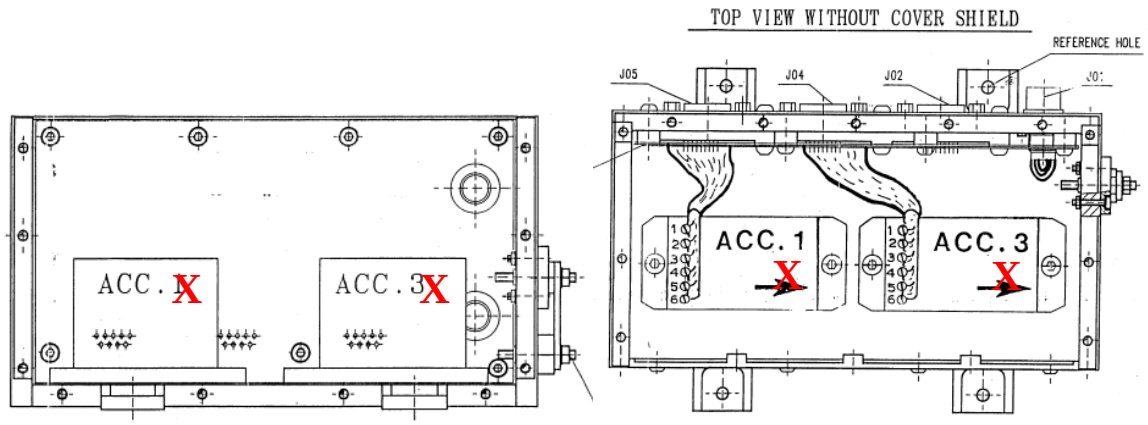

Figure 3

Finally, these positions are introduced in the CAD probe file in order to know these points in the probe reference frame. This gives (from R2):

	X	Y	Z	Distance from X axis
ACC1	112,06	-391,06	-284,41	483,55
ACC 3	112,06	-328,49	-240,87	407,34

Table 5

Hence, the distance to CoG for the different mission phases is the following (considering CoG position from Table 3 above):

Mission phases	Distance from CoG	
	Acc1	Acc3
Begin entry	489,51	413,57
End entry	489,47	413,44
Under main with FRSS	491,14	415,36
Under main without FRSS & DISR cover	488,17	412,14
Under drogue	486,97	411,08
Descent module without any parachute	487,49	411,66

Table 6

A2.5 POSITION DETERMINED MANUALLY

A manual measurement with a ruler is performed on several drawing of the probe Experiment platform top view from R2 (and placed below as Figure 4). Nb: The maximum diameter of the experiment platform as report on the following figure is 1300mm.

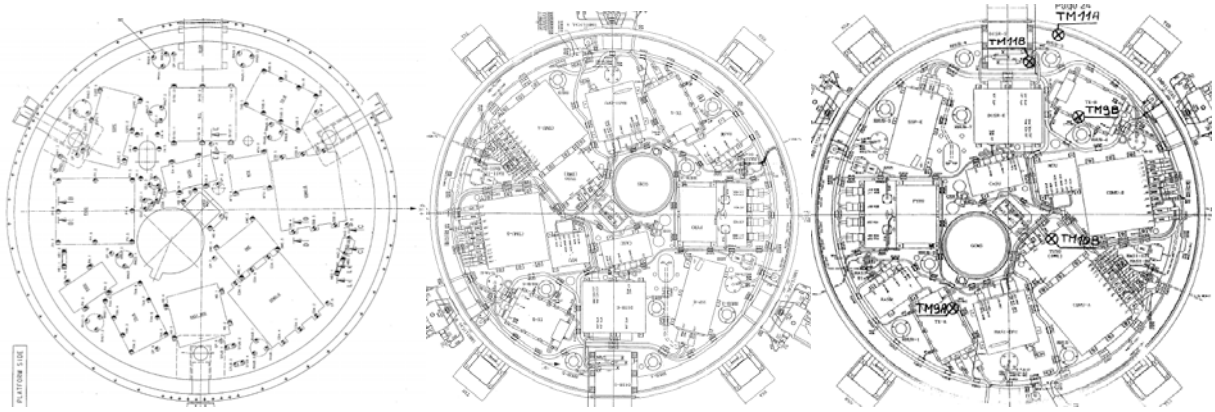

Figure 4

	Inserts	Equipment implementation	Thermistors implementation
RA	479 mm	477 mm	476 mm
RB	394 mm	402 mm	398 mm

Table 7

It can be derived from these manual evaluations a “mean distance” for both RASU accelerometers:

- RA = ~477 mm
- RB = ~398 mm

A2.6 SYNTHESIS

The different evaluations are synthesised on the following figure which presents RASU accelerometers position in the Y/Z plane.

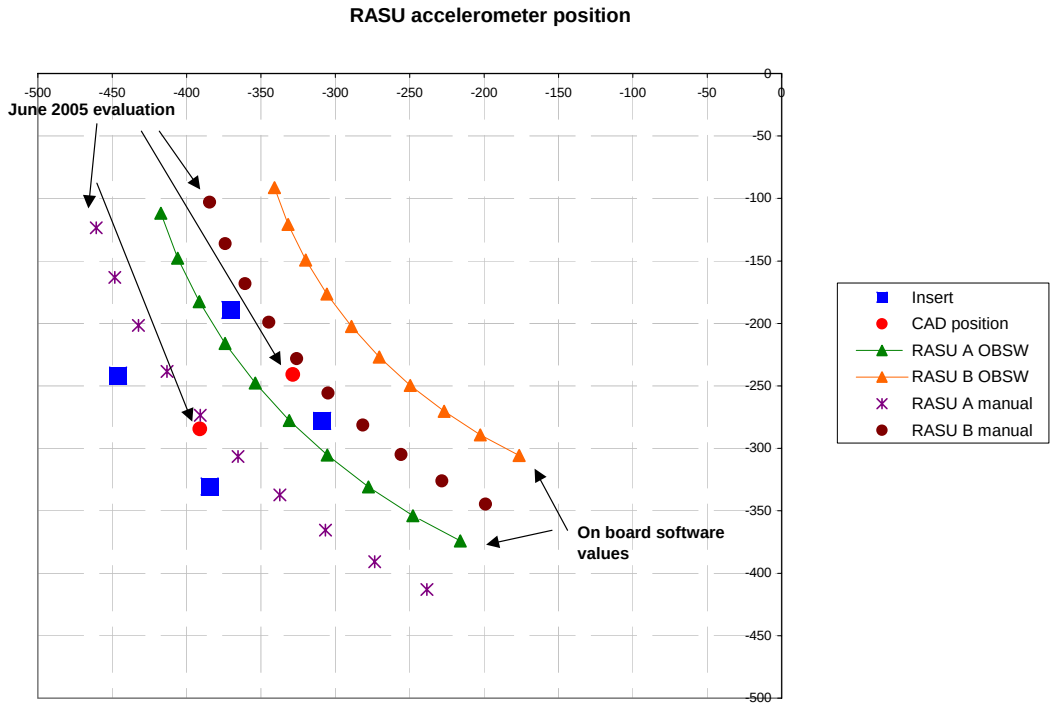

Figure 5

In order to possibly validate updated RASU accelerometers locations based on CAD's co-ordinates, we have compared here below the DDB Spin A & B as measured during the mission, with the Spin reconstructed from different sets of data (essentially Receiver AGC) (see Figure 6), with the DDB Spin A & B if it had been calculated with CAD's co ordinates (see Figure 7).

The results are clear : the Spin corrected with CAD's RASU accelerometers positions fits much better with the post mission reconstructed spin.

As a conclusion, it appears that the approximation used in the flight POSW for the computation of the Spin were slightly erroneous, and the confirmed RASU accelerometers location is the one indicated in table 6, and recalled hereafter :

Mission phases	Distance from CoG	
	Acc1	Acc3
Begin entry	489,51	413,57
End entry	489,47	413,44
Under main with FRSS	491,14	415,36
Under main without FRSS & DISR cover	488,17	412,14
Under drogue	486,97	411,08
Descent module without any parachute	487,49	411,66

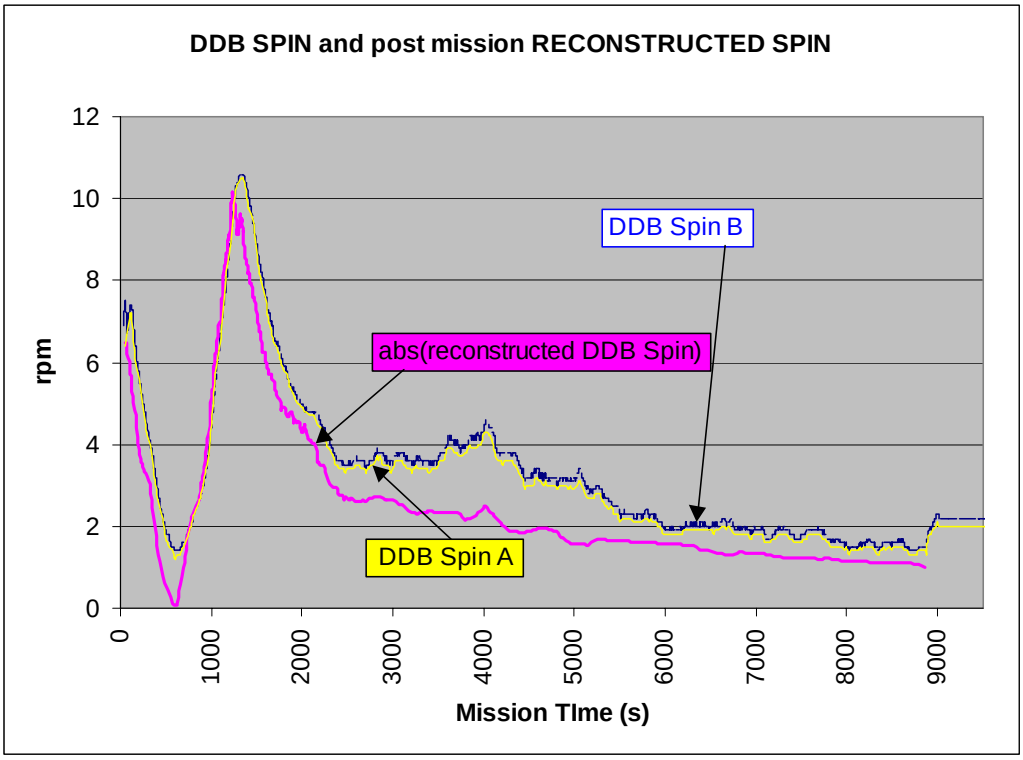

Figure 6

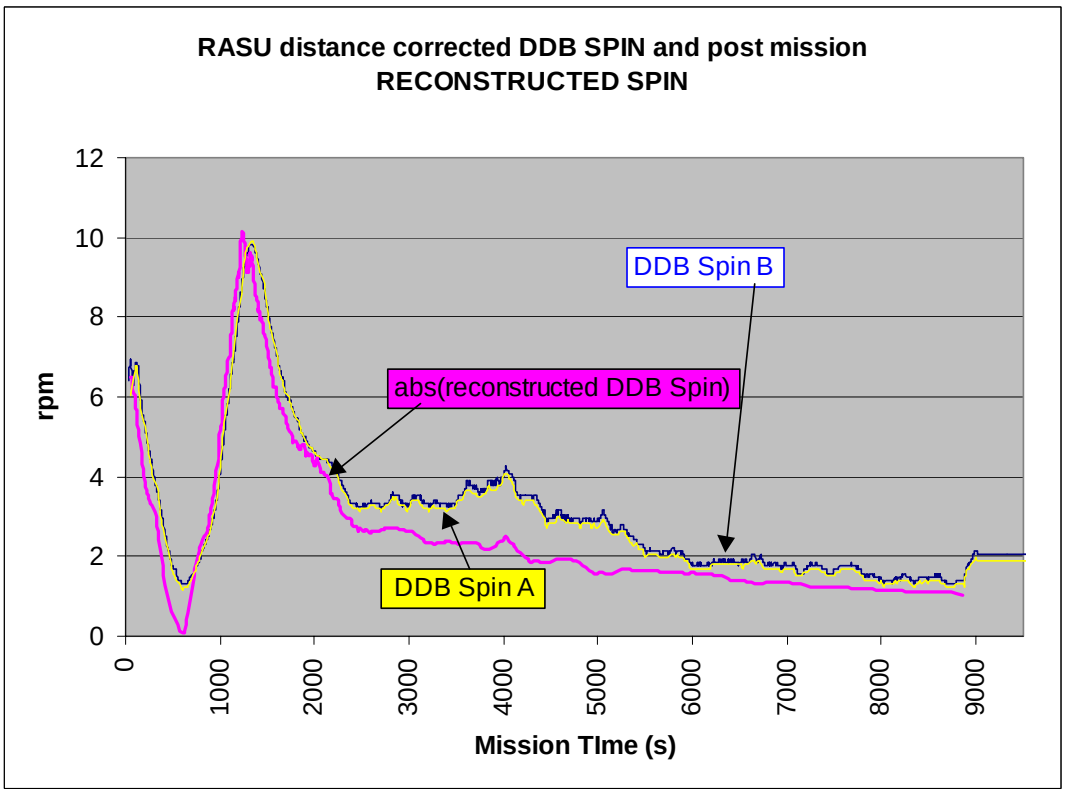

Figure 7